



QEX

\$5

September/October 2008

www.arrl.org

A Forum for Communications Experimenters

Issue No. 250



WØXI gives us an in-depth analysis of the “simple” crystal set, and shows us some of the electronic principles we can learn from these radios.

ARRL The national association for
AMATEUR RADIO

225 Main Street
Newington, CT USA 06111-1494



Two of the **LIGHTEST** and **MOST COMPACT** Amplifiers in the Industry!



HL-1.5KFX

HF/50MHz Linear Power

Features

- Solid State.
- The amplifier's decoder changes bands automatically with most ICOM, Kenwood, Yaesu.
- The amp utilizes an advanced 16 bit MPU (microprocessor) to run the various high speed protection circuits such as overdrive, high antenna SWR, DC overvoltage, band miss-set etc.
- Built in power supply.
- AC (200/220/235/240V) and (100/110/115/120V) selectable.
- Equipped with a control cable connection socket, for the HC-1.5KAT, auto antenna tuner by Tokyo Hy-Power Labs.

Specifications

Frequency:
1.8 ~ 28MHz all amateur bands including WARC bands and 50MHz

Mode:
SSB, CW, RTTY

RF Drive:
85W typ. (100W max.)

Output Power:
HF 1kW PEP max.
50MHz 650W PEP max.

Circuit:
Class AB parallel push-pull

Cooling Method:
Forced Air Cooling

AC Power:
AC 240V default (200/220/235)
– 10 A max.
AC 120V (100/110/115)
– 20 A max.

Dimensions:
10.7 x 5.6 x 14.3 inches
(WxHxD)/272 x 142 x 363 mm

Weight:
Approx. 20kgs. or 45.5lbs.

Optional Items:
Auto Antenna Tuner (HC-1.5KAT)
External Cooling Fan (HXT-1.5KF for high duty cycle RTTY)

Accessories Included:
Band Decoder Cables included for Kenwood, ICOM and some Yaesu



HL-1.2KFX

750W PEP Desktop Linear

Features

- Solid State.
- This world-class compact 750W HF amplifier is the easiest to handle and operate.
- The amplifier's broadband characteristics require no further tuning once the operating band is selected.
- The amplifier allows operation in full break-in CW mode due to the use of the amplifier's high speed antenna relays
- Quiet operation allows for even the weakest DX signals
- The amp utilizes a sophisticated circuit to run the various high speed protection circuits.

Specifications

Frequency:
1.8 - 28MHz all amateur bands including WARC bands

Mode:
SSB, CW, RTTY

RF Drive:
75 - 90W

Output Power:
SSB 750W PEP max.,
CW 650W, RTTY 400W

Circuit:
Class AB parallel push-pull

Cooling Method:
Forced Air Cooling

AC Power:
1.4kVA max. when TX
AC 100/110/115/120V,
AC 200/220/230/240V

Dimensions:
9.1 x 5.6 x 14.3 inches
(WxHxD)

Weight:
Approx. 33lbs.

More Fine Products from TOKYO HY-POWER



HC-1.5KAT

HF 1.5KW
Auto Tuner



HL-350VDX

VHF 330W
Amplifier



HC-200AT

HF/6m 200W
Auto Tuner
Lightning Tuning Speed



TOKYO HY-POWER LABS., INC. – USA
Technical Support
28301 Tomball Parkway, Suite #500-210
Tomball, TX 77375
Phone 713-818-4544
e-mail: thpsupport@airmail.net

TOKYO HY-POWER LABS., INC. – JAPAN
1-1 Hatanaka 3chome, Niiza Saitama 352-0012
Phone: +81 (48) 481-1211 FAX: +81 (48) 479-6949
e-mail: info@thp.co.jp
Web: <http://www.thp.co.jp>



Exclusively from Ham Radio Outlet!

www.hamradio.com

Western US/Canada 1-800-854-6046	Southeast 1-800-444-7927	Northeast 1-800-644-4476
Mountain/Central 1-800-444-9476	Mid-Atlantic 1-800-444-4799	New England/Eastern Canada 1-800-444-0047



QEX (ISSN: 0886-8093) is published bimonthly in January, March, May, July, September, and November by the American Radio Relay League, 225 Main Street, Newington, CT 06111-1494. Periodicals postage paid at Hartford, CT and at additional mailing offices.

POSTMASTER: Send address changes to: QEX, 225 Main St, Newington, CT 06111-1494 Issue No 250

Harold Kramer, WJ1B
Publisher

Larry Wolfgang, WR1B
Editor

Lori Weinberg, KB1EIB
Assistant Editor

Zack Lau, W1VT
Ray Mack, W5IFS
Contributing Editors

Production Department

Steve Ford, WB8IMY
Publications Manager

Michelle Bloom, WB1ENT
Production Supervisor

Sue Fagan, KB1OKW
Graphic Design Supervisor

David Pingree, N1NAS
Senior Technical Illustrator

Advertising Information Contact:

Janet L. Rocco, W1JLR
Business Services
860-594-0203 – Direct
800-243-7768 – ARRL
860-594-4285 – Fax

Circulation Department

Cathy Stepina, QEX Circulation

Offices

225 Main St, Newington, CT 06111-1494 USA
Telephone: 860-594-0200
Fax: 860-594-0259 (24 hour direct line)
e-mail: qex@arrl.org

Subscription rate for 6 issues:

In the US: ARRL Member \$24, nonmember \$36;

US by First Class Mail: ARRL member \$37, nonmember \$49;

International and Canada by Airmail: ARRL member \$31, nonmember \$43;

Members are asked to include their membership control number or a label from their QST when applying.

In order to ensure prompt delivery, we ask that you periodically check the address information on your mailing label. If you find any inaccuracies, please contact the Circulation Department immediately. Thank you for your assistance.



Copyright ©2008 by the American Radio Relay League Inc. For permission to quote or reprint material from QEX or any ARRL publication, send a written request including the issue date (or book title), article, page numbers and a description of where you intend to use the reprinted material. Send the request to the office of the Publications Manager (permission@arrl.org).

About the Cover

Phil Anderson, WØXI, gives us an in-depth analysis of the “simple” crystal set. Our cover shows one crystal set that Phil designed and built. As Phil’s article shows, we can learn many electronics principles from these radios.



In This Issue

Features

3 SID: Study Cycle 24, Don’t Just Use It
By Mark Spencer, WA8SME

10 A Great Teacher: The Crystal Set
By Phil Anderson, WØXI

15 The Rechargeable Battery “Cycler”
By Bertrand Zauhar, VE2ZAZ

22 Press-n-Peel Circuit Board
By Jim Kocsis, WA9PYH

26 Receiver Performance Measurement and Front End Selectivity
By Henry J. Rech

31 Optimum Lossy Broadband Matching Networks for Resonant Antennas
By Frank Witt, A11H

Columns

41 Letters to the Editor

43 In the Next Issue of QEX

43 Upcoming Conferences

44 Out Of The Box
By Raymond Mack, W5IFS

Index of Advertisers

American Radio Relay League:.....	Cover III
Atomic Time:.....	42
Down East Microwave Inc:.....	9
Kenwood Communications:.....	Cover IV
National RF, Inc:	9
Nemal Electronics International, Inc:.....	25
RF Parts	21, 23
Teri Software:.....	9
Tokyo Hy-Power Labs, Inc:	Cover II
Tucson Amateur Packet Radio:	40

The American Radio Relay League

The American Radio Relay League, Inc. is a noncommercial association of radio amateurs, organized for the promotion of interest in Amateur Radio communication and experimentation, for the establishment of networks to provide communications in the event of disasters or other emergencies, for the advancement of the radio art and of the public welfare, for the representation of the radio amateur in legislative matters, and for the maintenance of fraternalism and a high standard of conduct.



ARRL is an incorporated association without capital stock chartered under the laws of the state of Connecticut, and is an exempt organization under Section 501(c)(3) of the Internal Revenue Code of 1986. Its affairs are governed by a Board of Directors, whose voting members are elected every three years by the general membership. The officers are elected or appointed by the Directors. The League is noncommercial, and no one who could gain financially from the shaping of its affairs is eligible for membership on its Board.

"Of, by, and for the radio amateur," ARRL numbers within its ranks the vast majority of active amateurs in the nation and has a proud history of achievement as the standard-bearer in amateur affairs.

A *bona fide* interest in Amateur Radio is the only essential qualification of membership; an Amateur Radio license is not a prerequisite, although full voting membership is granted only to licensed amateurs in the US.

Membership inquiries and general correspondence should be addressed to the administrative headquarters:

ARRL
225 Main Street
Newington, CT 06111 USA
Telephone: 860-594-0200
FAX: 860-594-0259 (24-hour direct line)

Officers

President: JOEL HARRISON, W5ZN
528 Miller Rd, Judsonia, AR 72081

Chief Executive Officer: DAVID SUMNER, K1ZZ

The purpose of *QEX* is to:

- 1) provide a medium for the exchange of ideas and information among Amateur Radio experimenters,
- 2) document advanced technical work in the Amateur Radio field, and
- 3) support efforts to advance the state of the Amateur Radio art.

All correspondence concerning *QEX* should be addressed to the American Radio Relay League, 225 Main Street, Newington, CT 06111 USA. Envelopes containing manuscripts and letters for publication in *QEX* should be marked Editor, *QEX*.

Both theoretical and practical technical articles are welcomed. Manuscripts should be submitted in word-processor format, if possible. We can redraw any figures as long as their content is clear. Photos should be glossy, color or black-and-white prints of at least the size they are to appear in *QEX* or high-resolution digital images (300 dots per inch or higher at the printed size). Further information for authors can be found on the Web at www.arrl.org/qex/ or by e-mail to qex@arrl.org.

Any opinions expressed in *QEX* are those of the authors, not necessarily those of the Editor or the League. While we strive to ensure all material is technically correct, authors are expected to defend their own assertions. Products mentioned are included for your information only; no endorsement is implied. Readers are cautioned to verify the availability of products before sending money to vendors.

Larry Wolfgang, WR1B

lwolfgang@arrl.org

Empirical Outlook

It has been a busy and fun summer, but even as I write this in early August I realize that summer will be over all too soon! The September/October issue brings fall, and a return to our "normal" activities — whatever that means — at least for many of us. I hope you have managed some time to relax and refresh, and I hope some of that time involved Amateur Radio, in whatever way you enjoy our hobby.

The ARRL/TAPR Digital Communications Conference has been held in September for a number of years. As I thought about arrangements to travel to Chicago for this year's DCC (Sep 26-28), I realized that when I attended the event last year in Windsor Locks, CT, it was one of my first "duties" as *QEX* Editor. Has it really been a year already? The Sep/Oct 2007 issue was the first to list my name as Editor of our little magazine, so I guess it has. It seems like a good time to reflect on where we've been, or where we've come in that last year, and where we may be headed in the future.

With the Jan/Feb 2008 issue we made a few tweaks to the cover design and also brought out a new style for the inside of the magazine. I believe we have improved the presentation of our articles, and I haven't heard any complaints, so I hope you like it. Of course with every issue I think our Graphics Design Supervisor, Sue Fagan, KB1OKW, has come up with a cover that she will never be able to top, but then the next issue comes along and she does it again!

A year ago, our *QEX* circulation was just under 6000 copies per issue, and had been holding fairly steady at that number since at least early 2006. (I don't have circulation numbers going back earlier than that.) Now, that isn't a very large circulation, as magazines go, but it put *QEX* just about at the "break-even" point, financially. Clearly, there are opportunities to improve our position, economically.

Throughout 2008 we have seen a fairly steady circulation growth. With this issue, we have broken the 7000 copy circulation barrier! This is a very encouraging trend, because I believe it means that you like what you have been seeing, and perhaps have even been telling your friends. Thank you!

So, where do we go from here? We certainly want to continue producing a top-notch magazine with the technical content you want to read. Everyone at ARRL HQ (and those contributors who don't work here) knows every article won't please every reader, but I would like to think that every issue has some articles that appeal to every reader. What would you like to see? I am open to your ideas and criticisms. Let me know what you think.

As time permits, I would like to expand our Web site (www.arrl.org/qex) to include more interesting content. Except for the thumbnail cover images and sample articles from each new issue, that Web page has been pretty stagnant. I keep dreaming about ways to dress up the files download section, perhaps even making that more than a simple link on the main *QEX* page. So far it has only been a dream, though.

"As time permits" seems to be the magic phrase for a lot of things. We face a number of challenges to producing each issue. You will notice that this issue has only 44 pages between the covers, instead of the normal 64. There are a number of reasons for that, but two stand out. The first is that we are beyond the "to the printer date," so we have run out of time to add more content. The second reason is that there is not a lot of material in the "articles accepted" file. New articles have been coming in at about the same pace as we have been printing them. Planning the articles to fill each issue can be difficult without a backlog of material waiting to be printed.

The goal of our ARRL Technical Editorial Team is to ensure the technical accuracy and viability of each article accepted for publication, whether that be for *QST* or *QEX*. We also struggle to evaluate how interesting a given article will be to a majority of our readers. An article may show a really neat project, but if it doesn't look like something other hams will be able to duplicate, or would be interested in duplicating even if they could, we are reluctant to accept it for publication. Not every article that comes in for possible use in one of our magazines can be accepted for publication.

That said, I hope more of you will make the time to share your work with our readers by submitting articles about your latest project or technical interest. A fact of the publishing world is that we need to have material on hand to publish. Without you, we can't print all of this interesting and educational material!

SID: Study Cycle 24, Don't Just Use It

This VLF receiver system automatically logs received-signal data and displays it on your computer screen.

Hams are eagerly awaiting the arrival of sunspot Cycle 24 and the anticipated improvement in the marginal band conditions that we have endured the past few years. Instead of just using Cycle 24 and the improved ionospheric conditions, why not expand your knowledge of the ionosphere by joining a small group that is monitoring and studying the ionosphere through simple VLF receiver systems? Monitoring the ionosphere is also an excellent science activity for schools, and what is described below would make not only a novel conversation piece in your shack for eye-ball QSOs and stimulate conversations during your on-the-air QSOs, it also would make an excellent science fair project.

Background

The Earth's ionosphere refracts, or bends, radio waves and allows hams to talk over great distances well beyond the visible horizon. The ionosphere reacts strongly to the intense X-ray and ultraviolet radiation released by the Sun. This radiation strips the outer electrons away from their parent gas atoms, which make up the atmosphere, creating a region of ions that refract some radio waves while absorbing others depending on the wavelength and arrival angle of the wave. A somewhat more simplistic model of the ionosphere would be to consider that region of ions as forming a reflecting surface, or mirror, which returns some of the radio waves to Earth. Understanding the mechanics of the ionization of the ionosphere and how it affects the radio frequencies we use is part of the fun and mystique of the hobby. During significant solar events, where unusual radiation levels are released, however, there can be dramatic and sudden changes in the ionization of the ionosphere that disrupts radio communications. These significant and

sudden solar events are called sudden ionospheric disturbances, or SIDs.

Very low frequency (VLF) radio waves are partially refracted and partially absorbed by the lowest region of the ionosphere (the D region), which begins approximately 40 km above the Earth's surface. Using a receiver to monitor the signal strength from distant VLF transmitters, and noting unusual changes as the waves return from the ionosphere, you can directly monitor and track SIDs. This method of observation takes advantage of signals from several powerful transmitters operating in the VLF band between 16 kHz and 24 kHz. These transmitters are used to communicate with submarines that are underway. Some of these sources operate more or less continuously and offer a good stable radio wave point source. A partial list of VLF stations and frequencies given are in Table 1.

The SID Receiver Station

The construction and operation of a SID receiver station is well documented by various groups engaged in monitoring the ionosphere.¹ In this article I will touch on the bits and pieces that I put together to make a SID receiver system and add to the discussion a unique interface that stores collected data (to preclude tying up a computer all day long) and then dumps the stored data to a computer running Microsoft *Excel* for display using

¹Notes appear on page 9.

Table 1
VLF Stations and Frequencies

Cutler, ME	24.0 kHz
Jim Creek, WA	24.8 kHz
LaMoure, ND	25.3 kHz

a free software macro. This receiver can be easily and affordably duplicated so that you, or your local school, can begin monitoring Cycle 24.

Figure 1 is an overview of the SID receiver. A photo of the actual SID receiver set-up is shown in Figure 2. The receiver is mounted on an interior wall of my house, like a picture. Follow along with the block diagram as the individual components of the receiver are described.

Antenna

The antenna is a capacitor tuned, inductively coupled loop antenna.² The sides of the loop antenna are approximately 18 inches. The capacitor tuner is made of a bank of 100 pF and 1000 pF capacitors connected in parallel or series. They are switch-selected and connected to the loop of 125 turns of no. 26 magnet wire. See Figure 3. The capacitor bank allows 50 pF capacitance steps between 50 pF to 4000 pF. This is more than enough range to tune the loop antenna to the desired receiving frequency. An inductive loop of approximately 25 turns of no. 26 magnet wire is connected to the receiver. As mentioned in the on-line documentation, I experienced some adverse detuning of the receiver while trying to tune the antenna, and the inductive loop took care of that problem.

VLF Receiver

The receiver design is called the Gyrator.³ Far Circuits produces some circuit boards for the three variants of the Gyrator.⁴ I used the Gyrator II variant because the circuit is improved over Gyrator I, but I didn't want the ADC features that were included in Gyrator III. I modified the board and circuit slightly. Figure 4 shows the receiver board. I drilled a hole in the board and installed a BNC connector for an antenna jack. I used multi-turn potentiometers for the tuning and volume

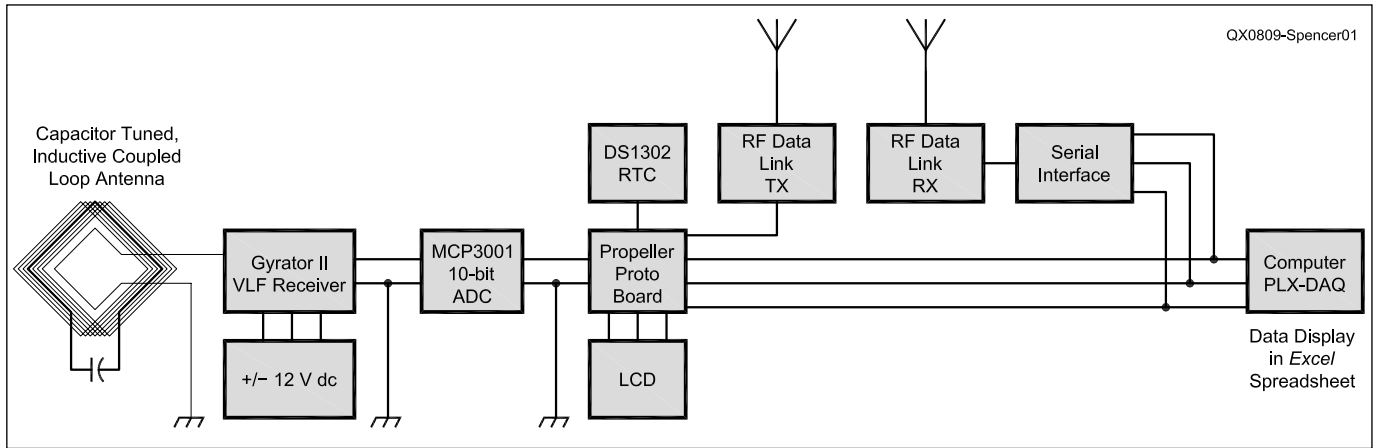


Figure 1 — This block diagram illustrates the operation of the SID VLF receiver, data collection and computer interface circuits.

controls. Tuning of the Gyrator receiver is very sensitive and the multi-turn potentiometer helped get accurate and stable reception on the desired frequency. Since the Gyrator II circuit is based on high gain op-amps, the circuit has a tendency to self oscillate. The volume control multi-turn potentiometer helped to keep the circuit under control. Finally, I changed the receiver output filter capacitor from the specified 10 pF to 100 pF to help alleviate the rapid amplitude changes that were caused by receiving weak signals. Amplitude changes caused by SIDs are not that rapid, and I found the higher capacitance made a better data plot, at the expense of making tuning the antenna, receiver, and aiming the loop a little more difficult because of the sluggish amplitude changes.

SID Interface

The interface between the Gyrator II and the computer is unique to the designs published on the web. The center piece of the interface is the Parallax Propeller micro-controller and prototyping board shown in Figure 5. The Propeller has eight parallel programmable interface controllers (PIC) that share resources and 32 input/output (I/O) lines. The Propeller uses either the high level Spin language, assembly, or a combination of both. Parallax has a library of programming objects for various display, keyboard, and mouse devices just to name of few. This prototyping board is reasonably priced, and has a large prototyping area. It has all the voltage regulation and communication ports needed for the basic operation and programming of the Propeller.

The board is populated with a 10-bit analog to digital converter (ADC) that converts the signal strength output of the receiver into digital values between 0 and 1023 (equal to 0 and 5 V). A real-time-clock device with battery backup is also added to the board.

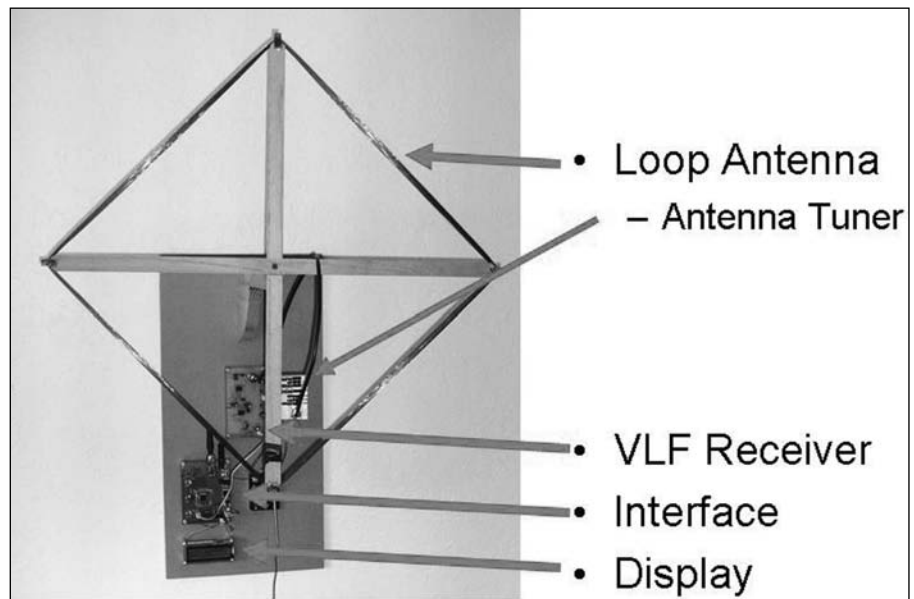


Figure 2 — This photo shows the loop antenna and receiver system mounted on the wall of the author's house.

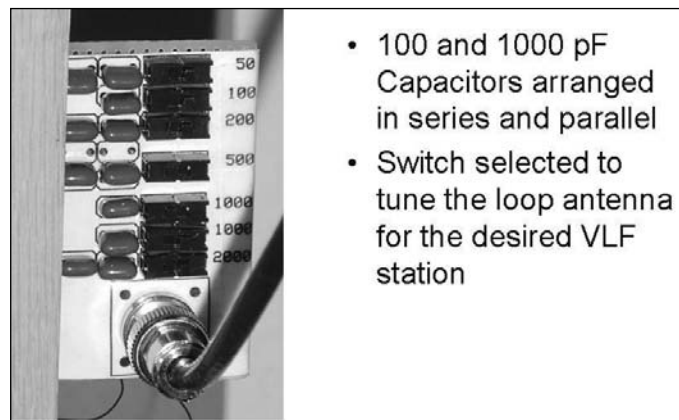


Figure 3 — Here is a close-up view of the antenna tuner. Various series and parallel capacitor combinations are switched in to tune the loop antenna for the desired VLF station.

The clock provides time-stamp data. A liquid crystal display (LCD) is connected to the board to display the time and the real-time ADC value. Though the LCD is not necessary for the operation of the SID receiver, it is a convenient way to monitor the station operation when not connected to the computer. To round out the interface board, a 70 cm data link transmitter module is connected to the serial port of the board to allow the collected data to be sent to the display computer without the need for a serial cable umbilical cord. This is a convenient feature if the receiver is not co-located with the display computer.

Push button switches and indicator LEDs allow the user to select various programmed features to operate the interface. One button allows the user to use the Microsoft *Hyper Terminal* program to set the real time clock. One button allows the user to start collecting and storing time and ADC data in the RAM that is part of the prototyping board and Propeller circuit. The final button allows the user to send the stored data either over a serial cable or over the data link to the display computer. If these were not enough options, the interface also sends the collected time and ADC data in real time to the display computer while it is simultaneously recording the data.

The circuit diagram of Figure 6 details the components added to the prototyping board and the connections between the individual components and the power and I/O pin numbers of the Propeller.

Interface Software

The software that is needed to program the Propeller for this interface is available from the author by e-mail request. A ZIP file containing the current software as of press time is also available for download from the ARRL Web site.⁵ One each of the eight PICs in the Propeller are programmed to read the ADC, read the real time clock, display the time and ADC value on the LCD, and convert the time and ADC values and send them to the serial port. The program is set to begin storing data at 4 AM local time and record time and ADC value every 15 seconds until 9 PM local time. This interval covers sunrise to sunset. The collection period can be easily changed in software.

Datalink Receiver

The receive side of the data link includes a receiver module and a MAX232 based interface that converts the TTL output of the receiver module into RS232 voltage levels required by the computer's serial port. See Figure 7. The circuit diagram for the data link receiver interface is shown in Figure 8.

Display Software

On the display computer side of the system, download and install PLX-DAQ.⁶ This

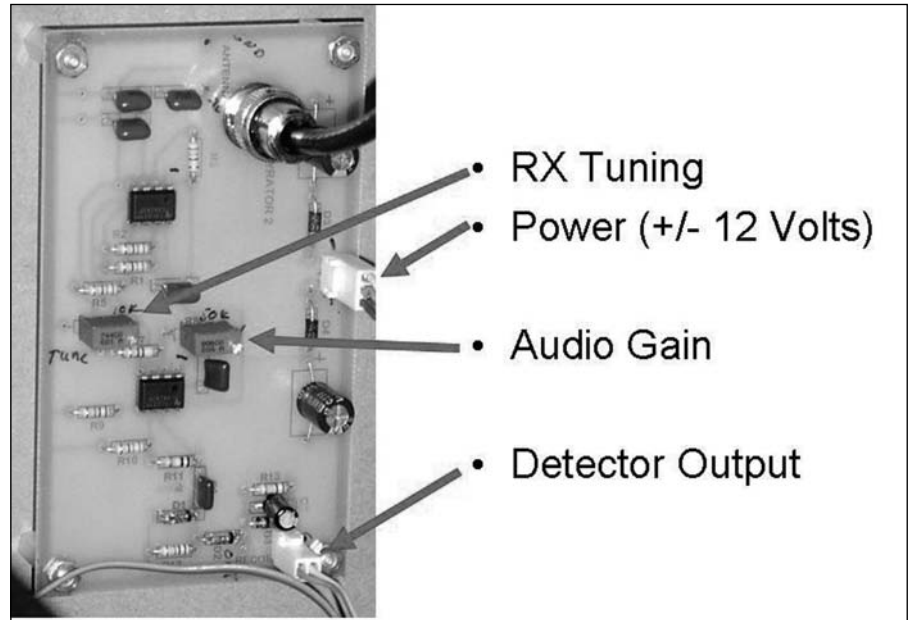


Figure 4 — This photo shows the Gyrator II receiver circuit board.

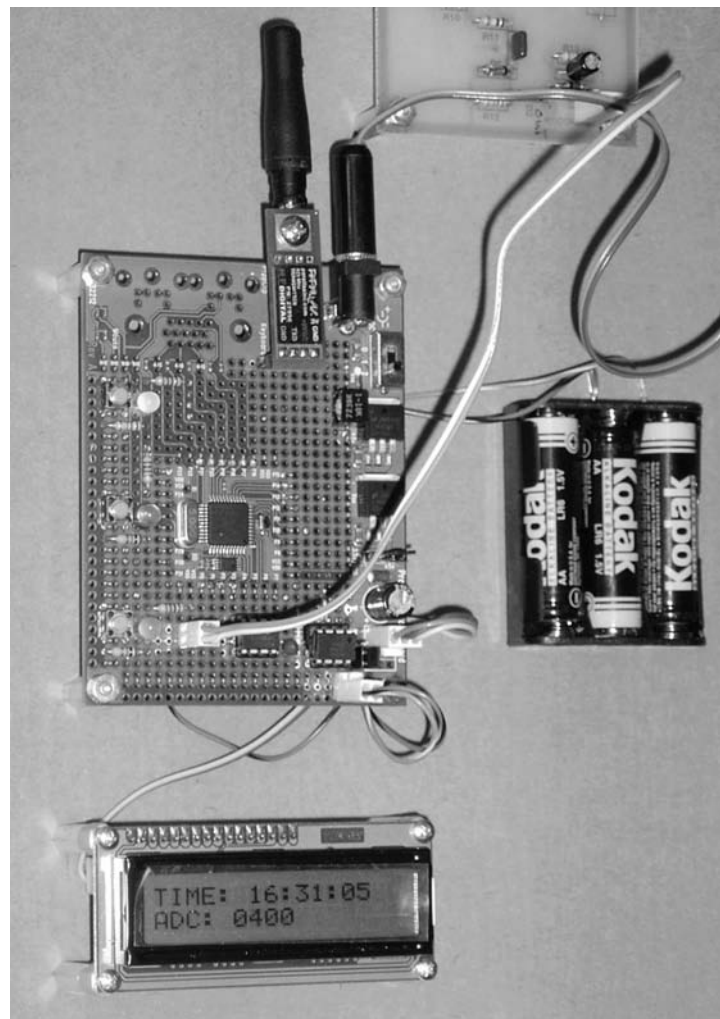


Figure 5 — Here is the Parallax Propeller microcontroller and prototyping board with an LCD and RF datalink transmitter.

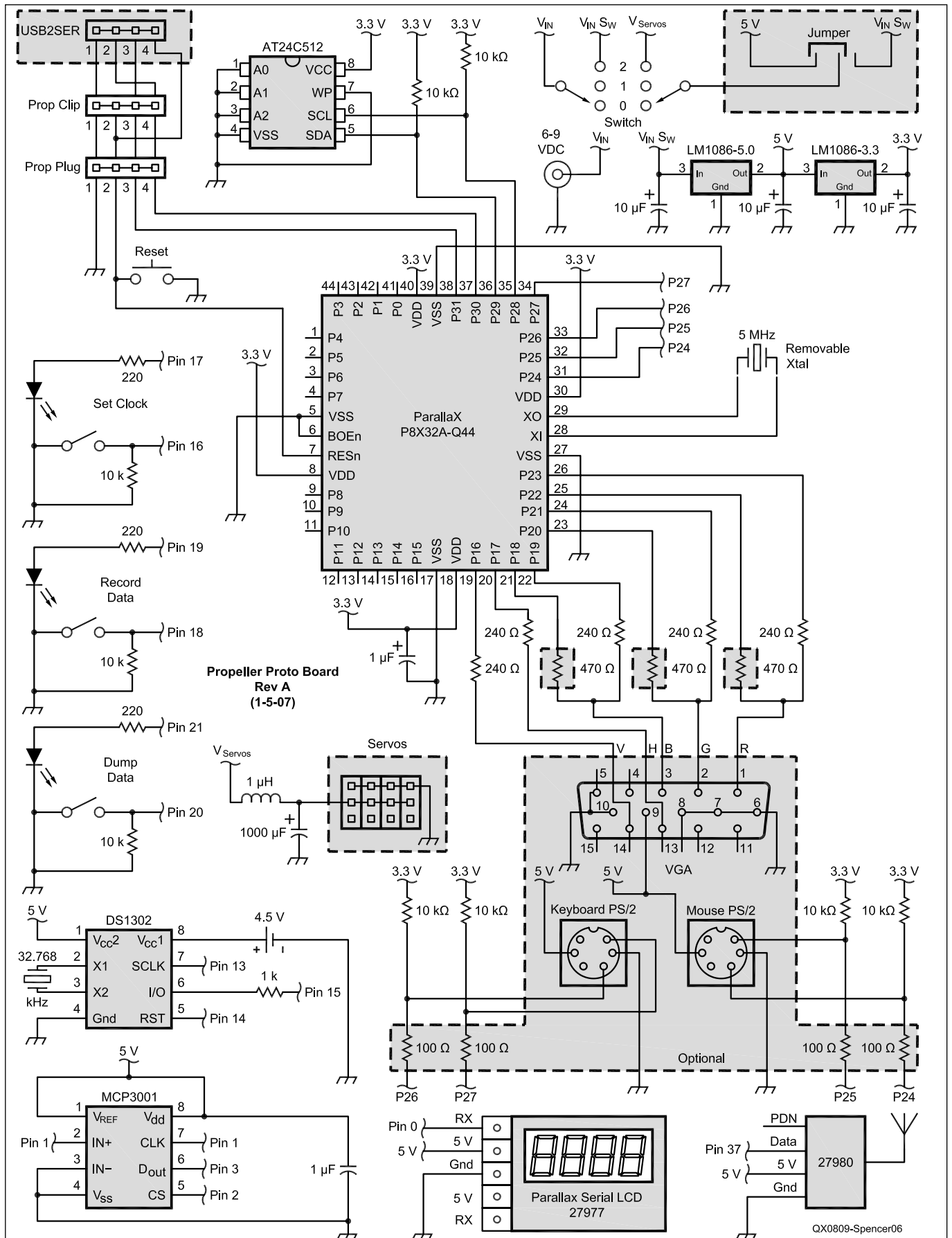


Figure 6 — This schematic diagram shows the SID interface circuit, including the Parallax Propeller prototyping board.

is a macro that is designed for use with *Excel*. The PLX-DAQ will capture the data collected and sent by the SID receiver and interface, and put the data values into the cells of an *Excel* spreadsheet. The math and graphic capabilities of *Excel* are then used to graphically display the data. The *Excel* template that is used to produce the following graphics is available from the author upon e-mail request. (This file is also included in the ZIP file available for download from the ARRL Web site. See Note 5.)

Data Interpretation

The real value of the SID receiver system is the interpretation of the graphic displays produced, and many times, more questions are raised than answered. Figure 9 is a typical collection from a quiet 24-hour period. The most obvious signal variations are those caused by the Sun's radiation. During daylight, the Sun's ionizing radiation penetrates deep into the ionosphere, producing enough free electrons at altitudes down to the D-region to allow radio waves to refract and return to Earth from that region. The air density is still relatively high at that height, though, so the electrons soon lose energy through collisions with air molecules, and consequently there is a lot of absorption too.

At night, the electrons in the lowest regions dissipate by recombination, and thus the region becomes transparent to radio waves. Refraction then takes place from regions at 80 km altitude and above, and with lower absorption due to the longer mean free path of electrons in the lower air density. Long distance paths improve, while signals

from closer transmitters may reduce.

The Sun's elevation is added to this plot. You can see that in the mornings, the ionosphere becomes illuminated when the sun is still some 10 degrees below the horizon as seen from ground level. While the sun is above the horizon, signal levels vary roughly in proportion to the sun elevation. After sunset, it takes the ionosphere nearly until midnight to recover. This pattern repeats from day to day.

The graphic in Figure 10 shows the data collection from just before sunrise until

sunset. Notice the apparent noisy signal between 1330 Z and 1530 Z (0630 and 0930 local time). This is called scintillation. The cause of this scintillation is thought to be because the "reflecting under-surface" of the ionosphere is uneven, which means that the signal arrives at the receiver via multiple paths, each of which is continually varying in amplitude and phase due to the constant fluctuation of the ionosphere. The result is chaotic random interference, and the received signal amplitude therefore constantly varies around its mean level, producing the slow

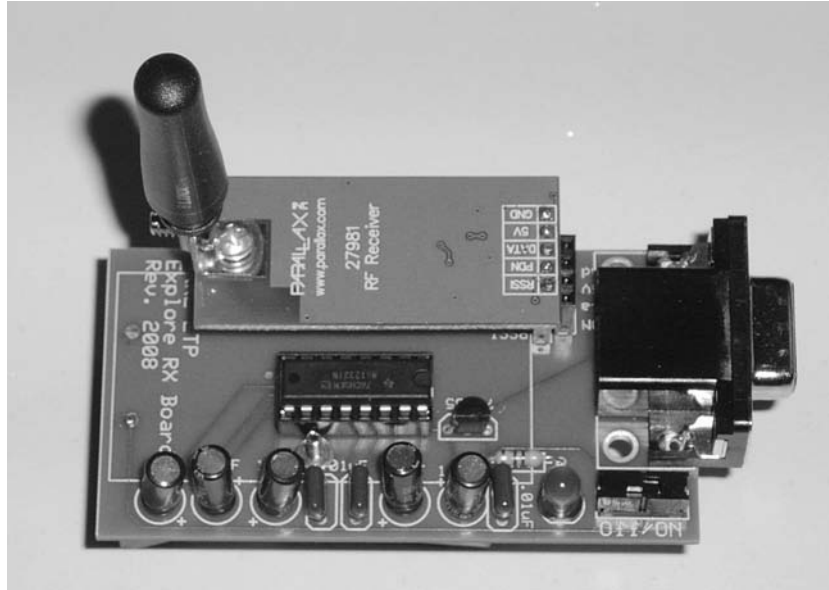


Figure 7 — The datalink receiver and serial interface connects to the display computer to feed the collected data into the computer for display in an *Excel* spreadsheet.

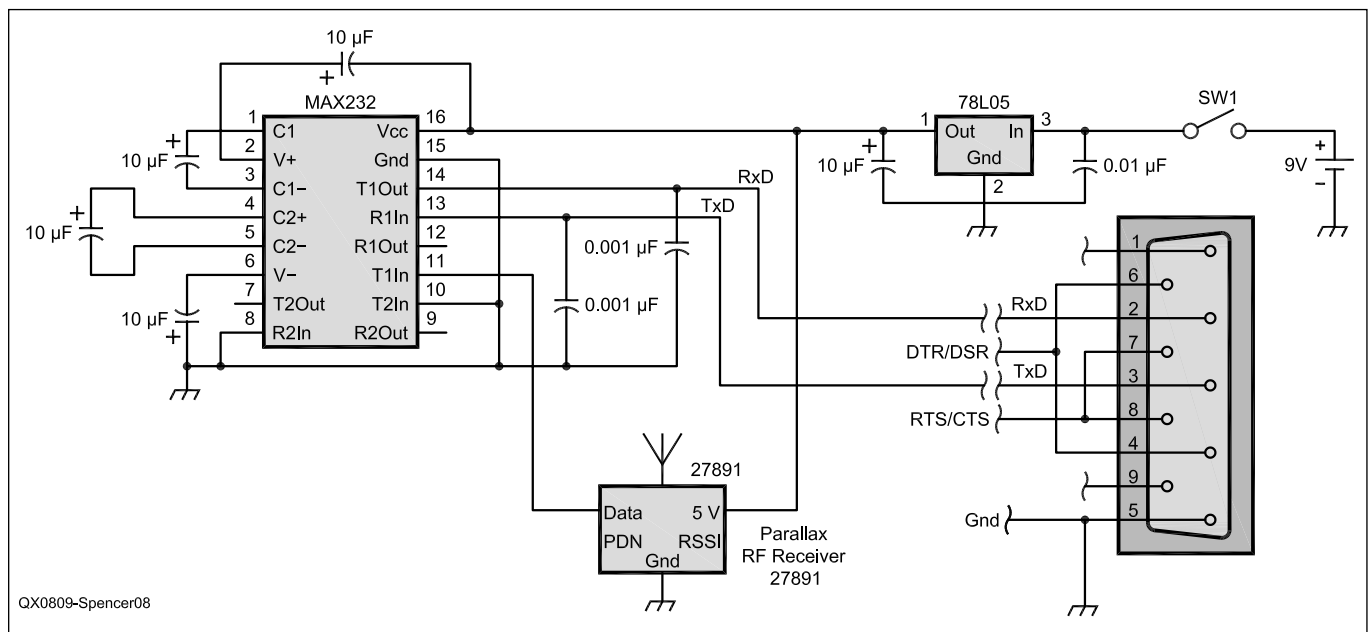


Figure 8 — This schematic diagram shows the schematic diagram of the datalink receive module and serial interface.

fading well known to HF operators, as well as more rapid variations which can readily be observed when the signal amplitude is sampled more rapidly as is done with the SID receiver.

The amount of scintillation is portrayed by the thickness of the signal trace, and varies constantly — slowly waxing and waning, presumably as patches of turbulent ionosphere drift across the path of the signal. This variation of scintillation does not repeat from one day to the next.

Notice the rapid increase in signal strength at around 0100 Z (1800 local time). I have observed similar increases over a number of days, with some minor variations in the time of occurrence. I am not sure what is causing this; if the occurrences were more random in time I would suspect the cause of the step change is the direct effect of an electromagnetic pulse associated with a strong sferic (lightening strike), which causes a localized upset in the D-region ionization, but I am not confident that this is the reason.

The graphic in Figure 11 shows another dawn to dusk collection. Notice there is scintillation just after sunrise, and a similar step change just before sunset. The numerous spikes in the late afternoon are caused by lightning strikes in the area (not necessarily in the immediate area, the storms could be hundreds of miles away).

The collection depicted in Figure 12 gave me some concern. I had made some changes to the system and it appeared to suddenly stop working! It turns out that the VLF transmitters are periodically turned off for maintenance. This was the case here.

I have not had the opportunity to witness an actual SID event, but I am ready when one occurs. Now that I have a good collection of graphics that represent quiet times, I will have a baseline for comparison when a SID occurs. A SID would cause a major disruption in the ionosphere that would show up as a major deviation from the normal curve. For instance, a solar flare would cause extra ionization in the upper regions of the ionosphere that are bathed with intense X-rays, and causing changes in radio wave propagation. This increase in ionization would penetrate down to the D-region and in turn cause an observable deviation in the measured signal strength of VLF signals as indicated by the collected data graph. The Web documentation has numerous examples of what a SID event would look like on the graphics and how to correlate the data to other sensors monitoring the Sun.^{7,8}

Conclusion

The SID receiver will give you an opportunity to explore VLF techniques as well as learn more about the ionosphere that we

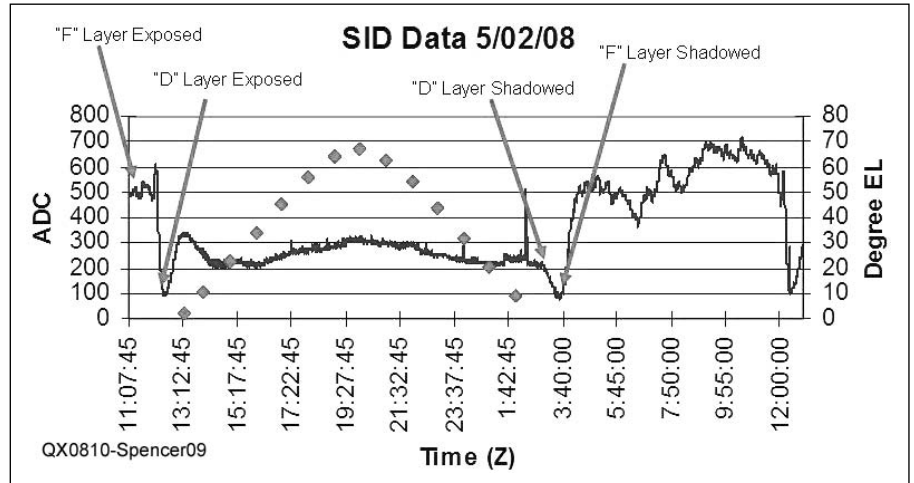


Figure 9 — A graph showing one 24 hour data collection period. You can see the propagation changes that result from sunrise and sunset, as well as the sun elevation throughout the daylight hours.

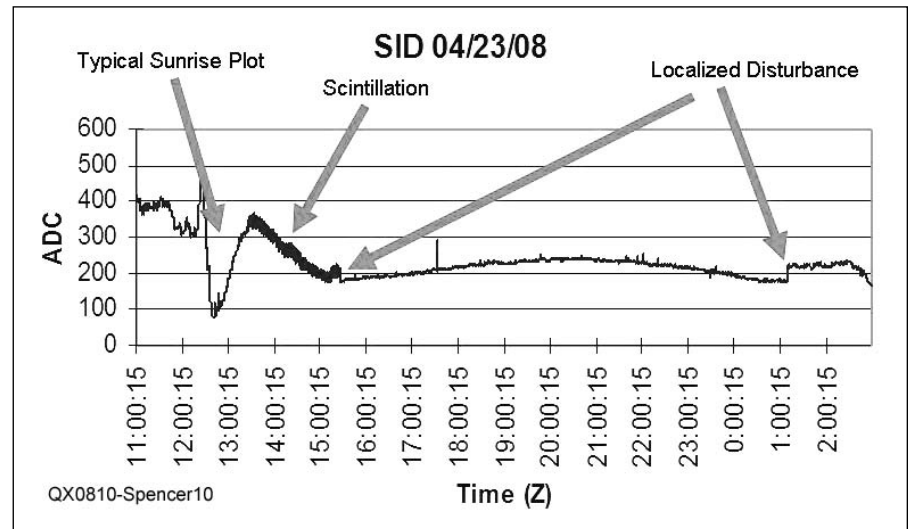


Figure 10 — This graph shows an approximately 2 hour scintillation pattern just after sunrise.

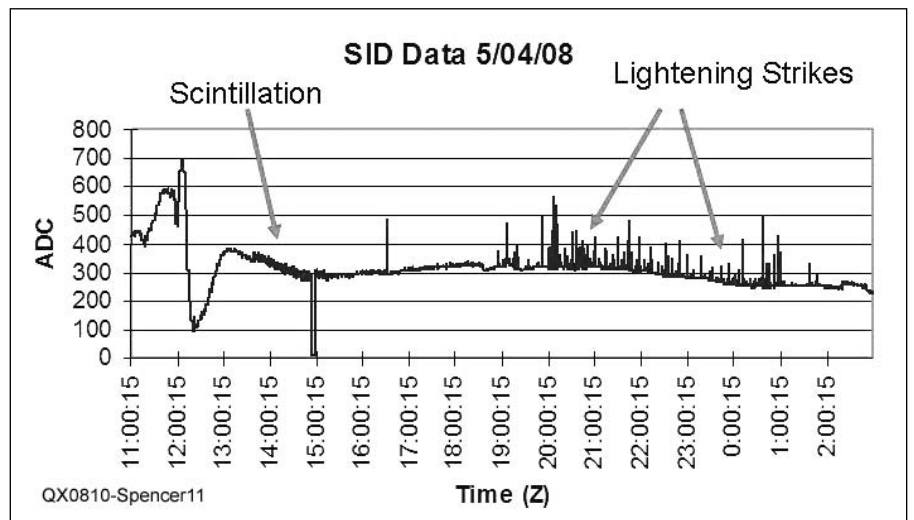


Figure 11 — Multiple lightning strikes were plotted during the afternoon, local time on this day.

depend on so much for our communications. Why not give it a try? Happy graphing.

Notes

- ¹Selected SID Information: www.aavso.org/observing/programs/solar/sid.shtml, solar-center.stanford.edu/SID/AWESOME/Goddard.pdf
- ²Antenna notes: www.aavso.org/observing/programs/solar/antenna.shtml
- ³RX notes: www.aavso.org/observing/programs/solar/minimalVLF.shtml
- ⁴Circuit Board Source: www.farcircuits.net/
- ⁵A ZIP file of the software files associated with this article are available on the ARRL Web site. These files were current as of the to-printer date. Go to www.arrl.org/qexfiles and look for the file **9x08_Spencer.zip**.
- ⁶PLX-DAQ software download: www.parallax.com/tabid/441/Default.aspx
- ⁷Interpreting Collected Data: <http://www.dcs.lancs.ac.uk/iono/data/summary/interpret/>
- ⁸Government reports of SID events for correlation: www.swpc.noaa.gov/Data/goes.html and www.swpc.noaa.gov/ftpmenu/indices/events.html

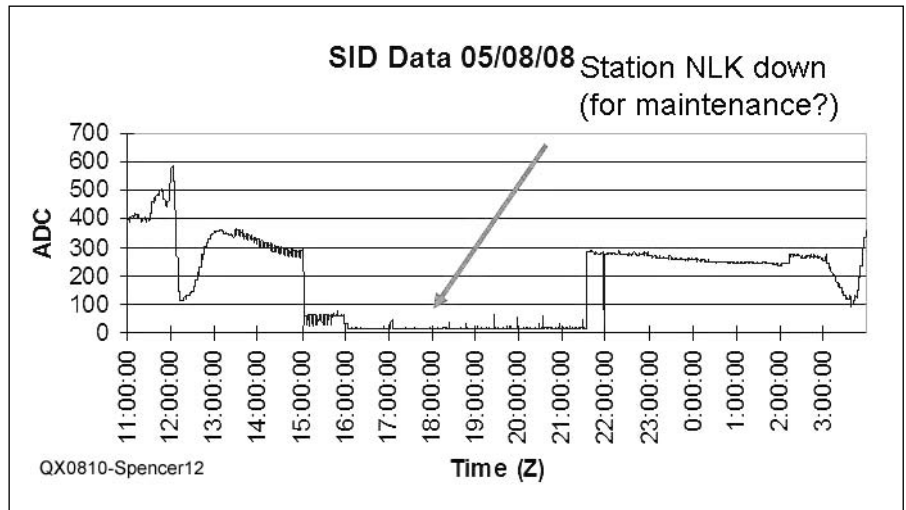


Figure 12 — If the signals seem to totally disappear, it may be because the station was shut down for maintenance, as was later confirmed to be the case on this day.

QEX

A picture is worth a thousand words...

With the **ANTENNA MODEL™** wire antenna analysis program for Windows you get true 3D far field patterns that are far more informative than conventional 2D patterns or wire-frame pseudo-3D patterns.

Describe the antenna to the program in an easy-to-use spreadsheet-style format, and then with one mouse-click the program shows you the antenna pattern, front/back ratio, front/rear ratio, input impedance, efficiency, SWR, and more.

An optional **Symbols** window with formula evaluation capability can do your computations for you. A **Match Wizard** designs Gamma, T, or Hairpin matches for Yagi antennas. A **Clamp Wizard** calculates the equivalent diameter of Yagi element clamps. **Yagi Optimization** finds Yagi dimensions that satisfy performance objectives you specify. Major antenna properties can be graphed as a function of frequency.

There is **no built-in segment limit**. Your models can be as large and complicated as your system permits.

ANTENNA MODEL is only \$90US. This includes a Web site download and a permanent backup copy on CD-ROM. Visit our Web site for more information about **ANTENNA MODEL**.

Teri Software
P.O. Box 277
Lincoln, TX 78948

www.antennamodel.com
e-mail sales@antennamodel.com
phone 979-542-7952

NATIONAL RF, INC.

VECTOR-FINDER
Handheld VHF direction finder. Uses any FM xcvr. Audible & LED display
VF-142Q, 130-300 MHz \$239.95
VF-142QM, 130-500 MHz \$289.95

ATTENUATOR
Switchable, T-Pad Attenuator, 100 dB max - 10 dB min BNC connectors
AT-100, \$89.95

TYPE NLF-2
LOW FREQUENCY ACTIVE ANTENNA AND AMPLIFIER
A Hot, Active, Noise Reducing Antenna System that will sit on your desk and copy 2200, 1700, and 600 through 160 Meter Experimental and Amateur Radio Signals!
Type NLF-2 System: \$369.95

DIAL SCALES
The perfect finishing touch for your homebrew projects. 1/4-inch shaft couplings.
NPD-1, 3 1/4 x 2 3/4, 7:1 drive \$34.95
NPD-2, 5 1/8 x 3 5/8, 8:1 drive \$44.95
NPD-3, 5 1/8 x 3 5/8, 6:1 drive \$49.95

NATIONAL RF, INC
7969 ENGINEER ROAD, #102
SAN DIEGO, CA 92111

858.565.1319 FAX 858.571.5909
www.NationalRF.com

Down East Microwave Inc.

We are your #1 source for 50MHz to 10GHz components, kits and assemblies for all your amateur radio and Satellite projects.

Transverters & Down Converters, Linear power amplifiers, Low Noise preamps, coaxial components, hybrid power modules, relays, GaAsFET, PHEMT's, & FET's, MMIC's, mixers, chip components, and other hard to find items for small signal and low noise applications.

We can interface our transverters with most radios.

Please call, write or see our web site
www.downeastmicrowave.com
for our Catalog, detailed Product descriptions and interfacing details.

Down East Microwave Inc.
19519 78th Terrace
Live Oak, FL 32060 USA
Tel. (386) 364-5529

A Great Teacher: The Crystal Set

Many have built crystal sets, but few have analyzed them in this much detail!

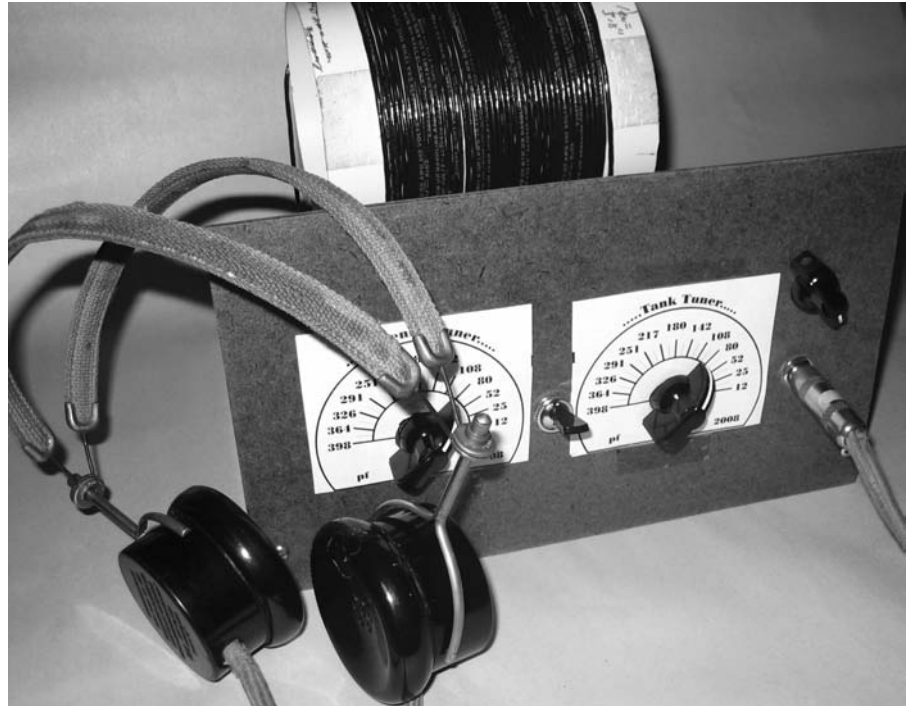
Figure 1 displays the schematic of a typical AM broadcast band crystal set system. The antenna is assumed to be an end-fed vertical or “L,” the tuner consists of a simple parallel tuned circuit featuring a multi-tapped coil, and the detector assembly uses a germanium diode with blocking capacitor and headphones. The job of the antenna is to capture the radio waves passing by. The tuner — or tank — is added to select a desired station from the many captured. The detector assembly works triple-duty, accommodating the tank, stripping audio from the AM modulated radio frequency (RF) signal, and producing audio (pressure waves). Yes; the lowly crystal set system does all that!

As TV ads are noted to say, “But wait, there’s more!” The *more* in this case is sometimes less. Unless the antenna, tank, and detector assembly are purposely designed to work together, results are often disappointing. Moving the antenna tap along the coil may not provide a good impedance match. Using small wire for the coil will limit Q, and hence selectivity. Ignoring the impedance match between the antenna-tank system and the diode can also reduce results.

Fortunately a number of architectures/systems have evolved that are capable of producing satisfying results with just a few inexpensive parts. The antenna can be inductively or capacitive-coupled to the tank; the tank coil can be wound on a low-loss solenoid or toroid form; the coil wire can be Litz or large single or multi-strand; a diode with favorable characteristics can generally be selected; and a tap on the coil or a transformer can be used to match the tank and diode with phones or other loads.

Today’s Crystal Set

I’ve picked a low-cost architecture to investigate in some detail: a crystal radio system consisting of a capacitive-coupled end-fed antenna, a solenoid coil design with moderate Q and output tap — an auto-transformer, if you will — and a germanium diode for the detector, with a resistor and ear-piece load. As you’ll see, decent crystal-set



performance can be had with such a simple design and inexpensive set of parts.

The schematic for such a set is shown in Figure 2 and a front shot of the bench model is pictured in the lead photo. At first glance the schematic looks like the one given in Figure 1, but let’s look more closely. A matching air variable capacitor, C_m , is inserted between the end-fed antenna and the tank. A fixed capacitor, C_2 , is placed in parallel with the air variable tank capacitor, C_1 , to extend tuning to the bottom of the band (525 to 800 kHz). The headphones denoted in Figure 1 are replaced by a high impedance ear piece and 32 kΩ resistor. Note that the ear piece is designated as a 25 nF capacitor.

Our approach shall be as follows: analyze and model the antenna match; design, simulate and bench test the tapped coil; investigate the antenna-tank match with the detector assembly using *Spice*; and estimate power

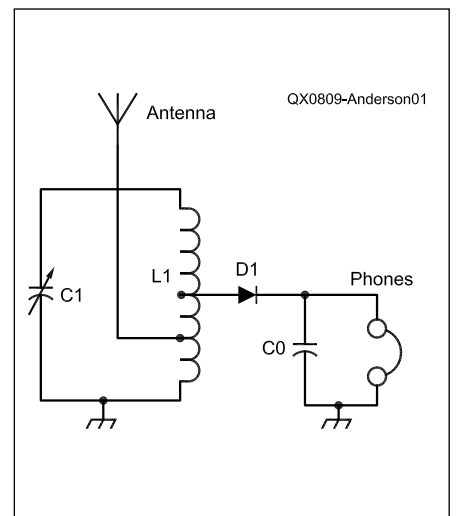


Figure 1 — This schematic diagram represents a generic crystal set

dissipation in the detector and load given varied signal levels at the antenna input.

Matching the Antenna

With inductively coupled (double-tuned) sets, one resonates the antenna with an inductor to maximize current and adjust coupling for selectivity. With this set, the object is to convert the resistance of the antenna to a very high value and connect the antenna assembly to the top of the tank.¹ Any capacitance left over will be added in parallel with the tank. As such, *we're not really matching the antenna to the tank, but striving for step-up transformer action of the voltage and resistance.*

A 50 to 150 foot end-fed antenna for the AM band can be modeled as shown in Figure 3A. It has a voltage source, an antenna and ground system resistance of 20 to 50 Ω, and a distributed capacitance of 100 to 500 pF. Using an antenna bridge, the impedance of my antenna, 30 feet up and 60 feet horizontal to the west, measured 32 Ω with 400 pF at 400 kHz and 30 Ω with 501 pF at 1 MHz.² The following analysis shows how the added series capacitor, C_m , provides the voltage step-up desired.

The voltage source, in the circuit of Figure 3A, can be converted into a current source — a source substitution — by shorting its output and calculating the resulting current. The initial impedance is then placed in parallel with the current source, as shown in Figure 3B.

$$I_a = \frac{V_a}{R_a - jX_a} \quad [\text{Eq 1}]$$

where R_a is the resistance and X_a is the capacitive reactance of the antenna model.

The series impedance of the current source can, in turn, be converted, *at one frequency*, into a parallel combination, R_{ap} and C_a , without changing the circuit operation. This substitution is called “a series-to-parallel equivalent,” using the following equations:³

$$R_{ap} = \frac{R_a^2 + X_a^2}{R_a} \approx \frac{X_a^2}{R_a} \quad [\text{Eq 2}]$$

$$X_{ap} = \frac{R_a^2 + X_a^2}{X_a^2} \approx X_a \quad [\text{Eq 3}]$$

This conversion results in the circuit shown at Figure 3C. Pushing capacitor C_a aside, let's convert the remaining current source and resistor R_{ap} back into a voltage source.

$$V_1 = I_a R_{ap} = \frac{V_a}{X_a} (R_{ap}) = V_a \frac{X_a}{R_a} \quad [\text{Eq 4}]$$

Note that the new voltage source, at Figure 3D, less any capacitance, is equal to the original antenna source times the ratio of the antenna's reactance to its resistance. Since the reactance is much larger than the resistance for the AM broadcast band, the voltage presented to the tank circuit, now including C_a , has been stepped up substantially. *In effect, the RC series circuit of the antenna acts like a voltage step-up transformer.* Rearranging Equation 4 and substi-

tuting X_a from Equation 2, we rediscover a transformer-like turns ratio:

$$\frac{V_1}{V_a} = \frac{\sqrt{R_a R_{ap}}}{R_a} = \sqrt{\frac{R_{ap}}{R_a}} = n \quad [\text{Eq 5}]$$

That leaves us with a simple voltage source, which has a resistance that can be used in simulation with the tank circuit and detector assembly.

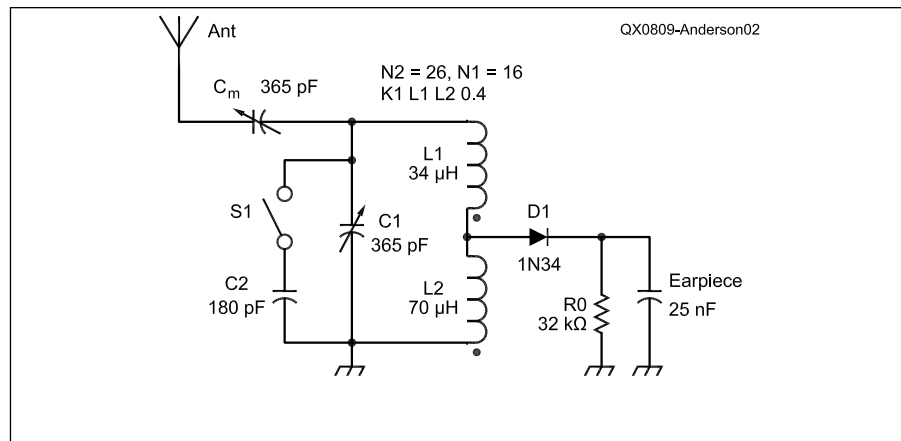


Figure 2 — This schematic diagram shows the capacitive-coupled, coil-tapped crystal set we will analyze in this article, and as shown in the lead photo.

Parts List			
Qty	Name	Value	Designations
2	variable capacitors	365 pF	Cm, C1
1	ceramic cap	180 pF	C2
1	SPST Switch		SW1
1	coil	133 μH	L1
1	germanium diode	1N34	D1
1	resistor	32 kΩ or 47 kΩ	R _o
1	ear piece	Hi-Z	CO

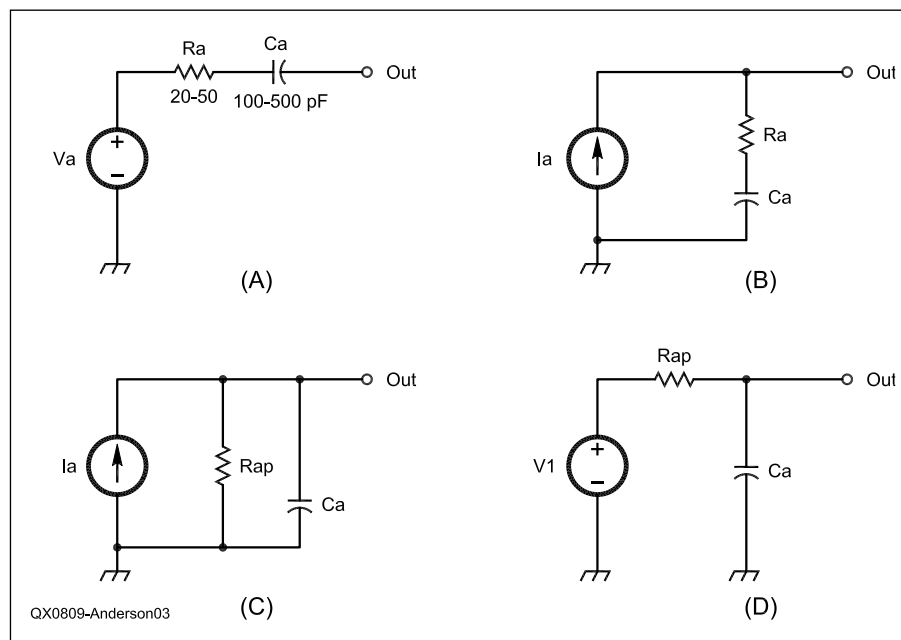


Figure 3 — Parts A through D show antenna equivalent circuits.

Building the Tank Circuit

Regarding the best energy transfer from the tank circuit to the detector assembly for weak signals, current thinking is to match the effective resistance of the tank and antenna in combination with the detector diode's crossover resistance.⁴ Intuition leads us to think that this process is like optimizing the flow of power to a resistive load driven by a battery with equal source resistance. The situation turns out to be a bit more subtle at RF, with a detector circuit involved, but let's start with this thought. We will show with the simulation example that our intuition is heuristic!

After fiddling with the design — simulating, building, and bench testing several tanks — I arrived at a workable solution for the tank circuit, given the matches desired. I can now present it as if it were a derivation (kind of like in a textbook where derived equations precede the examples).

Initially, I chose to build the tank circuit with a 140 μH coil with an output tap, an inexpensive 365 pF air variable capacitor, and a 180 pF disc capacitor, switched in to enable coverage of the band from 525 to 800 kHz. The lower inductance value somewhat avoids the problems of bunching up tuning and lowering tank Q because of using an inexpensive air variable capacitor at the top end of the band. I chose to build the coil on a thin-walled 4.2 inch diameter length of PVC sewer pipe, using No. 18 stranded wire. While Litz or solid wire provide for a higher Q, there are advantages to using stranded wire: it's cheaper, easier to wind and solder and the jacket expands the winding pitch to 0.09 inches. In addition, I chose to set the tap so that the impedance looking into the tap would match the ubiquitous 1N34 diode. This arrangement avoids the use of expensive inter-stage audio transformers, which allow diode attachment at the top of the tank circuit. You give up a bit of performance with this arrangement. With these ideas in mind, let's look at the coil.

To match the diode, we need to know its crossover resistance, R_x . While diodes vary from batch to batch and by manufacturer, let's assume a 1N34 has a saturation current of about 1000 nA, operation at room temperature, and an m factor of 1.3. Hence:

$$R_x = \frac{0.025m}{I_0} \approx 32 \text{ k}\Omega \quad [\text{Eq 6}]$$

In addition, when the coil is wound with 42 turns and tapped at 26 turns, as noted in Figure 6, the output to input turns ratio (of this auto-transformer) is

$$N = \frac{N_1}{N_1 + N_2} = \frac{26}{26 + 16} = 0.61 \quad [\text{Eq 7}]$$

This calls for an antenna and tank total resistance match of

$$R_{\text{tank}} = \frac{R_x}{N^2} = \frac{32k}{0.38} \approx 84 \text{ k}\Omega \quad [\text{Eq 8}]$$

For a simple starter set, this value is reasonable. For a high performance set, DXers would strive for 500 k Ω to 700 k Ω perhaps.

Modeling and Checking the Tank Coil

Since our coil is an air solenoid, wound on a thin form, coupling between the windings is not as tight as it would be on a ferrite toroidal core, for example. We can still model the total coil as an auto-transformer by measuring the mutual inductance between the portions of the coil on each side of the tap. Figures 4 and 5 denote the measurement setup at 580 kHz. A 4017B B&K RF generator was used to drive a launch coil with 12 turns of No. 22 wire wound on a 3.5 inch ABS form. The resulting signal was inductively coupled to the coil assembly under test.

The coil, at that time, consisted of 12 turns for L2 and 30 turns for L1, all close-wound in the same direction.

The tank circuit was resonated at 580 kHz by adjusting C1, an air variable capacitor. C1 was then disconnected and its value measured with an 810C B&K capacitance meter. Total inductance, with coils aiding (dots in same direction), was calculated to be 142.5 μH . Coil L2 was then unwound, rewound in the opposite direction (on the same form), the circuit was again resonated, C1 was measured, and the total inductance calculated to be 78.1 μH . Mutual inductance was then estimated to be:

$$M = \frac{L^2 - L}{4} = 16 \mu\text{H} \quad [\text{Eq 9}]$$

The individual inductances of the coils were then calculated, using a modified Wheeler's equation:⁵

$$L_{22} = \frac{r^2 N^2}{10Np + 9r} = 21 \mu\text{H}, \quad L_{11} = 86 \mu\text{H} \quad [\text{Eq 10}]$$

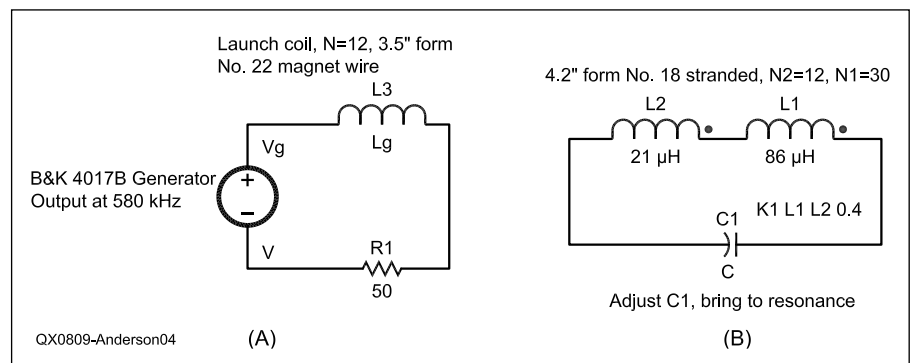


Figure 4 — These schematic diagrams show the connections for the mutual inductance test setup.

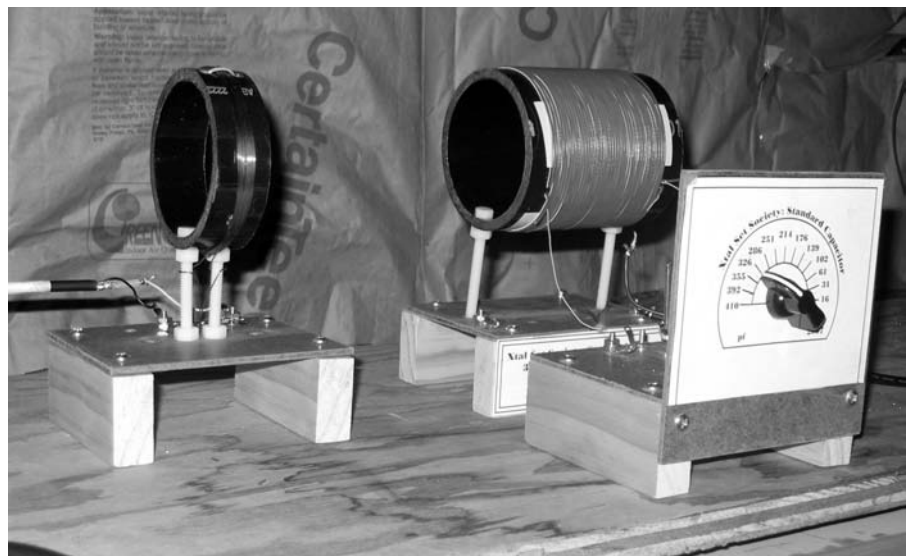


Figure 5 — This photo shows the mutual inductance test setup.

where:

r is the radius of the coil

N is the number of turns

p is the winding pitch, in this case 0.09 inches.

Hence, the coupling coefficient for the two sections is:

$$k = \frac{M}{\sqrt{L_{22}L_{11}}} = 0.4 \quad [\text{Eq 11}]$$

To check the coil model and to prepare for a full simulation of our crystal set, I carried out a *Spice* simulation, as denoted in Figure 6.⁶ I am happy to report that the results agree with the measurements made on the bench! Our coil is modeled as an autotransformer with the *Spice* declaration “K1 L1 L2 0.4” — it says that L1 and L2 are combined and have a coupling coefficient of 0.4. Note that the effective turns ratio is:

$$N = \frac{N_2}{N_1 + N_2} = 0.28 \quad [\text{Eq 12}]$$

As noted in Figure 6B, a frequency sweep simulation of the circuit is in agreement, stepping the primary voltage down from ~53 to 15 mV at 580 kHz, a ratio of 0.283. This is simply another confirmation of Clarke’s derivation that high-Q RF tank circuits, at the point of resonance when properly tapped, act like a transformer.⁷ Hence, the load seen by the transformer primary is:

$$R_{\text{primary}} = \frac{R_{\text{tap}}}{(N)^2} = \frac{6.53 \text{ k}\Omega}{(0.28)^2} = 83.3 \text{ k}\Omega \quad [\text{Eq 13}]$$

This is further confirmed by calculating the tank Q from the sweep graph, Figure 6B:

$$Q = \frac{f_0}{\text{bandwidth}} \approx \frac{580 \text{ kHz}}{7 \text{ kHz}} = 82 \quad [\text{Eq 14}]$$

Therefore, the *effective* parallel resistance of the tank circuit, with the given load is:

$$R_p = QX = Q(2\pi f_0 L) = 82(2\pi \times 0.580)(140) = 41.8 \text{ k}\Omega \quad [\text{Eq 15}]$$

Clearly, the Q has been halved by the effective reflection of 6.5 kΩ of resistance from the secondary into the primary, in parallel with its inherent antenna and coil losses modeled by ~82 kΩ. Flipping it around — reflecting the primary impedance into the secondary, the diode “sees” roughly 6.5 kΩ.

Thinking about “Today’s Crystal Set,” shown in Figure 2, if we wish to use a 1N34 detector that has a crossover resistance of about 32 kΩ, we’ll have to change the turns ratio of our example above. We need to match (or transfer to the primary if you will) 32 kΩ to 80 kΩ. A turns ratio of 0.62 does the trick.

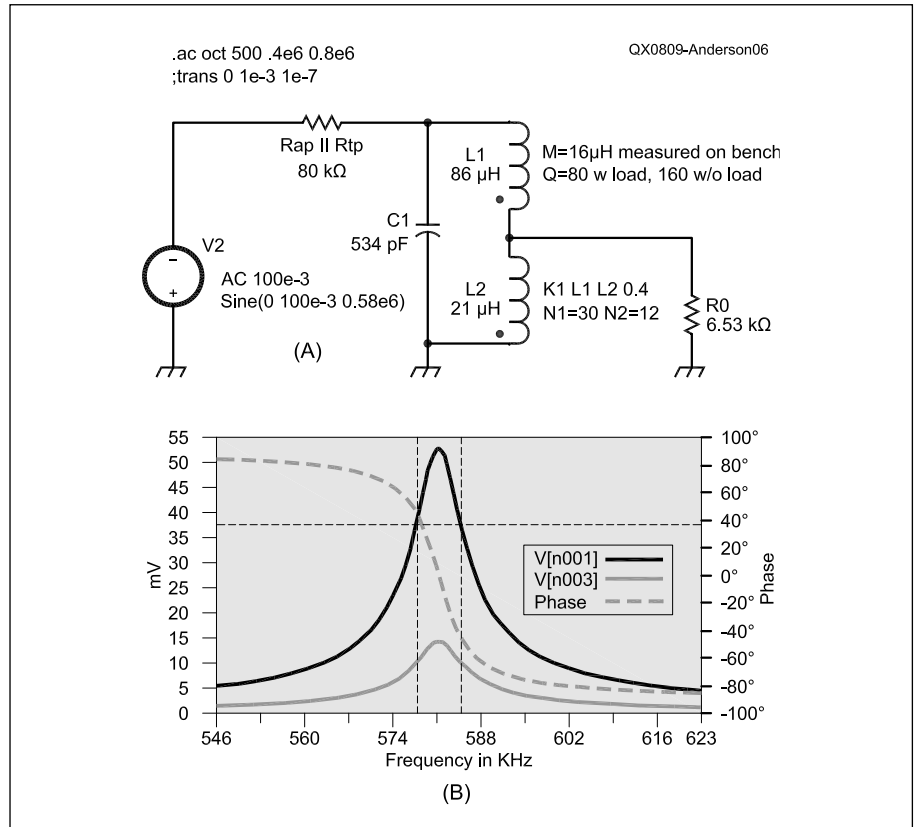


Figure 6 — Part A shows the *Spice* model for the tuned circuit autotransformer. Part B shows the *Spice* output results of the tank Q measurement.

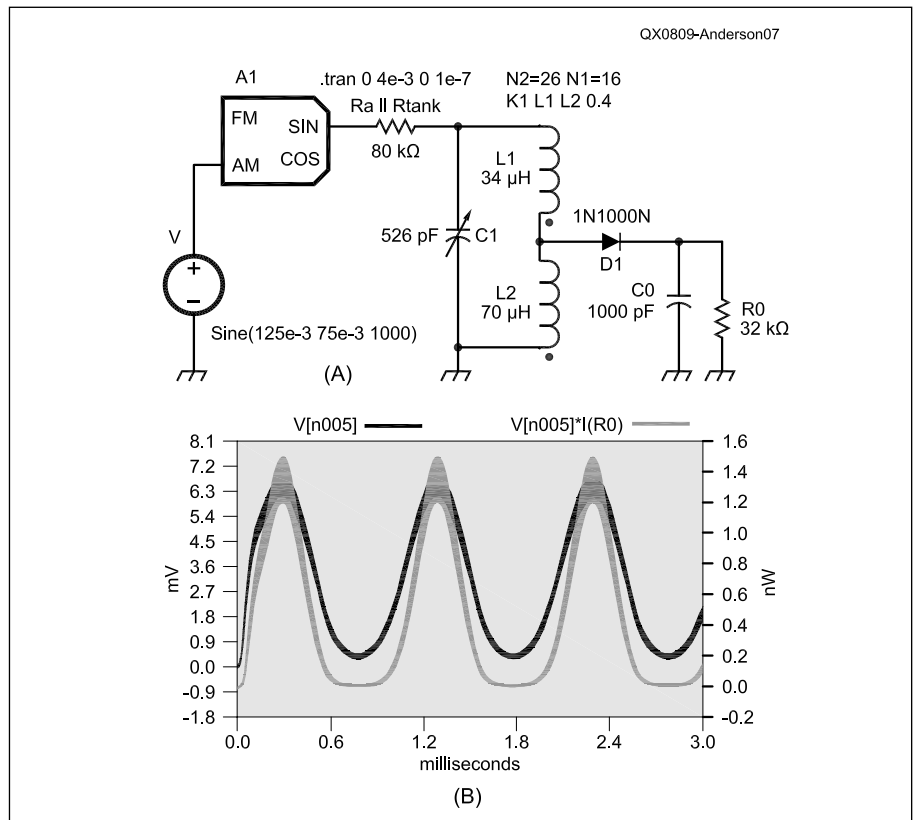


Figure 7 — Part A shows the *Spice* crystal set circuit simulation. Part B shows the *Spice* output waveform and power dissipation results.

Simulating the Full Crystal Set

We've finally arrived at the best part — simulating the full crystal set. The *Spice* schematic for doing so is shown in Figure 7A, with the results shown in Figure 7B. Let's do a bit of housekeeping first. Sources V and A1 combined simply generate an AM signal and together with resistor Ra replace our antenna and ground source presented in Figure 3D. Our tank circuit has been updated to provide an input-to-output turns ratio of 0.61. The 1N1000N diode is fictitious in name; I simply give my *Spice* diode models a part number that names their saturation current value. You can't buy a 1N1000N diode. As noted earlier and in Table 2, the crossover resistance of a diode with an I_o of 1000 nA has a crossover resistance of about 32 k Ω . As per our earlier discussion, the turns ratio now provided will reflect a resistance of 32 k Ω into the primary of the tank of about 80 k Ω , matching the loss there. We'll now run a series of simulations to show that, approximately, *the maximum peak power of the audio signal obtained at the output occurs when the total antenna and tank resistance matches the crossover resistance of the diode, given that the output load is roughly the same value, too.*

Voltage source V in Figure 7 sets the RF carrier level, modulation level, and audio frequency. For example, the directive "sine(125e-3 75e-3 1000)," noted on the drawing, sets the RF level at 125 mV_{peak}, the modulation at 75 mV_{peak}, with an audio frequency of 1000 Hz. The ratio of the RF and audio levels sets the modulation percentage; hence, 75/125 provides for 60%. This statement is varied to produce more or less drive. Source A1 determines the RF frequency and is set to 580 kHz. You may wonder why I chose 580 kHz instead of the usual standard of 1 MHz. It's simply because WIBW, a 5000 W station 20 miles from me, broadcasts on 580, and can be used as a real comparison to the simulation.

A tabulation of five simulation runs is noted in Table 1. Each run notes the drive level at the tap output and resulting audio voltage, peak power across the load, R_o , in nW and dBm. With each succeeding run the drive voltage is reduced by 1/2. The first three entries are certainly very strong signals, producing loud copy in my Baldwin headphones or a Hi-Z ear piece. Once the tap voltage level drops below 74 mV_{p-p}, listening level begins to drop. Note that the output voltage, V_o , at first drops by 1/2 in concert with the tap voltage. At a diode input drive of 75 mV_{p-p}, V_o drops to 1/3, from 74 to 21 mV_{p-p}. In the last entry, V_o drops from the last entry to near 1/4, from 22 to 6 mV_{p-p}. Peak power out, of course, drops even faster. With the tap at 37 mV_{p-p}, peak output is at -58 dBm. Our basic set gives up at about this point; at least I noted that when using Baldwin phones and a matching Bogen

Table 1
RF Voltage In — Power Out

V_{tap} (mV _{p-p})	V_o (mV _{p-p})	Peak Power Out (nW)	Average Power Out (nW)	Peak Power Out (dBm)
600	350	6300	2900	-22.01
300	157	1150	463	-29.39
150	74	170	62	-37.70
75	21.5	18	6.3	-47.45
37	6.5	1.4	4.7	-58.54

Table 2
Tank — Diode Matching for Maximum Power

I_o (nA)	Peak Power Out (nW)	Rx at Peak (k Ω)	Power Out (nW)
600	1.06	54	1.06
700	1.28	46	1.28
800	1.37	41	1.37
900	1.44	36	1.44
1000	1.7	33	1.7
1100	1.74	30	1.74
1200	1.74	27	1.74
1300	1.7	25	1.7
1400	1.7	23	1.7
1500	1.63	22	1.63
1600	1.5	20	1.59

transformer in place of the 32 k Ω resistor. In comparison, very high impedance DX sets report minimum discernable signal levels at around -67 dBm or lower. (See Note 4.)

We finish by looking at what happens when the resistance at the tap (from the antenna and tank circuit) does not match the crossover resistance of the diode installed. I simulated this by leaving the tank circuit and load constant and substituting various diode models, 1N1000N, 1N900N, and so on. These results are tabulated in Table 2. Note that the match is very broad except when diodes with an Rx much larger or smaller than the antenna tank resistance are used. *Maximum power at the load, R_o , is noted as 1.7 nW when the diode's resistance of about 32 k Ω matches that of the tap output and load.*

We've just brushed the surface here. The *Spice* simulation circuit of Figure 7 could be used to generate volumes of data. We could look at the relatively high currents circulating in the tuned tank circuit. We could crank up the Q of the tank and run the simulations again, thereby investigating weak signal reception. We could investigate what the current spikes in the diode look like at the peak of each RF cycle for heavy and weak signal drives. We'll save these investigations for another time.

Notes

¹Ed Richley, "The Design of Unpowered AM Receivers Using Detectors Made From Rocks (Part 2 of 3)," *The Xtal Set Society Newsletter*, Vol 5, No. 2, March 1, 1995. Available at www.midnightscience.com.

²Phil Anderson, "XS-800 Antenna Measurement Bridge," www.midnightscience.com/article2.html.

³H. Skilling, "Electrical Engineering Circuits," "Series & Parallel Equivalent Circuits," p 97, Wiley, 1959.

⁴B. Tongue, <http://www.bentongue.com/>.

⁵"Inductance of a Single Layer Solenoid," www.midnightscience.com/formulas-calculators.html.

⁶There are many variations of the *Spice* circuit simulation program. One convenient version, available for free download is the Linear Technology *LTSpice*. See www.linear.com/designtools/software/index. JSP. The author's *Spice* files are available for download at the ARRL Web site. Go to www.arrl.org/qexfiles and look for the file 09x08_Anderson.zip.

⁷Kenneth Clark, *Communication Circuits: Analysis and Design*, p 38, Addison-Wesley, 1978.

Phil Anderson, W0XI, was first licensed as a teenager in 1953 as KN0HSB. He graduated from the University of Kansas in 1963 with a BSEE, and then earned an MSEE from Syracuse University in 1967. He added a DocEng degree from the University of Kansas in 1971. He was an engineer at IBM in Poughkeepsie, NY between 1963 and 1969. Phil founded Kantronics in 1971, and retired in 2002. He founded the Xtal Set Society in 1991, and is still playing with crystal sets!

In 1969 Phil took (and passed) the Novice through Amateur Extra Class license exams in one sitting at the FCC Field Office in Kansas City. He is co-inventor of the GTOR communications protocol and co-designer of the Kantronics KPC-2, KPC-3, KPC-4, KPC-9612, KAM, KAM-XL and several pager controllers as well as 144, 220 and 440 MHz RF amplifiers. His current technical interests include ultrasonics, QRP, powerless devices, mm waves and radio astronomy. Phil is also a proud grandfather!



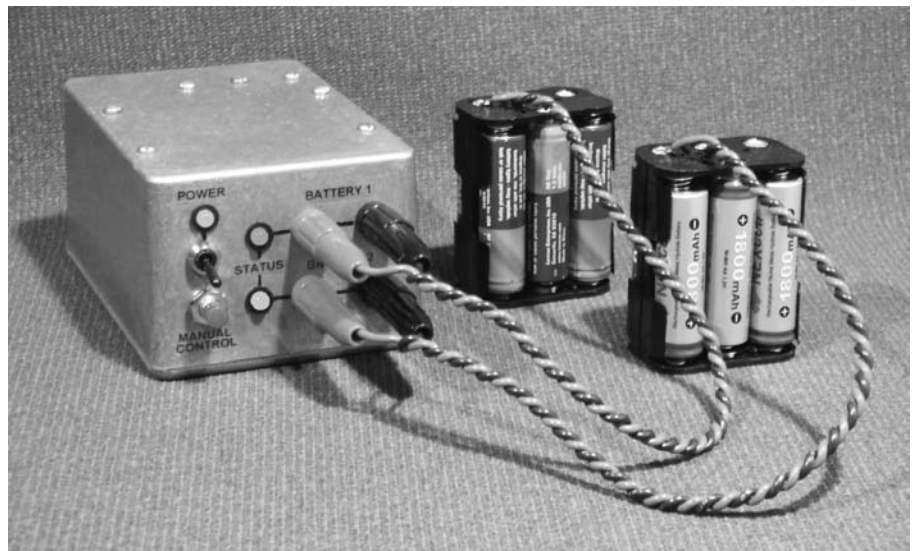
The Rechargeable Battery “Cycler”

With this computerized periodic discharger/charger, you will always be ready for action...and for an emergency!

I am a sporadic handheld radio user. I find my dual-band radio mostly useful during the few hamfests I attend every year. I used to recharge the batteries the week prior to an event. I have, however, been caught far too often with my handheld radio battery packs in a depleted state when I needed them for unplanned activities. Even worse, I was never truly ready for an emergency situation requiring portable Amateur Radio communications. Are you ready to deploy? Always?

Nickel cadmium (NiCd) or Nickel metal hydride (NiMH) rechargeable cells are very economical and provide a lot of energy per weight, but they have drawbacks. The biggest issue is shelf life. These cells can lose up to 50% of their capacity within a month after recharging. Another concern is the now infamous “memory effect.” Whether the naming is appropriate or not, whether the effect is real or exaggerated, most manufacturers still recommend a regular discharge/charge cycle to maintain the energy storage capabilities. These rechargeable battery characteristics are well documented, and are worth reading about.¹

Looking around on the market, I could not find a device that would do what I needed: an autonomous and periodic discharger/charger for my battery packs. Once again, if you can’t find it, design it! So I have designed and constructed a discharger/charger circuit that I call the Rechargeable Battery “Cycler.” The Cycler will periodically discharge and recharge nickel cadmium (NiCd) or Nickel metal hydride (NiMH) battery packs so that they are always fresh and ready to deliver. A few years ago, I elected to use AA-size cell holder packs made specifically for my radio. AA-size rechargeable batteries are easier and cheaper to replace than custom-made battery packs. Whether you use sealed custom made battery packs that fit your handheld radio or regular rechargeable cells, this charger will do the job right.



Here is a list of key features of the design:

- It is a microcontroller-based approach, which brings a lot of features and flexibility into the unit. The device can easily be reconfigured when the battery specifications change.
- The Cycler supports one or two battery packs with distinctive configuration settings for either pack.
- The Cycler is designed to accommodate NiCd or NiMH battery cells of capacity C from 500 mAh to 5000 mAh, assuming the recommended C/10 charging current for 10 to 12 hours is used.
- The cycler can accommodate one to ten cells per battery pack.
- The firmware also offers a battery restoration mode, during which the batteries are discharged and recharged a number of times without any idle period between the cycles.
- A Windows-based software tool allows the user to configure the Cycler in a matter of minutes via an RS-232 link. After con-

figuration, the personal computer (PC) can be disconnected. All settings are saved in nonvolatile Flash memory.

- When left connected to the Cycler, the Windows tool provides discharge and charge data logging capabilities. This allows voltage-curve plotting using the built-in graph engine or using a third-party spreadsheet program.
- The following parameters can be configured via the Windows tool for both batteries: number of cells, battery capacity, end-of-discharge voltage, discharge current, charge current, charge duration, overall cycle period and number of conditioning cycles.
- All the electronics are integrated onto a small double-sided circuit board.

I could go on with the list of features, but instead let me explain how the battery cycler system works.

System Description

Figure 1 shows the system’s circuit schematic. The circuit is fairly simple and easy

¹Notes appear on page 21.

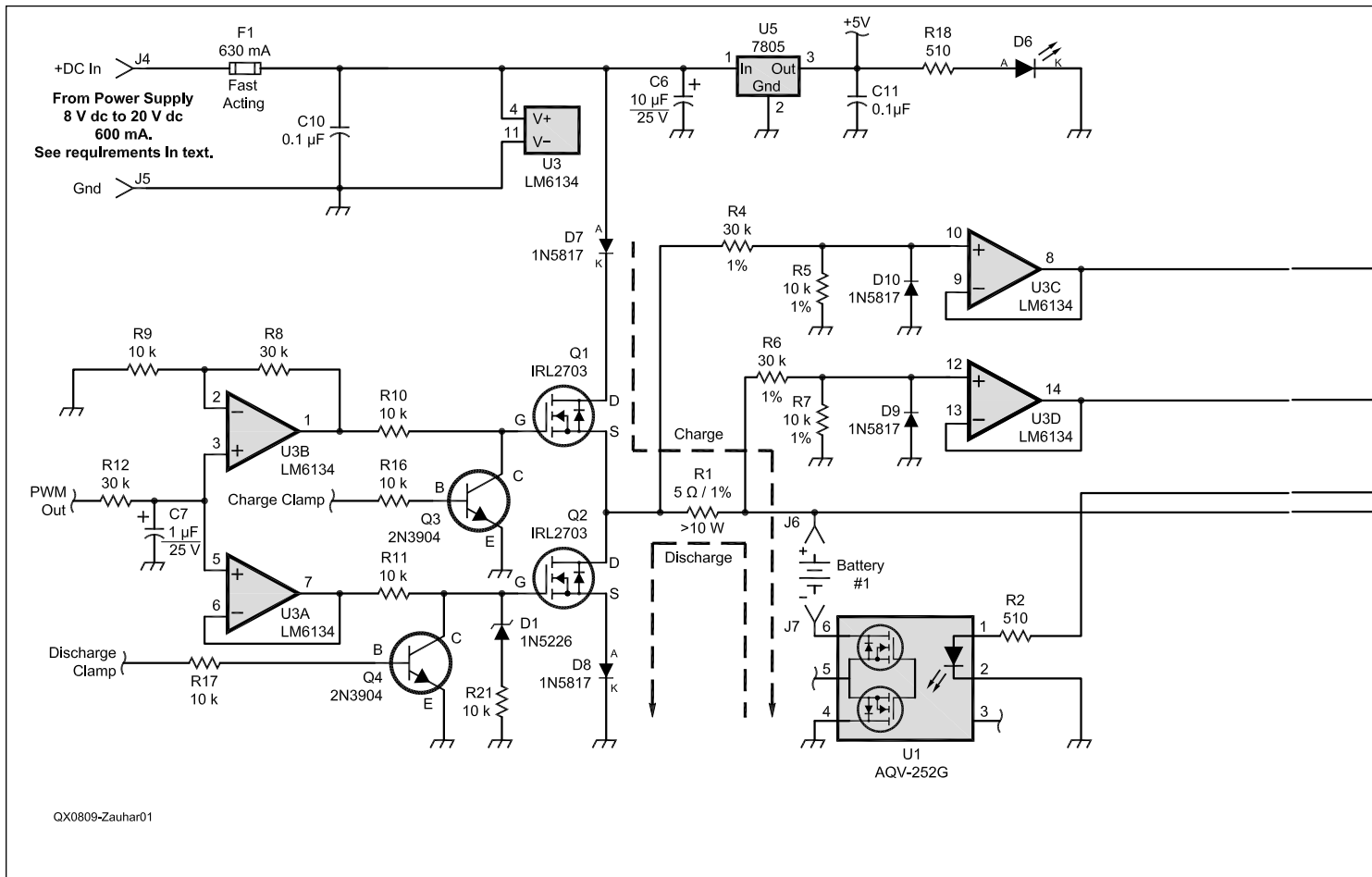


Figure 1 — Circuit schematic of the Rechargeable Battery “Cycler.”

Parts List

Component Reference

- C1, C8, C9, C10, C11
- C2, C3, C4, C5, C7
- C6
- D1
- D2, D3, D6
- D4, D5, D7, D8, D9, D10
- F1
- PB1
- Q1, Q2
- Q3, Q4
- R1
- R5, R7, R9, R10, R11, R16, R17, R21
- R4, R6, R8, R12, R13
- R2, R3, R14, R15, R18, R19, R20
- U1, U2
- U3
- U4
- U5
- U6
- Sockets for U1, U2
- Socket for U3
- Socket for U4
- Socket for U6
- Insulation kits for Q1 and Q2
- Enclosure

Description

- 0.1 μ F, 25V or higher, radial
- 1 μ F, 16V or higher, electrolytic, radial
- 10 μ F, 25V or higher, electrolytic, radial
- 1N5226B, 3.3 V Zener Diode, DO-35 package
- Bi-color (Green-Red) LED, 5 mm, two leads.
- 1N5817 Schottky diode, DO-41 package
- 0.630 A Fast Acting fuse. “Pico II”, Axial
- Momentary push button, SPST, Normally Open
- IRL2703 MOSFET Transistor, TO-220 package
- 2N3904 NPN Transistor, or equivalent
- 5 Ω , 1%, 15 W, TO-220 package
- 10 k Ω , 1%, 1/4 W, axial
- 30 k Ω , 1%, 1/4 W, axial
- 510 Ω , 1/4 W, axial
- Panasonic AQV-252G family Solid-State Relay, DIP-6 package.
- LM6134 Quad Operational Amplifier, DIP-14
- Microchip PIC18F1220 micro-controller, DIP-18 package, programmed part. See Note 3.
- 7805 Voltage Regulator, TO-220 package
- MAX232 Conversion chip, DIP-16 package
- IC Socket, 6-pin, 0.3” spacing, low profile
- Shorten socket with heated hobby knife blade.
- IC Socket, 14-pin, 0.3” spacing, low profile, optional
- IC Socket, 18-pin, 0.3” spacing, low profile, recommended
- IC Socket, 16-pin, 0.3” spacing, low profile, optional
- Thermally conductive, electrically insulated pad, plus hardware.
- Hammond 1590T Aluminum Enclosure, suggested

Part Number

- Digikey: 399-4329-ND or equiv.
- Digikey: P1196-ND or equiv.
- Digikey: P1176-ND or equiv.
- Digikey: 1N5226B-TPCT-ND or equiv.
- Digikey: 160-1038-ND or equiv.
- Digikey: 1N5817-TPCT-ND (lot of 10) or equiv.
- Digikey: F2312-ND or equiv.
- Digikey: EG2015-ND or equiv.
- Digikey: IRL2703PBF-ND
- Digikey: 2N3904-APCT-ND (lot of 10) or equiv.
- Digikey: MP930-5.00F-ND
- Digikey: P10.0KCACT-ND (lot of 10) or equiv.
- Digikey: P30.0KCACT-ND (lot of 10) or equiv.
- Digikey: P510CACT-ND (lot of 10) or equiv.
- Digikey: 255-1791-5-ND
- Digikey: LM6134BIN-ND
- Digikey: PIC18F1220-I/P-ND
- Digikey: LM7805CT-ND or equiv.
- Digikey: 296-1402-5-ND or equiv.
- Use Digikey ED3108-ND or equiv.
- Digikey: ED3114-ND or equiv.
- Digikey: ED3118-ND or equiv.
- Digikey: ED3116-ND or equiv.
- Digikey: 4724K-ND or equiv.
- Digikey: HM159-ND or equiv.

The Hardware

Printed Circuit Board

I designed a double-sided circuit board to integrate the hardware.⁴ The dimensions are 2.3×2.8 inches (5.8×7.1 cm). Integrated circuit (IC) sockets are optional but recommended; this is especially applicable to the microcontroller and the solid-state relays. A fine tip soldering iron should be used for all components. Take all electrostatic discharge (ESD) precautions. The ICs and the MOSFETs are ESD sensitive devices, so care should be taken to guarantee a static-free environment when assembling the unit.

You may decide to build the circuit using other techniques such as breadboard and point to point wiring. The layout is not critical since there are no high-speed signals carried. Take care in proper dc supply decoupling using the $0.1 \mu\text{F}$ capacitors near the ICs. Keep in mind the current to be carried on the outputs when selecting wire size for the solid-state relays, the MOSFETs and the power resistor.

Enclosure

Figure 2 shows the Hammond diecast aluminum project box I used to enclose my Cyclor board. This type of enclosure offers two advantages. It has a thick wall that dissipates the heat generated by the MOSFETs and the power resistor, and it helps reduce EMI radiation in the shack.

Other enclosures can be used as long as you keep power dissipation in mind. Under worst case conditions, the two MOSFETs (Q1 and Q2) and the power resistor (R1) could dissipate up to 6 W in total. These three devices must have their tabs mounted to the enclosure wall or a decent sized heat-sink for proper heat dissipation. Make sure to electrically insulate the MOSFET metallic tabs from the enclosure because these are not at ground potential. Insulation and heat conductive kits are available to do this. (See the parts list.)

There is more information on how to put everything together using the suggested enclosure on my Web site. (See Note 2.)

Battery Wiring

Wiring to the batteries is straightforward. Like any battery charger, the positive circuit board pad (+) connects to the positive battery terminal; the negative (-) circuit board pad connects to the negative battery terminal. This is done independently for both batteries (though the two positive (+) pads actually connect to a common point in the circuit). Colored banana plugs and jacks are a good idea for interfacing at the enclosure end. [I would use polarized connectors, such as Anderson PowerPole connectors. — Ed.] I strongly recommend using colored wiring as

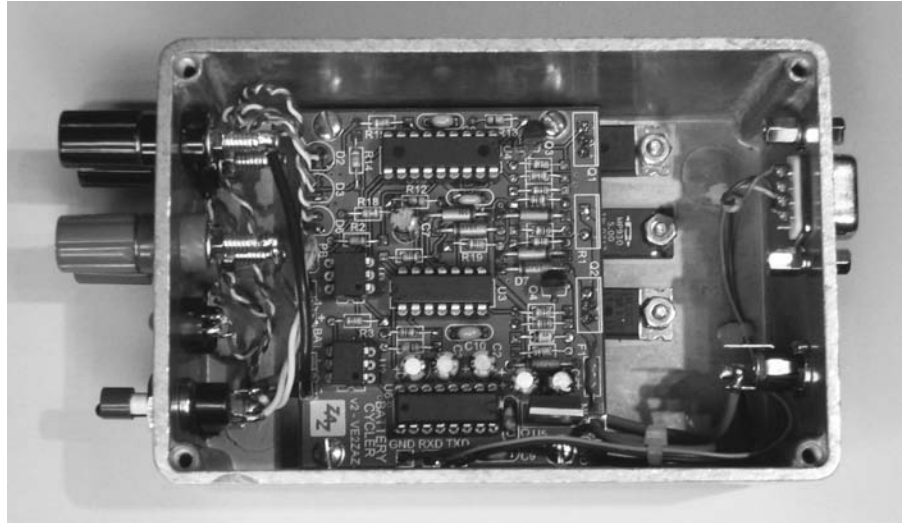


Figure 2 — The completed Battery Cyclor system in a Hammond diecast aluminum project box.

well, to help avoid battery reversal. Alligator clips or mini-grabbers will do a good job of connecting to the batteries. I use AA-size cell holders equipped with soldering tabs. A bit of creative thinking will likely be required to connect to sealed custom battery packs. One thing to understand here is that the wiring and terminals in the chain show some resistance. This will cause the voltage measured by the Cyclor to be different from the actual battery voltage, potentially by as much as a few tenths of a volt. So keep the wiring short, use wires of proper gauge and make sure you have good connections all the way back to the circuit board.

DC Supply

A suitable external dc power supply for the Cyclor board is required. The supply voltage has to be at least 5 V higher than the expected fully charged battery voltage. This fully charged voltage turns out to be around 1.6 V per cell when still connected to the charger. A minimum dc supply of +8 V dc is required, but do not exceed +20 V dc. The maximum expected current is 100 mA more than the charge current set by the user. Assume a maximum current of 600 mA, to be on the safe side.

I have found that laptop power supplies make great power sources for this application. The output of these units typically ranges from +12 V dc to +18 V dc, with at least 1 A of available current.

The Firmware and Software

I have created a *Windows* program to configure the Battery Cyclor; this makes the man-machine experience friendlier. The compiled *Windows* software is packaged in an installer program, and is available for download from

my Web site. The software will run under just about any 32-bit *Windows* version. Figure 3 shows screen shots of the *Windows* Battery Cyclor Configuration Tool, showing the system configuration, battery configuration and results log tabs highlighted. As seen in the figure, the tool is tab-based, with features distributed over several tabs.

The first tab provides the ability to set the number of batteries (one or two) connected. It also provides the ability to configure the type of discharge/charge cycle (periodic mode or battery restoration mode), the number of days in a cycle and the number of cycles during a battery restoration mode.

The second tab is where you set the battery parameters, such as the battery capacity, the number of cells, the end of discharge voltage threshold, the discharge current, the charge current and the charge duration. These parameters are individually set for both batteries. Charge and discharge parameters are filled in by the tool but can be changed if required. Note that the charge and discharge current ranges from 50 mA to 500 mA, which corresponds to a C/10 charge current for batteries ranging from 500 mAh to 5000 mAh. The combinations of voltages and currents are validated by the tool to ensure that the Cyclor can carry out what is requested. From the above entries, the cycle duration in days is also verified to ensure that the stages requested can be executed within the allocated time.

Another tab provides log and alarm download capabilities. This is useful to find out the current Cyclor stage, the duration of the previous stages, if there were issues detected during the entire cycle, the battery voltage and current values, and so on. More information on this is available in the

Operation section.

Finally, there is a settings transfer tab (not shown in Figure 3), where you will be able to read the current settings from the Cyclor or write new settings to it. After selecting the computer COM port, reading from or writing to the Cyclor is just a matter of pressing a button. A progress bar informs you of the status of the transfer. Everything completes in a matter of a few seconds. After reading the settings from the Cyclor, all fields in the various tabs are updated with the currently configured settings. A change to only one field involves a read-modify-write process. There is nothing special to perform in order to save the data to non-volatile memory. A “Write Settings” command will permanently save the data inside the microcontroller. After configuration is complete, the user can disconnect the cable or leave it connected for log and alarm monitoring purpose.

Operation

The best way to explain how the PIC firmware operates is by using flowcharts. Figure 4 shows the firmware flow for the two cycle modes available, namely the periodic mode and the battery restoration mode. The periodic mode (Figure 4A) is the regular mode to maintain optimum battery performance. At a repeating period (in days) set by the user, the batteries get discharged and then recharged, battery no. 1 first, followed by battery no. 2. If the Cyclor is configured to service only one battery, battery no. 2 is skipped. These stages are followed by an idle stage (nothing happening) that runs until the period set by the user is reached. The Cyclor then starts a new cycle as described above.

The battery restoration mode (Figure 4B) is used to repeatedly cycle the batteries with the intent of restoring their charge holding capability. In this mode, the batteries are discharged and then recharged, battery no. 1 first, followed by battery no. 2. This discharge/charge cycle repeats without idle period until the number of cycles set by the user is reached. These cycles are followed by the off stage, which turns off any activity on the Cyclor. From there, pressing the Manual Stage Control button will initiate a regular periodic cycle with the previously configured settings. Note that the restoration cycles do not begin until the user depresses the button.

The first time the unit is powered up, the Cyclor firmware is set to the off stage. Depressing the Manual Stage Control button advances the Cyclor to the next stage in the cycle, as shown in the flow chart on Figure 4A. Repeatedly pressing the button, within less than 3 seconds, advances to the next stages in rotation. When the button is left alone for 3 seconds, the selected stage begins. Note that the currently running stage is still

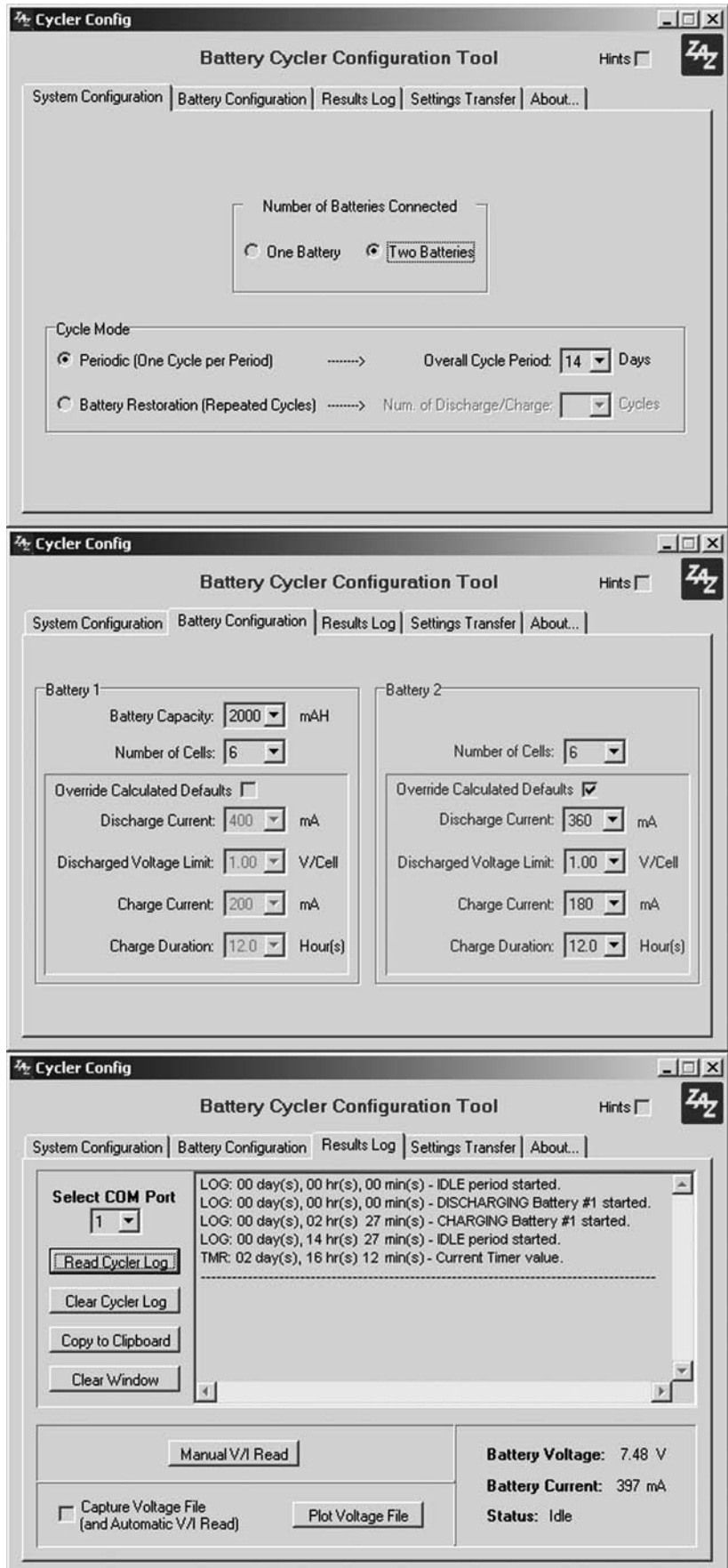


Figure 3 — Screenshots of the Battery Cyclor Windows configuration tool, with the system configuration, battery configuration and results log tabs highlighted.

executed until the 3-second delay expires. Also note that the cycle timer is reset every time a stage is initiated via the Manual Stage Control button.

LEDs

There are three light emitting diodes (LEDs) equipped on the Cycler. The first two (D2 and D3) are bi-color LEDs. Having a green/red LED pair in a single package enables the generation of three colors: green, red and amber. The latter is generated when both green and red LEDs alternate at a fast rate. In our application, amber indicates the discharge stage, red indicates the charge stage and green indicates the idle stage. Extinguished LEDs indicate the off stage. The battery no. 2 LED can also be seen permanently off, which indicates that the second battery channel is disabled.

In addition to solid colors, there are two LED flashing scenarios that may be seen. The first one happens when the user manually toggles between the stages, triggering the 3-second delay mentioned previously. The flashing rate will be about three Hertz. After the 3 second delay, the selected stage begins and the LEDs are solid colored. The second flashing scenario will occur when the Cycler detects a low battery voltage or is unable to generate the right amount of current. The corresponding battery LED will flash at a fast rate, indicating an alarm on that battery. More description of this feature is provided in the Alarm section below.

The third LED (D6) merely indicates the power on/off status of the cycler. A bi-color LED can be used there as well, but only one color will be shown.

Logs, Readings and Alarm Messages

As seen on Figure 3, the Battery Cycler provides the user with information messages via the *Windows* tool. These messages can be consulted under the “Results Log” tab. The Log buffer has sufficient memory space to keep the logs and alarms of an entire cycle.

Whenever a new stage begins, a log message is generated, along with a timestamp generated by the internal timer. This allows the user to verify that the various stages occur as planned. The built-in timer starts at zero at power up and whenever a new cycle begins. It has a resolution of two minutes and an accuracy of $\pm 2\%$.

In addition to log messages, there are also alarm messages generated. Examples of such messages are: “Unable to generate the specified charge current” and “Insufficient battery voltage during idle stage.”

Another informative feature is the battery voltage and current display and logging. Pressing a button in the “Results Log” tab provides a reading of the instant battery voltage and current as seen by the PIC. This feature is available during the charge and discharge stages. This voltage and current reading can also be automated so that the results get logged onto the PC. When enabled, the automatic voltage/current read feature takes a reading every 30 seconds and saves the values along with a timestamp (in seconds) in a text file for further analysis. This “voltage file” can be plotted directly within the software using the built-in graph engine. An example plot is shown on Figure 5. The voltage file can also be analyzed and plotted using any third-party spreadsheet program

(Microsoft *Excel*, *Open Office Calc*, or other programs). When analyzing a discharge stage voltage file, the plot feature also calculates and displays the battery capacity in mAh. The calculation is rather simple: the discharge current is multiplied by the discharge time. This assumes that you have captured the whole discharge stage in the voltage file, of course. The calculation will show you the “real” capacity of your batteries, not the theoretical one. Be prepared for some disappointment here...

Built-in Robustness

The Cycler will gracefully recover from a power outage or disconnection. If the power outage occurs during a charge or discharge stage, the Cycler will restart in the discharge stage. If the Cycler recovers from a power outage while it was in the idle stage or in the off stage, it will restart in that same stage.

The Cycler also has various anomaly detectors implemented in firmware. Whenever these trigger, an alarm log is generated. Here is a list of anomalies and actions.

- The Cycler will abort the charge stage if it is unable to generate the charge current requested by the user.
- The discharge stage will continue if the cycler is unable to generate the discharge current requested by the user, but an alarm log will be generated.
- The Cycler monitors the health of the batteries during the idle stage at a two-minute interval. If the battery voltage falls below the end-of-discharge threshold voltage configured by the user, the corresponding LED flashes at a fast rate and an alarm is gener-

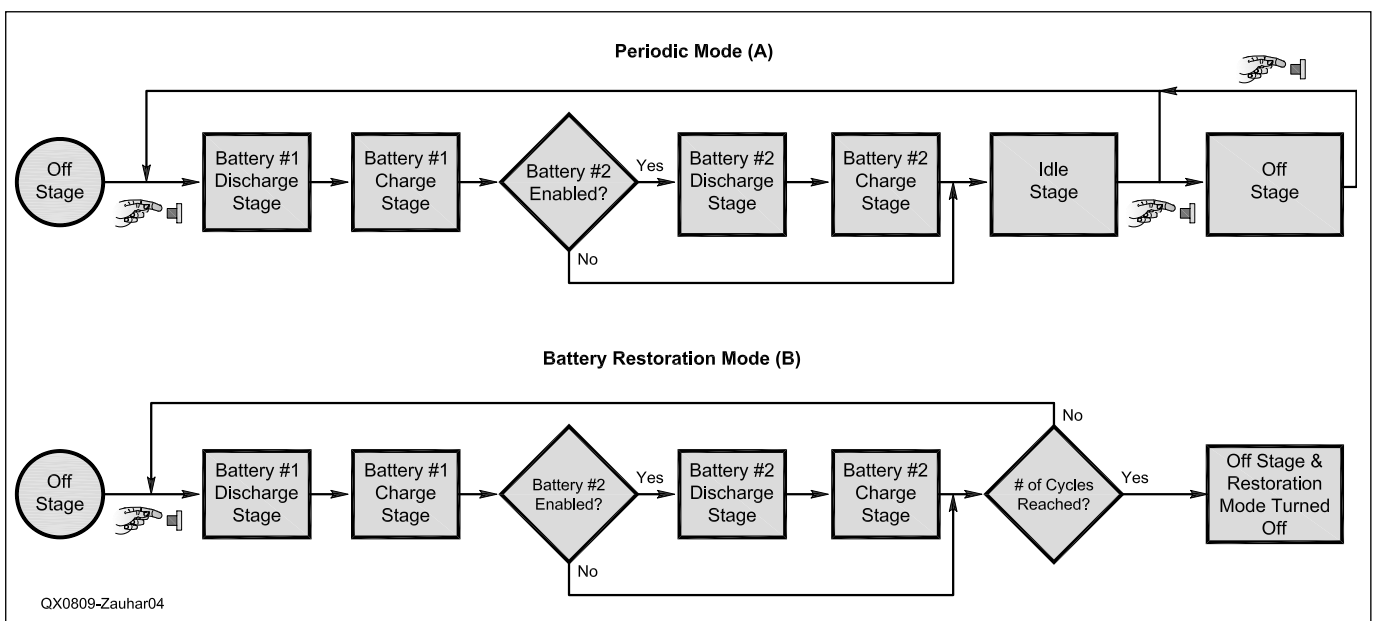


Figure 4 — Flowchart of the Cycler firmware operation for the two supported modes.

ated.

- The discharge stage will end if the battery voltage does not fall below the end-of-discharge threshold within a time limit calculated as 150% of the theoretical discharge time.

- The Cyclor is also equipped with a fuse (F1) that will protect the battery and the circuit if a fully charged battery is inadvertently connected with its polarity reversed. If the generated current is high enough, the fuse will blow. Otherwise, the Cyclor will still generate an alarm claiming that the requested discharge current cannot be produced, which should raise user suspicion about the wiring.

Accuracy and Resolution

The Cyclor voltage and current reading accuracy and resolution call for some additional explanation. The design intent was to create a circuit that would have sufficient accuracy and resolution to properly charge and discharge batteries. In that sense, it is not meant to replace an accurate voltmeter or ammeter. The user must keep this in mind when analyzing the readings.

Assuming that the component tolerances meet those specified in the parts list, the Cyclor absolute worst case accuracy on the voltage readings is estimated to be $\pm 6.5\%$. The current reading has an absolute worst case accuracy of $\pm 24\%$. These accuracy errors are worst case scenarios assuming at-the-limit component tolerances, which is a very unlikely scenario. In fact, if the resistors of the same value come from the same batch, which is usually the case when you purchase them new, then the overall accuracy will be much better. This is what I measured on the two prototype assemblies I put together. The accuracy errors are mainly generated by (from the largest to the smallest contributor):

- Difference in resistance between R5 and R7.
- Difference in resistance between R4 and R6.
- The +5V supply rail accuracy (U5), which is used as the reference for the highest value (4095) read by the PIC microcontroller ADCs,
- Resistance tolerance of R1.

Assuming a more-or-less stable temperature, the offsets on the voltage and current reading can be measured manually using an accurate meter and taken into account if trying to derive a better accuracy.

When making a voltage/current reading via the *Windows* tool, the resulting voltage and current values represent an average of 30 readings. This is done by the *Windows* tool to null out any ripple caused by the firmware when maintaining the current to the user-

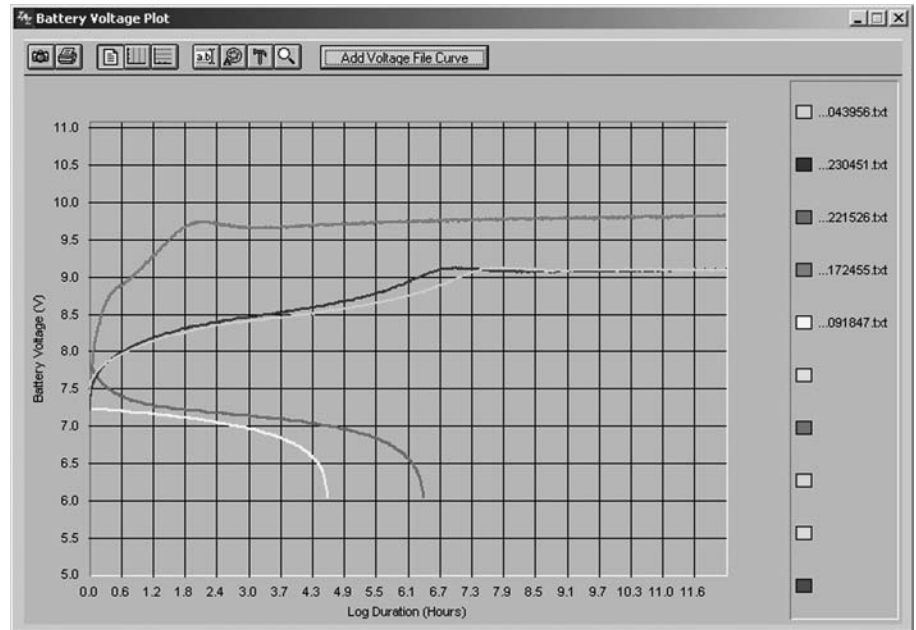


Figure 5 — Various charge and discharge curves can be displayed concurrently by the Battery Cyclor *Windows* configuration tool.

requested value. As a result, two decimals are provided on the voltage values. This additional resolution provides much better trend analysis and plotting clarity. The user must remember though that the accuracy study provided above still applies. In other words, better resolution does not translate into better accuracy.

Conclusion

This Rechargeable Battery Cyclor fulfills what few other commercial chargers do — it keeps my rechargeable handheld radio batteries fresh and ready for action. Not only does it keep them charged up, but it cycles them at regular intervals so that their useful life is maximized.

Assuming a reasonably stuffed junkbox, you will be able to assemble and own the Cyclor for around \$60 US. This compares favorably with off-the-shelf high-tech universal chargers, which are not autonomous...

Now you will be able to claim you are always ready for emergency action! That by itself is reassuring, isn't it?

Notes

¹Wikipedia, the free online encyclopedia, provides a good overview of Nickel Cadmium and Nickel Metal Hydride battery technologies and how to optimize their performance. See en.wikipedia.org/wiki/Ni-Cd and en.wikipedia.org/wiki/NiMH for more information.

²I maintain a Web site where I provide updates to this project, source files and additional comments. Please visit ve2zaz.net.

ve2zaz.net for more details. The PIC program files and *Windows* configuration software files are also available for download from the QEX Web site. Go to www.arrl.org/qexfiles and look for the file **09x08_Zauhar.zip**. The files available on the QEX Web site are the latest versions as of press time, but ve2zaz.net may have more recent files.

³For those of you who cannot program Microchip PIC18F series micro-controllers, I make pre-programmed PIC microcontrollers available for purchase. Please contact me via e-mail for more details.

⁴I distribute high quality, fully etched, plated-through bare circuit boards for this project. Please contact me via e-mail if you are interested in obtaining a circuit board.

Bertrand Zauhar has been a radio amateur as VE2ZAZ since 1984. He holds an advanced amateur license. Bertrand has designed for the hobby — among other things — a micro-controller-based radio T/R Sequencer (QST, March 2007), a GPS-Derived Frequency Standard (QEX Sept/Oct 2006), an L-band transmit converter (Amsat Journal, May/June 2003), a 1 to 12 GHz frequency counter prescaler, a microprocessor-based repeater controller, several amateur satellite antennas and an RF-sensing alarm (73 Amateur Radio, May 1998). Bertrand received his Electronics Engineering degree in 1989 from École Polytechnique de Montréal. Since then, his professional engineering career has been spent working for Nortel at the Montréal and Ottawa locations. In his current position, he is an electronics hardware design engineer on optical transmission equipment.



Press-n-Peel Circuit Boards

*Looking for a way to make a circuit board for your next project?
Here is a simple technique for homemade boards.*

Here's a new way to make printed circuit boards at home. The only chemicals are some very inexpensive etchant and some very common household items. No special equipment is required and you can go from artwork on your computer to a finished board in about an hour!

Until a few years ago, I used the photo technique to make printed circuit boards. That method required photo sensitized circuit board material and a special light source. The boards I made using that technique always came out with missing or very thin tracks, and all the tracks had very rough edges. I think the resist layer just wasn't thick enough and allowed the etchant to remove some of the copper.

A few years ago I saw an ad for a product called Press-n-Peel Blue manufactured by Techniks Inc, Ringoes, NJ.¹ It consists of plastic sheets that act as a carrier for the toner from a laser printer. The artwork is printed on the Press-n-Peel Blue media, and then a common household hand iron is used to transfer it to the bare copper clad circuit board material. The toner and Press-n-Peel Blue material forms the resist.² When my first board came out very professional looking I threw out all my photo technique materials.

FAR Circuits provides high quality circuit boards for many of the projects in *QST* and *QEX*.³ What do you do, however, if you want to design and produce your own board for a circuit you've developed? Press-n-Peel Blue is the answer. Read on and I'll lead you through the steps needed to make a high quality circuit board at home for your next project.

Requirements

You will need the following:

1) A computer program to compose the actual artwork on your computer. The program must have the ability to produce a mir-

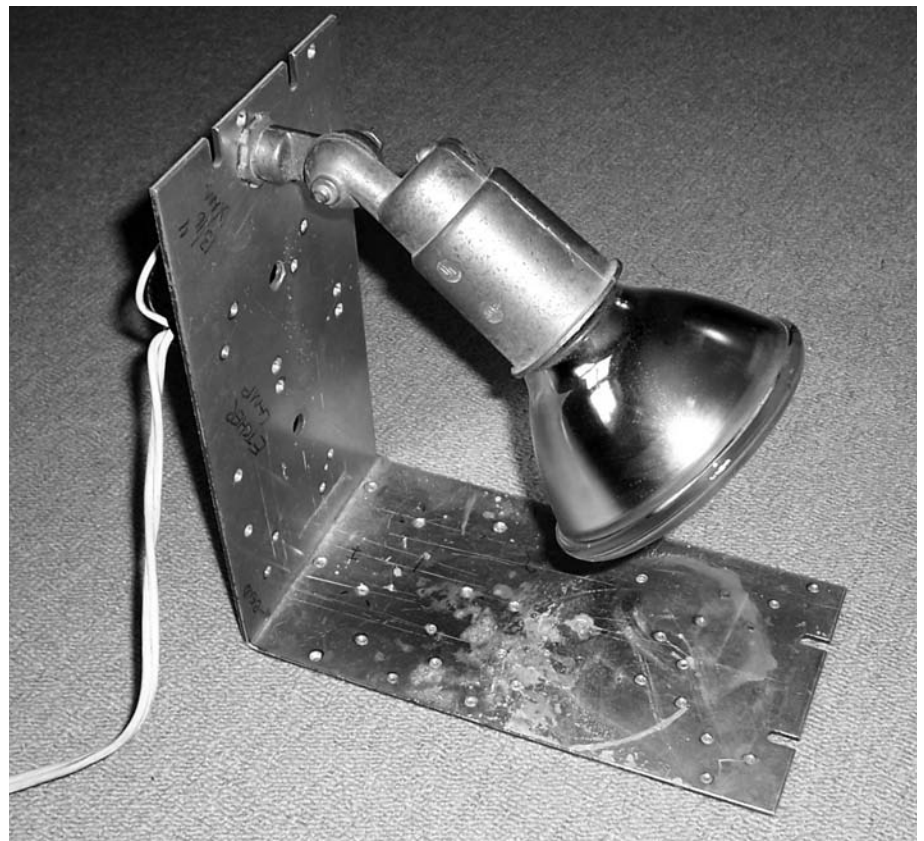


Figure 1 — A heat lamp for speeding up the etch process. There is nothing fancy here! I use a 60 W floodlamp, a single outdoor floodlight fixture and a 120 V ac cord and plug.

ror image of the artwork since Press-n-Peel Blue reverses the image when it is applied to the circuit board.

2) A laser printer that uses black toner — an inkjet printer will not work. (I use a laser printer that I picked up at a garage sale for \$10.)

3) A common household handheld clothing iron. Even with wash-and-wear clothes being the norm, most homes have an iron available. I often see them at garage sales.

4) A piece of parchment paper. This is available at most grocery stores. (I'm using

the same piece that I've used to make dozens of circuit boards.)

5) A wooden cutting board or other flat piece of wood. I use a short length of 2 by 4 for smaller boards.

6) A small utility knife or single edged razor blade.

7) A small plastic tray for etching the circuit board.

8) Optionally (to speed etching) a 60 W spotlight mounted on a bracket. The board will etch faster if the liquid is heated slightly. See Figure 1.

¹Notes appear on page 25.

- 9) A small roll of 3M Scotch® Magic Tape.
- 10) A steel wool scouring pad, such as an SOS or other cleaning pad.
- 11) Scotch® Super 33+ electrical tape (only required if your board has a ground plane).
- 12) Very fine sandpaper.
- 13) Nail polish remover (\$1.50 for a 6 fluid ounce bottle).
- 14) Press-n-Peel Blue.

How-to steps

1) Add a 1-inch-long test-strip pattern to your artwork. It can be seen in several of the figures. This is needed so that you can verify that your artwork is the correct size. (The first time I plotted some artwork, it came out half-size because the scaling in my software was set to 50%. Another time the scaling was set to 110%. I didn't notice until I placed an IC on the board and the tracks didn't line up with the pins! That little test pattern will save you time, etchant and board material.)

2) Create a mirror image of the artwork.

3) Print out the artwork on plain paper. Flip the printed page over and look through the paper to make sure the artwork looks proper when viewed facing a bright light. Now is the time to make changes because this is what your board will look like when you're finished.

4) Measure the length of the 1-inch-long track added in Step 1. If it isn't exactly 1 inch long adjust the scaling in your software.

5) Once you've verified that the artwork is properly scaled and mirrored, pull out the printer paper tray and write an "X" on the upper right edge of the top sheet of paper as it sets in the paper tray, then replace the paper tray. Print out the artwork again.

6) Cut a piece of the Press-n-Peel Blue to cover the printed artwork plus ½ inch on each side. Using 3M Scotch Magic Tape around the edges, attach the Press-n-Peel to the page just printed, covering the artwork completely. **The dull side of the Press-n-Peel must be visible.** (Using a plain piece of paper as the "carrier" for the Press-n-Peel will allow you to print artwork for a small board without wasting the unused portion of a sheet of Press-n-Peel. I have used this technique in several printers and never had a jam.) Put this "carrier" back into the paper tray with the "X" in the same position as in step 5.

7) Print the artwork on the Press-n-Peel. See Figure 2. Remove it from the carrier and trim off the tape. Touch only the outer edges, because any oil from your hands may prevent the Press-n-Peel Blue from adhering to the copper clad circuit board material.

8) Start heating the iron now. Set it between "acrylic" and "polyester". Turn off the "steam" feature.

9) Prepare the copper clad circuit board material by lightly sanding it with very fine sandpaper. Rinse it in water, then scour it lightly in circular motions using a steel wool pad. Rinse it again until *all* residue has been removed. Hold it upright by the edges with one corner pointed downward, and allow it to drip dry. Use a piece of facial tissue to dry it completely and make sure there are no fibers left on the board. Cleanliness is required if you want a professional looking circuit board with no breaks in the tracks!

10) If your board needs a ground plane, cover the entire bottom with Scotch 33+ electrical tape. Overlap the pieces about 0.100 inch and cut each piece ½ inch longer than needed. After the bottom is completely covered, trim the ends of the tape using a utility knife or single edged razor blade. Press down

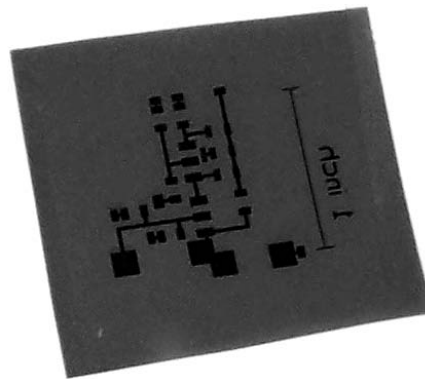


Figure 2 — This photo shows a small piece of Press-n-Peel on the "carrier" page.

on the ends where the pieces overlap so there is no path for the etchant to enter and remove areas of the ground plane.

11) Put the following on the cutting board or 2 by 4 piece of wood in this order: a paper towel folded twice, the copper clad circuit board with the cleaned side up (and optional ground side down), the Press-n-Peel Blue circuit pattern, dull side down, a single sheet of parchment paper. Make sure the Press-n-Peel is centered on the circuit board with at least ¼ inch overlapping on each edge. See Figure 3.

12) Apply the iron and push down gently. See Figure 4. You want only enough pressure to transfer the heat. If you use too much pressure the track will spread out, producing shorted tracks and pads. If you don't use enough pressure the pattern may not attach securely to the circuit board material. Move the iron back and forth and rotate it for 2 minutes.

13) Remove the iron and parchment paper. Remove the circuit board material with the Press-n-Peel attached (use long nosed pliers — the board is very hot at this point!). Hold the circuit board under cold water for 15 to 20 seconds to quench it. Remove it from the water and lift one corner of the Press-n-Peel material, then peel it off the circuit board completely. See Figure 5.

14) Check the artwork for any breaks in the tracks. If the artwork is missing in critical areas you can remove the Press-n-Peel pattern using sandpaper and try again. I have found that sometimes small areas of the board are missing some Press-n-Peel etch resist. If

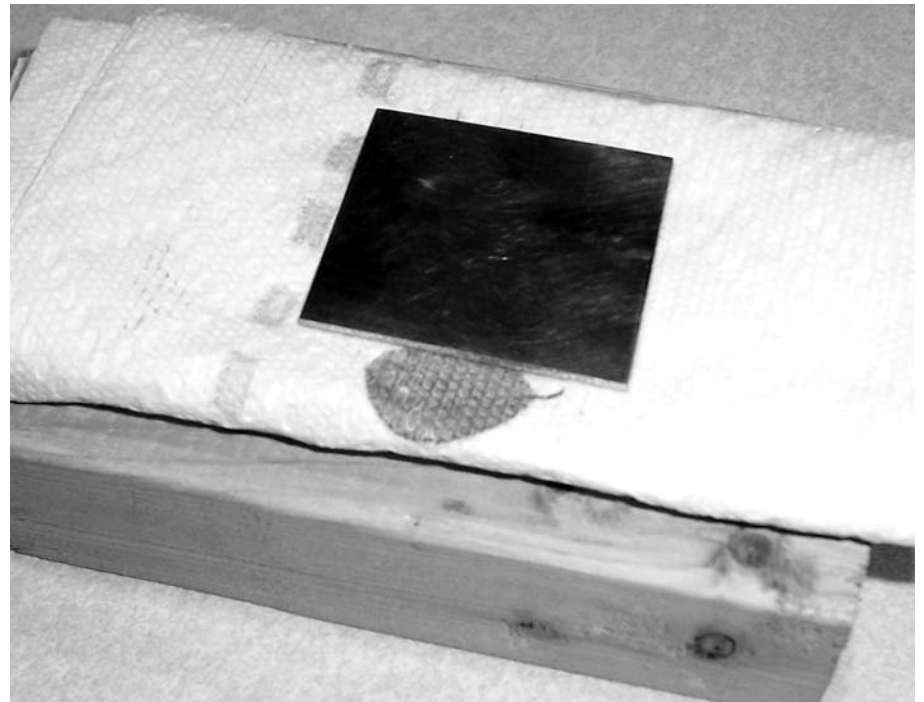


Figure 3 — This stack includes the 2 × 4, paper towel and clean copper clad circuit board material.



Figure 4 — The Press-n-Peel circuit pattern and parchment paper are placed on top of the material stack shown in Figure 3. Then the iron is used to heat the Press-n-Peel material to transfer the etch resist to the circuit board material.

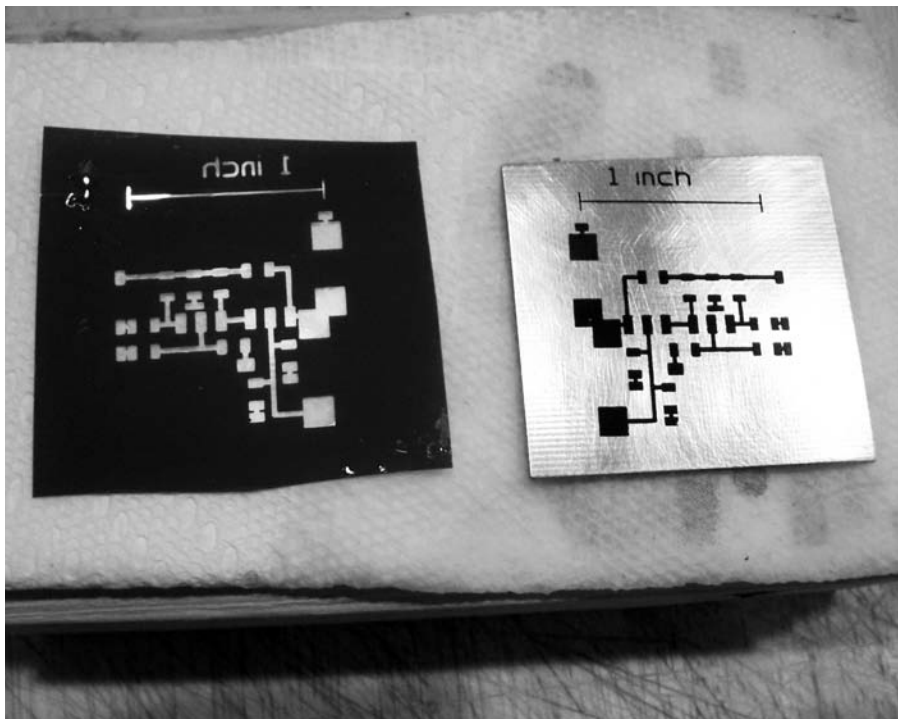


Figure 5 — The copper clad circuit board material is on the right, with resist pattern after ironing. The Press-n-Peel material on the left is missing the track and pads.

these areas didn't affect circuit operation I just went ahead and etched the board.⁴

15) If the artwork looks okay, put the circuit board material in the plastic tray and cover it with etchant. The proper quantity of etchant is just enough to completely cover the board material when the tray is on a level surface.

16) If you've constructed the heat lamp/bracket assembly, turn it on and place it about 6 inches from the plastic tray. See Figure 6.

17) Gently rock the tray back and forth every 10 to 15 seconds. After a few minutes the copper will turn a lighter color. In about 20 to 30 minutes the circuit board will be completely etched. See Figures 7 and 8.

18) Remove the circuit board from the plastic tray and rinse in water. If you applied the Scotch 33+ Electrical Tape to provide a ground plane, remove the tape.

19) The Press-n-Peel Blue instructions say to use fine sandpaper to remove the resist. Instead, I've successfully used nail polish remover to remove most of the Press-n-Peel/toner, then just a little cleanup with very fine sandpaper so that less copper is removed. (Better yet is the solvent methyl ethyl ketone — MEK — but it's not readily available. I happen to have access to some at work.) Rinse the circuit board again with water and dry with a paper towel. Now it is ready for soldering. See Figure 9.

Performance

Using the exact techniques described here I've made various boards for projects I've designed. One of them was a microwave downconverter for 2.4 GHz, complete with LO, mixer and LNA. If this technique works at that frequency it will work for any project! The manufacturer states that 0.005 inch track can be produced. Using Press-n-Peel, I have made boards with 0.010 inch wide tracks that came out perfect.⁵

Ground connections are made by drilling a small hole (0.020 inch diameter) through the board, placing a short piece of wire in the hole, bending both sides flat and soldering both sides.

Many parts are now available only in surface mount technology (SMT). Some home constructors may not like this fact but Press-n-Peel is well suited for making boards for SMT components. SMT parts do not require holes for mounting — this is a time-consuming and tedious task. Consider the accuracy required when drilling 14 or more hole locations for a single DIP IC so that the leads slip into place easily and you will start to appreciate SMT parts!

Materials Availability

Press-n-Peel Blue is available from All Electronics (www.allelectronics.com) priced at \$17.50 for ten 8½ × 11 inch sheets.



Figure 6 — The circuit board with resist is placed in a small plastic tray under the heat lamp.

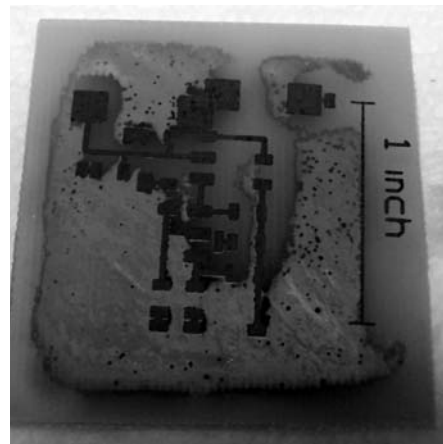


Figure 7 — Here is the circuit board after 15 minutes in the etchant. It's almost done!

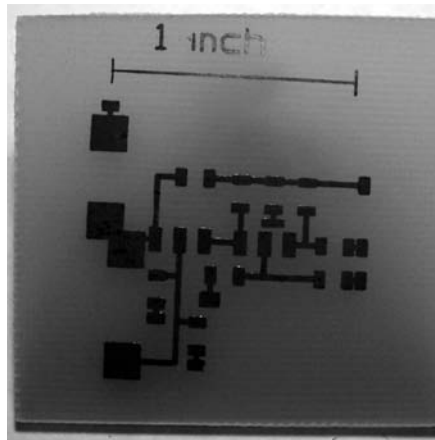


Figure 8 — Etching is complete after 20 minutes.

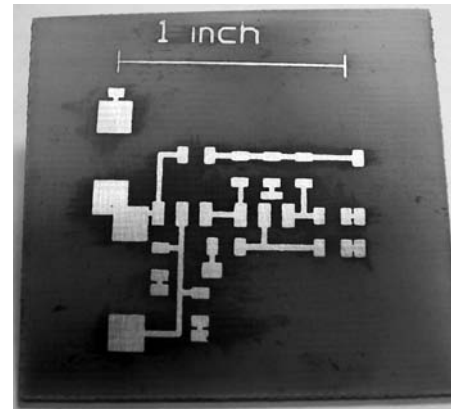


Figure 9 — The board after removing the Press-n-Peel/toner with nail polish remover and very fine sandpaper. Now we are ready to solder!

homebrew downconverter for 2400 MHz amateur satellite work. He was first licensed in 1964 as WN9LDB. He passed his General class exam in 1965 and his Extra class exam in 1986.

Jim's interests are casual DXing, CW on HF, low power CW, especially during ARRL Field Day, homebrewing, satellite communications, cooking and baking and noncompetitive bicycling. He is anxiously awaiting the next high orbit bird launch to replace AO-40. Jim received a degree in physics from Indiana University in 1976.



Hosfelt Electronics (www.hostfelt.com) sells a pint of etchant (part number ER-3) for \$3.49 and both single sided and double sided circuit board material.

Notes

¹I am not an employee of Techniks, and have received no compensation for this article from them.

²I recommend using only Press-n-Peel Blue. They also make a paper based product called Press-n-Peel Wet. It produced boards of only fair quality. The "Blue" is far superior.

³FAR Circuits, 18N640 Field Court, Dundee, Illinois 60118; www.farcircuits.net

⁴The only possible causes of failure to make

a good board are: (1) too much or too little pressure when ironing and (2) dirt/dust/oil on the board or Press-n-Peel. Use just enough pressure to transfer the heat and keep the board and Press-n-Peel Blue clean. If you follow my steps you can produce professional looking boards at home at very low cost.

⁵I am interested in hearing from you if you use Press-n-Peel Blue. Please e-mail me with any questions or comments.

Jim Kocsis, WA9PYH, is employed as a Test Engineer at Honeywell Aerospace. He has homebrewed small projects his entire ham career, including a 4 foot satellite dish and downconverter for 1691 MHz GOES reception and a

We Design And Manufacture To Meet Your Requirements

*Prototype or Production Quantities

800-522-2253

This Number May Not Save Your Life...

But it could make it a lot easier! Especially when it comes to ordering non-standard connectors.

RF/MICROWAVE CONNECTORS, CABLES AND ASSEMBLIES

- Specials our specialty. Virtually any SMA, N, TNC, HN, LC, RP, BNC, SMB, or SMC delivered in 2-4 weeks.
- Cross reference library to all major manufacturers.
- Experts in supplying "hard to get" RF connectors.
- Our adapters can satisfy virtually any combination of requirements between series.
- Extensive inventory of passive RF/Microwave components including attenuators, terminations and dividers.
- No minimum order.

NEMAL

Cable & Connectors
for the Electronics Industry

NEMAL ELECTRONICS INTERNATIONAL, INC.

12240 N.E. 14TH AVENUE
NORTH MIAMI, FL 33161

TEL: 305-899-0900 • FAX: 305-895-8178
E-MAIL: INFO@NEMAL.COM
BRASIL: (011) 5535-2368

URL: WWW.NEMAL.COM

Receiver Performance Measurement and Front End Selectivity

Some receiver tests may be better indicators of real-world performance than current dynamic range measurements.

Doug Smith's recent three articles dealing with receiver performance covered a great deal of ground.¹ That discussion highlights what a complex instrument a receiver is. It was clear from Doug's discussion that his endeavor was to break away from old ways of thinking and doing things. We all know what the prime goal of receiver performance is — the detection of wanted signals in the presence of strong off channel signals. From my perspective, nothing much has changed in the last 30 years or so regarding how we look at receiver performance measurement, at least in Amateur Radio circles, although there has been welcome recognition of the importance of the second order distortion performance of receivers (raised by Ulrich Rohde in the early 1990s and the importance of near channel strong signal performance (lack thereof) compared to further out strong signal IMD effects.² People like Rob Sherwood have been banging the drum on that one for 30 years.³ The ARRL has taken this on board (and now performs IMD tests at 2 kHz separation) as have the receiver manufacturers (by offering narrower bandwidth roofing filters).

While the current receiver testing regime has served the amateur fraternity well, I make a case for these tests to be supplemented by another test: the Noise Power Ratio test. I believe that front end selectivity allows the last drop of performance to be extracted from receivers and that the existing testing regime discriminates against receivers that have high front end selectivity. In some ways, I suspect that the way receiver performance is measured influences the way receivers are designed. An example of this is that once the ARRL began performing IMD tests at 2 and 5 kHz separation, receivers with roofing filters having similar bandwidths appeared on the scene.

I would also like to suggest ways that

¹Notes appear on page 30.

test results might be presented, such that the focus is on what really matters. No doubt this will be akin to treading on the hooves of certain sacred cows. It may well be that what is focused on influences the way receiver design is implemented. That is why it is important to carefully consider these issues.

Some of the matters I am about to discuss I raised in a letter published in *QST* over 10 years ago.⁴ So, I apologize for repeating myself, albeit at a very low rate!

Receiver Performance Test Results

Intercept Points

The first issue I would like to deal with is the way we use the results of receiver performance testing as practiced by the ARRL and followed in most of the literature.

The first thing to say is that IP3 is merely a calculation. It is a totally fictitious number that hardly bears any relationship to reality. Its calculation is based on two measurements, that of the noise floor (minimum discernible signal or MDS) and the level (IL3) of two test tones that raises the 3rd order IMD products above the noise floor. (Since 1993 the ARRL has been using an S5 reference level instead of the noise floor — I thank Michael Tracy, KC1SX, former ARRL Lab Test Engineer, for his very helpful discussions on this matter.)

These three are related by the formula:

$$IP3 = (1.5 \times IL3) - (0.5 \times MDS) \quad [\text{Eq 1}]$$

Plug in the measured (log ratio values in dB) IL3 and MDS and there's the IP3.

Now, this formula relies on the belief that receiving systems behave according to the so-called cube power law. Doug also pointed out this does not appear to be the always case and offered an explanation for this. I believe there may be an even more straightforward explanation to be found by delving into the mathematics of distortion products. The

amplitude coefficients derived for the third order terms ($2f_1 \pm f_2$, $2f_2 \pm f_1$) are governed by the cubic power as long as there are no 5th or higher odd order distortion products. If they are present, these higher order products generate their own 3rd order products and what's more is that the amplitude coefficients of these 3rd order products have terms to the power of 5 and not 3. So we have double jeopardy here.

Let the transfer equation for the receiver be:

$$y = Ax + Bx^2 + Cx^3 + Dx^4 + Ex^5 \quad [\text{Eq 2}]$$

Then, if two interfering signals are considered, the amplitude coefficient of the 3rd order product term generated by the 3rd order distortion only is:

$$= (3 \times C \times E1 \times E2^2) / 4 \quad [\text{Eq 3}]$$

where E1 and E2 are the amplitude coefficients of the two interfering signals.

If the 3rd order terms produced by the 5th order distortion are included then the amplitude coefficient of the 3rd order product term becomes:

$$= \{[(3 \times C \times E1 \times E2^2) / 4] + [(5 \times E \times E1 \times E2^4) / 4] + [(15 \times E \times E1^3 \times E2^2) / 8]\} \quad [\text{Eq 4}]$$

The question, then, is how large or small is E, because that will determine the influence of the 5th order generated terms — it will have to be very small indeed for the 5th order terms to have little impact on the total amplitude coefficient.

The same thing happens with the 2nd order products. If there is 4th order distortion, this distortion will yield 2nd order components with amplitude coefficients to the power of 4 and not 2.

A good very basic discussion of this can be found in Carson.⁵

This discussion may provide a basis for understanding why receivers do not appear to

conform to a cubic law. If the 3rd order term is anything like Equation 3, then Equation 1 is more or less irrelevant, and calculating the 3rd order intercept point in this way is nearly meaningless unless it is clear that 5th order distortion is at a very low level.

The other way in which the IP3 term has no bearing to reality is that compression will ensure that any intercept point could never be reached anyway. There is no need to comment on this any further as it has been well covered elsewhere.

The other significant point to raise about intercept points is that they can give false impressions about distortion behavior when comparing the intercept point from one order to another. Generally, the 3rd order intercept point for the high end receivers we see today are in the +10 to +25 dBm range, while the 2nd order intercept point range is from +60 to +80 dBm. At first glance it is tempting to say that the 2nd order performance of receivers isn't really an issue. When it is understood, however, that the 2nd order products come out of the noise in some receivers before the 3rd order products, then it is clear that the 2nd order performance of a receiver is important and that the relative intercept points very much belie this performance. Of course, the 3rd order products rise in amplitude at a higher rate.

Given all of the above, I believe it is preferable to express intermodulation performance not with intercept points but with the levels at which the IMD products exit the noise floor. These are real numbers. For sure there might be measurement issues to consider but why compound the problem by manufacturing fictitious numbers that have no relationship to reality. If receivers are to be compared, then the best way to do this is to compare the respective IL2 and IL3 numbers (and IL4 and IL5 for that matter).

Dynamic Range

The notion of dynamic range to my mind is symptomatic of another unhealthy fixation.

If we're talking about the 3rd order Spurious Free Dynamic Range (DR3), without knowing either the IL3 or the MDS, the dynamic range means virtually nothing. For instance, you cannot tell from a dynamic range figure whether the receiver in question is very noisy and the IL3 takes a while to crawl out above the noise floor or the reverse. If the DR3 of a crystal set was measured, it would not surprise me to find that it is comparable to some of the receivers on the market. If it was purchased at a \$/dB price comparable to a fully fledged receiver you might not be happy when you take it home and find it's not much good for receiving anything other than the local broadcast sta-

tion, yet it will happily deal with S9 +40 dB signals. A receiver with a dynamic range of 100 dB sounds a lot sexier than a receiver with an IL3 of -25 dBm but it might be exactly the same receiver. Knowing the IL3 actually tells you something real about the receiver and provides a sound basis on which to compare receivers. Comparing receivers based on DR3 alone without specifying the MDS or IL3 at the same time will not tell you much. When comparing receivers for strong signal performance, if you specify IL3, that is sufficient. If you specify DR3, you need to specify either IL3 or the MDS along with it, otherwise it is nonsensical.

Much the same can be said for the blocking/compression dynamic range. Without specifying the level at which blocking occurs (BL) or the MDS, then it doesn't mean that much for the same reasons that are mentioned above.

Noise Performance

There appears to be an increasing interest in specifying the noise performance of a receiver based on the Noise Figure (NF) because it is independent of bandwidth. While it is bandwidth independent in its formulation, the way the NF is derived is bandwidth dependent. Allow me to explain my point.

The noise equation, which is always invoked to characterize receiver noise behavior is:

$$\text{Minimum Discernable Signal} = -174 \text{ dBm} + 10 \log(\text{Bandwidth}) + \text{Noise Figure} \quad [\text{Eq 5}]$$


Rearranging terms, we have:

$$\text{Noise Figure} = \text{Minimum Discernable Signal} + 174 \text{ dBm} - 10 \log(\text{Bandwidth}) \quad [\text{Eq 6}]$$

This is one way the NF can be calculated. The MDS is measured in the usual manner (as practiced by the ARRL and other test labs) and then the measured value is applied to Equation 6. The measurement is performed at a nominal receiver bandwidth setting. The bandwidth applied to the calculation, however, should ideally be the measured half power noise bandwidth of the total receiving system. So this requires measurement. Also, as Doug has explained in his papers, bandwidth is a slippery customer. There is also passband ripple, shape factor and ultimate attenuation to consider — these will vary from receiver to receiver. So in this sense, the NF derived this way is not independent of the receiver bandwidth and bandwidth characteristics.

From my point of view, if I were evaluating a receiver's ability to copy a very weak signal compared to another receiver, what I would be interested in knowing is, what signal level at the antenna will produce a discernable sig-


from
MILLIWATTS to KILOWATTS
More Watts per Dollar



Taylor TUBES

**Quality
Transmitting
& Audio Tubes**


- COMMUNICATIONS
- BROADCAST
- INDUSTRY
- AMATEUR



Immediate Shipment from Stock

3CPX800A7	3CX15000A7	4CX5000A	813
3CPX5000A7	3CX20000A7	4CX7500A	833A
3CW20000A7	4CX250B	4CX10000A	833C
3CX100A5	4CX250BC	4CX10000D	845
3CX400A7	4CX250BT	4CX15000A	866-SS
3CX400U7	4CX250FG	4X150A	872A-SS
3CX800A7	4CX250R	YC-130	5867A
3CX1200A7	4CX350A	YU-106	5868
3CX1200D7	4CX350F	YU-108	6146B
3CX1200Z7	4CX400A	YU-148	7092
3CX1500A7	4CX800A	YU-157	3-500Z6
3CX2500A3	4CX1000A	572B	4-400A
3CX2500F3	4CX1500A	807	M328/TH328
3CX3000A7	4CX1500B	810	M338/TH338
3CX6000A7	4CX3000A	811A	M347/TH347
3CX10000A7	4CX3500A	812A	M382

- TOO MANY TO LIST ALL -




ORDERS ONLY:
800-RF-PARTS • 800-737-2787
Se Habla Español • We Export

TECH HELP / ORDER / INFO: 760-744-0700
FAX: 760-744-1943 or 888-744-1943

An Address to Remember:
www.rfparts.com

E-mail:
rfp@rfparts.com



RF PARTS COMPANY
Since 1967

nal at the speaker/phones. This is bandwidth dependent, so we can't ignore bandwidth. The noise power emerging from the speaker is a function of many factors, including shape factor, passband ripple and other factors that vary from receiver to receiver. But we don't have to specify these factors to characterize a particular receiver's ability to resolve weak signals. All we need to know is the noise power at the output at the chosen nominal bandwidth setting for the particular receiver in question so we can compare this measurement to another receiver of interest set at the same nominal bandwidth. It doesn't matter what the actual bandwidth is. The receiver's actual bandwidth is whatever it is, no matter what the nominal specification is. Comparing the NF of different receivers won't tell you how two receivers will perform relatively speaking unless the bandwidth characteristics of each are also specified. Then you will have some fun calculating the noise power in the speaker.

Cross Modulation

In the last 30 years, when it has come to third order distortion, the focus has shifted from cross modulation performance to two tone intermodulation performance. There was a time when cross modulation was the primary measurement.

For an IMD product to be detected, the generating signals have to be such that they add/subtract to leave a product in the wanted channel. In other than very heavy signal environments the probability of two discrete signals beating to leave products in-channel is low. It is more likely in a real world situation that a strong off-channel signal will cross modulate the wanted in-band signal. This could be a strong broadcast station or a CW signal, where the keying sidebands are impressed on the wanted signal. While cross modulation is a third order effect and can be vicariously measured by the IMD3 tests, it appears it is not given due consideration these days.

Summary

I believe the way test results are presented influences the way we think about receiver performance. From my point of view, what I would like to know is how sensitive a particular receiver is (what is the MDS) and at what point do IMD products (IL2 / IL3 / IL4 / IL5) begin to become a problem, and when does blocking (BL) show itself. These numbers can be directly used to compare receivers.

These numbers tell you almost everything you want to know. Dynamic range can be misleading as it is incomplete by itself. IP2 / IP3 are fictitious points. I suppose dynamic range sounds like a sexy number. It is normally a large number and is expressed in dB, which is a simpler notion to understand than dBm, and it doesn't have a negative sign in

front of it as does the IL2 and IL3 (usually) — negative signs are not very impressive!

I am hoping that the ARRL might begin to publish the IL2, IL3 and BL numbers as well as continue to publish MDS.

Front End Selectivity

There's an old saying: An ounce of prevention is worth a pound of cure. In times gone by, front end selectivity was a vital component in effecting strong signal performance. It in effect de-stressed the first mixer if not also the second. With the advent of strong mixers, narrow bandwidth post mixer filtering and the need for frequency agility and better receiver operability, front end selectivity became less important in the design of receivers. Personally, I believe this has not been a positive development.

It was not uncommon to find 3 to 4 ganged tuned circuits before the mixer in the old tube-based receivers such as in the then-state-of-the-art Collins R390 and the 75 series equipment.

Not all professional receiver designers followed the move away from the front end selectivity trend. For instance, Barrs felt front end selectivity was essential for receivers, particularly for those co-located with transmitters.⁶ He proposed a 4 gang tuned input circuit having a 20 dB to 27 dB attenuation 2.5% off tune (40 dB to 50 dB attenuation 5% off tune). Gikow went further and proposed cryogenic superconducting inductors for input filters to produce very high Q with bandwidths in the low kilohertz.⁷ This was for military applications. Extreme, certainly, but if you need it, you can get it.

It appears that after 30 or 40 years, Amateur Radio manufacturers are turning to front end selectivity to provide ultimate performance. For instance, the ICOM IC7800 and the Yaesu FT 1000MP Mark V have tracking preselectors. In the latter case, switching in the preselector reduces the MDS by 3 dB but increases the IP2 from 68 dBm to 102 dBm (IL2 goes from -28.5 dBm to -10 dBm).⁸ I have not seen the effect on third order performance published/measured. The preselector thus has a large impact on IMD performance without too much loss of sensitivity.

Peter Chadwick, in a May/June 2002 *QEX* article, asked the question "How much dynamic range do we need?"⁹ He used real world measured signal strength and density data to model the behavior of receivers in a high signal strength environment. Earlier papers by Winn and Sosin adopted a similar methodology but asked a slightly different question.^{10, 11, 12, 13, 14} How many signals can a receiver, with a specified IMD characteristic and specified front end filtering, resolve? Winn and Sosin both used real world signal

intensity and density data generated in Winn's case by Radio Suisse in 1968 and in Sosin's case from various unspecified reports and his own measurements. Using this data they were able to model the IMD product generation by receivers with specified dynamic ranges. A deficiency of this modeling was that only third order effects were studied and 2nd order effects were ignored (Sosin argued that input filtering mitigated this effect).

Winn set about demonstrating that high dynamic range circuitry was better than low dynamic range receivers with tuned front ends. In particular he was able to demonstrate that a receiver with an IMD ratio of 90 dB (measured with two 90 dBμV EMF signals applied to produce a 0 dBμV EMF product — equivalent to IP3 = +22 dBm) and a wide-band input filter was considerably superior to a receiver with an IMD ratio of 70 dB (measured with two 70 dBμV EMF signals applied to produce a 0 dBμV EMF product — equivalent to IP3 = -8 dBm) and a tuned filter with attenuation of 20 dB 12% off tune. However, his own figures demonstrated that adding a tuned input filter to the high dynamic range receiver would further increase the receiver's IMD performance and allow almost all of the available signals (that is, those above the antenna noise) to be resolved.

Sosin's aims were not that much different than Winn's and achieved similar results.

The study by Winn suggests that receivers with intercept points comparable to the best in today's world would benefit from selective front ends where weak signals are being copied.

Peter Chadwick's study was very interesting, highlighting that high noise figures are not a problem for HF and that effective (in the sense that it could be achieved with attenuation and not compromise the noise figure needs) IP3 levels of 20 to 30 dBm were required. The main question I have in regard to the study is about the input filters of the transceiver he used for the tests (a Yaesu FT102). I think this has an amateur band only receiver, so that the input filters are probably much narrower than sub-octave filters. To this degree, his results reflect not so much front end linearity but also front end selectivity to some extent.

(An interesting sidelight to these studies is that with each input filter/dynamic range combination, there is an optimum attenuator setting (which is non-zero) which maximizes signal resolution. The lower the front end selectivity the more the receiver benefits from input attenuation. Peter Chadwick's work demonstrated a similar phenomenon.) These three studies show that a receiver's performance is a function of both the receiver's internal characteristics and the signal environment in which it is "embedded."

Those designers putting aside front end

Table 1
Receiver Measurements Reported by Watson

	Noise Power for 40 dB NPR. (dBm/Hz)	Noise Figure (dB)	NPRFOM (dB/Hz)
Receiver A — Older tube design optimized for noise figure with broad input filter	-118	5	51
Receiver B — Modern design with high dynamic range mixers and RF amps with low pass input filter only	-99	10	65
Receiver C — Receiver B with suboctave filter	-86	7	81
Receiver D — Receiver B with preselector having 10% bandwidth	-77	10	87

selectivity argued that second order effects could be taken care of by octave front end filters and third order effects mitigated by the implementation of balanced front end circuits (RF amplifiers and mixers). This is true but the real world is not perfect, otherwise we would not be having this discussion and the ARRL nor anyone else would find it necessary to measure IL2 and IL3 and be concerned with IMD dynamic range. In reality, octave input filters don't have a rectangular response characteristic and balanced circuits are not always perfect.

It is commonly believed that 3rd order distortion is not a problem for far out signals, only for close in signals. It is not difficult to fabricate examples of both 2nd and 3rd order IMD using far out signals that will generate products that fall in-channel. If the off-channel signals are big enough or large enough in number it is not difficult to see how the receiver noise floor will be degraded — what might be termed dynamic sensitivity. Front end selectivity will ameliorate both far out 2nd and 3rd (and higher) order effects.

While strong mixer front ends using minimal front end selectivity give very good performance, if it is desired to squeeze that last ounce of performance from a receiver (after all, isn't this the premise of high end receiver design), then selective input circuits are necessary.

Noise Power Ratio

The previous discussion was about demonstrating the value of front end selectivity. It is also clear that receiver designers are giving more attention to front end selectivity. It would be interesting to know why. Is it because manufacturers are looking for a competitive edge? Do they recognize that mixer technology has gone as far as it can and that the next step in improving receiver performance is tracking preselectors? Is the market demanding more

effective front end selectivity?

If we are willing to accept that front end selectivity improves receiver performance, then I would argue the test regimes that are in use, such as the one the ARRL employs, discriminates against receivers that have strong front end selectivity. The battery of tests in use will not enable comparison of a receiver that has poor (that is wide band) front end selectivity to one that has strong front end selectivity. This is because the IMD tests are done at one or two close in offsets only and do not test the IMD response over a range of frequency separations. This means that two receivers with the same front end circuitry (mixer and RF amp) will perform the same on the tests, even though one may have superior front end selectivity.

In my original letter to *QST*, I suggested that the noise power ratio test as described by Watson might be a way of bringing front end selectivity into the receiver performance measurement equation.¹⁵ It is very difficult to find a great deal on this test technique in the literature. The earliest paper I have tracked down is by Dingley.¹⁶ The technique appears to have been used in the commercial receiver industry and it is only in the last few years that the academic literature has begun to mention the technique, albeit not in great detail. It appears also to be used for testing the intermodulation performance of RF power amplifiers. For example, see the *Microwave Journal* article by Katz.¹⁷ Peter Chadwick mentions its use in the testing of frequency division multiplexed telephone systems in the past.¹⁸

The technique requires feeding a receiver with high-power, wide-band white noise through a notch filter at the test frequency. The noise power in the receiver output is measured. The level of noise power that fills the notch stop band will be a function of the cross modulation and intermodulation (of all orders) distortion, reciprocal mixing performance of

From
MILLIWATTS
to **KILOWATTS**
More Watts per DollarSM

- **Wattmeters**
- **Transformers**
- **TMOS & GASFETS**
- **RF Power Transistors**
- **Doorknob Capacitors**
- **Electrolytic Capacitors**
- **Variable Capacitors**
- **RF Power Modules**
- **Tubes & Sockets**
- **HV Rectifiers**

ORDERS ONLY:
800-RF-PARTS • 800-737-2787
Se Habla Español • We Export

TECH HELP / ORDER / INFO: 760-744-0700
FAX: 760-744-1943 or 888-744-1943

An Address to Remember:
www.rfparts.com

E-mail:
rfp@rfparts.com

RF PARTS
COMPANY

the receiver and the front end selectivity. The more selective the receiver the lower will be the output noise power in the notch.

This is a fair test of receivers and would better reflect how they might perform relatively in real world signal environments.

The test would yield an all around figure of merit, which could account for receiver nonlinearity (intermodulation at all orders and cross modulation), reciprocal mixing and front end selectivity.

Watson defines the Notch Power Ratio:

$$\text{NPR} = \frac{\text{Out-of-notch noise power}}{\text{In-notch noise power}} \quad [\text{Eq 7}]$$

Watson then defined the Pnpr, which is the white noise input power spectral density (dBm/Hz) that produces a 40 dB NPR.

He then defined the Noise Power Ratio Figure of Merit (dB/Hz) as:

$$\text{NPRFOM} = \text{Pnpr} + 174 - \text{NF} \quad [\text{Eq 8}]$$

This NPRFOM is comparable to the dynamic range that is derived from the existing standard testing regime.

Watson reported some test work where he demonstrated how increasing the front end selectivity of a receiver directly resulted in significantly better NPRs. (See Note 15.) His results are summarized in Table 1. (The test was conducted on VHF/UHF receivers at 39 MHz.):

In comparing a receiver with a suboctave filter and one with a preselector, the tuned preselector degrades the receiver NF by 3 dB but significantly improves the NPRFOM (by 6 dB). The improvement in the NPRFOM of a receiver with a 10% bandwidth preselector compared to a receiver with a low-pass filter at the input is 22 dB. In an HF receiver, the loss in sensitivity would probably not be missed but the increase in IMD performance would be useful in high signal density environments.

This test work demonstrates that the technique will discriminate between receivers with different input selectivity and that input selectivity has a significant impact on receiver performance. The testing regime is also more representative of real world signal conditions and will provide a better insight as to how a particular receiver will behave in such conditions.

The above is not to argue for the abandonment of existing receiver performance testing regime. The existing regime while having measurement issues, has been time tested and provides useful information. However, it is deficient when it comes to providing

information which enables the comparison of receivers with different degrees of front end selectivity.

The NPR technique will more than likely require development. Matters such as the bandwidth of the applied white noise signal and the notch depth and bandwidth will need consideration.

Conclusion

I have suggested ways that receiver performance test results might be better presented so that focus can be directed to what matters in the comparison of receivers. I believe the concepts of the dynamic range and the intercept point, while very much ingrained in our thinking, can lead to confusion and lack of clarity. Some might think these suggestions trivial. However, I suggest that the ways we talk about receiver performance influences the ways we think about receiver design.

These days not too much reliance is placed on front end selectivity. Designers have relied on front end linearity to do the job. It is apparent though that if the ultimate performance is to be wrung from a receiver, front end selectivity becomes important in high signal density environments. It appears 40 meter work in Europe is still a challenge as is contesting and multi activity. If BPL takes hold (dare I speak these words), the average suburban listening post will become a signal quagmire despite the amateur bands being notched (a little like a street scale NPR test on your receiver!). And of course we have an upcoming turn up in the sunspot cycle which will multiply signal intensities and densities. If we begin to fairly test receivers, receivers with selective front ends will be seen in a new light.

The performance (in other words, the reception of weak signals in the presence of strong ones) of even the best receivers could well be enhanced by the use of outboard, highly selective filters.

Of course, the ultimate solution to an intractable IMD problem is to turn the set off and go have a game of golf!

Notes

¹Doug Smith, KF6DX, "In Search of New Receiver Performance Paradigms," Parts 1, 2 and 3, *QEX*, Nov/Dec 2006, Jan/Feb 2007 and Mar/April 2007.

²Ulrich Rohde, N1UL "Key Components of Modern Receiver Design," Parts 1, 2 and 3, *QST*, May 1994, June 1994 and July 1994.

³J. R. Sherwood and G. B. Heidleman, "Present-day Receivers — Some Problems and Cures," *ham radio*, Dec 1977.

⁴Henry Rech, "Modern Receiver Design," Technical Correspondence, *QST*, June 1995.

⁵R. S. Carson, *Radio Communications Concepts: Analog*, John Wiley and Sons, 1990.

⁶R. A. Barrs, "A Reappraisal of H.F. Receiver Selectivity," *The Radio and Electronic Engineer*, July 1982, Vol 52, No. 7.

⁷E. Gikow, "Wide Dynamic Range Preselectors," *IEEE Transactions on Aerospace and Electronic Systems*, Vol AES-2, No.1, Jan 1966.

⁸R. Lindquist, "Yaesu Mark V FT-1000 MP Tranceiver," Product Review, *QST*, Nov 2000, pp 64-69.

⁹P. Chadwick, "HF Receiver Dynamic Range: How Much Do We Need?" *QEX*, May/June 2002.

¹⁰R. F. E. Winn, "The Effect of Receiver Design in Communication Systems," *Proceedings of the IERE Conference on Radio Receivers and Associated Systems*, 1972, pp 193-204.

¹¹R. F. E. Winn, "Operational Aspects of H.F. Receiver Design," *Electronics and Power*, 13 June 1974.

¹²B. M. Sosin, "H.F. Communication Receiver Performance Requirements and Realization," *The Radio and Electronic Engineer*, Vol. 41, No. 7, July 1971.

¹³B. M. Sosin, "H.F. Receiver Reception Failure Factor," *Point-to-Point Communication*, Jan 1974.

¹⁴B. M. Sosin, "Performance of High Frequency Receiving Systems," *The Marconi Review*, First Quarter, 1976.

¹⁵R. Watson, "Receiver Dynamic Range Part II, Use One Figure of Merit to Compare Receivers," *Microwaves & RF*, Jan 1987.

¹⁶J. N. Dingley, "An Introduction to White Noise Testing of H.F. Receivers," *IERE Conference Proceedings No. 24*, July 1972, pp 227-241.

¹⁷A. Katz, "TWTA Linearization," *Microwave Journal*, April 1996.

¹⁸P. Chadwick, "In Search of New Receiver Performance Paradigms," Part 1 (Nov/Dec 2006)," *QEX*, Letters to the Editor, Jan/Feb 2007.

Henry Rech built his first crystal set when he was 10 years old (45 years ago). This stirred a lifelong passion for understanding and studying receiver design, although he has no academic technical qualifications as such. He has avoided becoming an Amateur Radio operator, but is fast running out of excuses with the demise of the CW test. In fact, he aims to complete his Australian advanced license exams in the next few months. He has a degree in economics and has had an involvement with the investment and mineral resources industries. He is currently a private financial markets trader, and enjoys sailing in his free time.



Optimum Lossy Broadband Matching Networks for Resonant Antennas

This analysis determines the optimum component values for obtaining a broadband match between a transmission line and an antenna, using a transformer and a resonator.

Reprinted by permission of the publisher, from *RF Design*, April 1990, pp 44-51, and July 1990, p 10.

This article was originally published in *RF Design* in 1990 and is reprinted here by permission of the publisher.¹ It is the primary reference for work AI1H has done on broadband matching documented in ARRL publications.^{2, 3, 4, 5, 6, 7, 8, 9} It is the only reference that contains the derivation of the pertinent formulas, and it ties it to the classic work on the subject by Fano.¹⁰

Examples of practical resonant antennas are the quarter-wave monopole, (n/2)-wavelength dipoles, where n is an odd positive integer, and the full-wave loop. Another example is a short non-resonant antenna, which has been made resonant by the addition of a reactive element. The resonant antenna has inherent broadband radiating properties, but its match bandwidth falls short of meeting requirements in many applications.

This paper addresses the problem of optimizing the design of a fixed matching network located between the transmission line and the resonant antenna. The matching network contains a transformer and a resonator. The analysis differs from previous results in that it yields explicit formulas, which provide maximum match bandwidth and which account for the incidental losses that are inherent in most practical matching networks.^{10, 11, 12} The goal of the optimization presented herein is to maximize the match

bandwidth for a given maximum standing wave ratio (SWR) over the operating band.

In his classic work, Fano¹⁰ addressed the same problem in a very general sense, but treated only the lossless case. Fano's generality included a wide class of load impedances and high order matching networks. He and others have observed that large match bandwidth improvements are possible with very simple matching networks.^{11, 13, 14} This paper treats such a case. A recent examination of the same single resonator matching network structure was reported by Hansen.¹² He recognized the importance of accounting for matching network loss, but did not include it explicitly in his evaluation. The value of the results described herein is that concise design formulas, which account for the losses in the matching network, are provided.

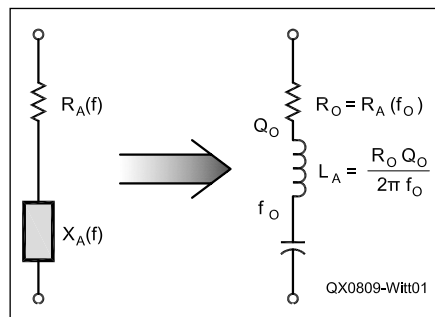


Figure 1 — Dipole approximate equivalent circuit used in the analysis. $R_A(f)$ includes both the radiation resistance and antenna losses.

Antenna Impedance

The analysis that follows applies to antennas whose impedance near resonance may be approximated by a series *RLC* circuit as shown in Figure 1. The use of this approximation makes the analysis tractable, and, as will be seen later, is accurate enough to provide useful design information. The results apply to the dual case as well, however this case will not be covered here.

It will be assumed that the real part of the antenna impedance, $R_A(f)$, does not vary much over the operating band. It is set equal to the value of the real part of antenna impedance at resonance, R_O . The antenna driving point impedance is thus established by three parameters: the resonant frequency, F_O , the real part of the antenna impedance at resonance, R_O , and the Q of the antenna at resonance, Q_O :

$$Q_O = \frac{F_O}{2R_O} \cdot \left. \frac{dX_A(f)}{df} \right|_{f=F_O} = \frac{2\pi F_O L_A}{R_O} \quad [\text{Eq 1}]$$

where L_A = antenna inductance.

Transformer Matching

Before treating the transformer/resonator matching case, it is helpful to consider the simplest form of matching network, which consists of a transformer whose bandwidth is large compared with the bandwidth of the resonant antenna.⁵ The topology, which assumes that the transformer losses are negligible, is shown in Figure 2A. Maximum bandwidth is not achieved when a perfect match (SWR = 1:1) exists at resonance. In Figure 3, the intentional mismatch at resonance is seen. That

¹Notes appear on page 40.

mismatch is achieved by driving the antenna with a generator whose impedance is greater than R_o , causing the SWR to equal S_L at resonance. A generator impedance lower than R_o will not yield optimum matching.

The analysis is facilitated by transforming the band-pass network of Figure 2A to the low-pass network of Figure 2B. The SWR versus frequency characteristic of Figure 3 shows the relationship between the band-pass and low-pass SWR characteristics. The midband frequency, F_o , is the geometric mean of the band edge frequencies, F_L and F_H . Of interest is the bandwidth, BW , at a particular SWR, S_M . The reflection coefficient looking from the line into the matching network is given by:

$$\rho(f) = \frac{R_o + j2\pi fL_A - Z_T N_z}{R_o + j2\pi fL_A + Z_T N_z} = \frac{(1 - S_L) + j\left(\frac{f}{F_o}\right)Q_o}{(1 + S_L) + j\left(\frac{f}{F_o}\right)Q_o} \quad [\text{Eq 2}]$$

where:

Z_T = transmission line characteristic impedance (ohms)
 N_z = transformer impedance ratio.

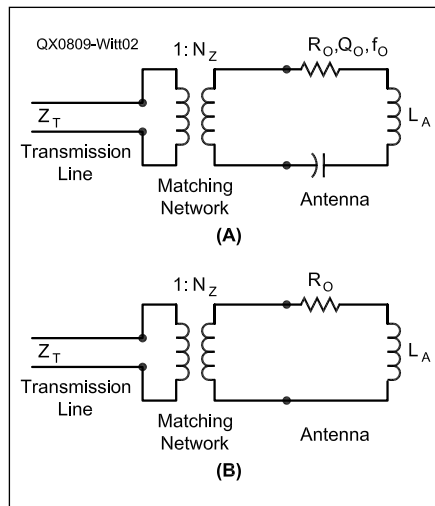


Figure 2 — Transformer matching. Part A shows the equivalent circuit. Part B shows the circuit after the band-pass to low-pass transformation.

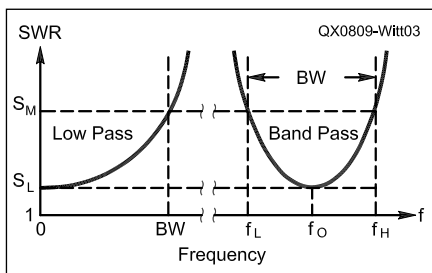


Figure 3 — SWR versus frequency for optimum transformer matching.

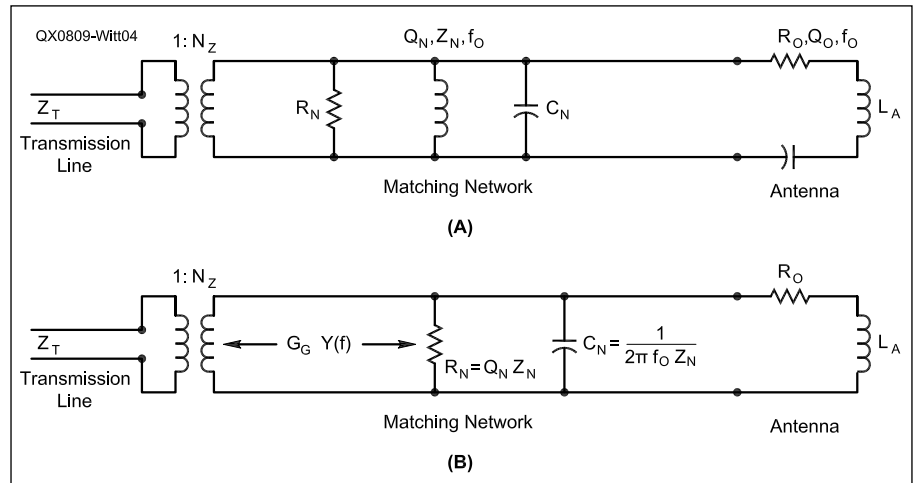


Figure 4 — Transformer/resonator matching. Part A shows the equivalent circuit and Part B shows the results after the band-pass to low-pass transformation.

Substituting $f = BW$ in Equation 2 and using

$$|\rho(BW)| = \frac{S_M - 1}{S_M + 1} \quad [\text{Eq 3}]$$

yields

$$BW = \frac{F_o}{Q_o} \left[\left(S_M + \frac{1}{S_M} \right) S_L - S_L^2 - 1 \right]^{\frac{1}{2}} \quad [\text{Eq 4}]$$

It is useful to define the normalized bandwidth, B_N , to be the product of the fractional bandwidth and the antenna Q :

$$B_N = \frac{BW}{F_o} \cdot Q_o \quad [\text{Eq 5}]$$

Also, the normalized reference bandwidth, B_{Nref} is defined to be the normalized bandwidth for the case when the antenna is perfectly matched at resonance. Using Equation 4 for $S_L = 1$ yields:

$$B_{Nref} = \frac{S_M - 1}{\sqrt{S_M}} \quad [\text{Eq 6}]$$

By setting

$$\frac{dB_N(S_L)}{dS_L} = 0$$

the value of S_L, S_{Lopt} , which gives the maximum bandwidth, may be determined:

$$S_{Lopt} = \frac{1}{2} \left(S_M + \frac{1}{S_M} \right) \quad [\text{Eq 7}]$$

Substitution yields the maximum normalized bandwidth, B_{Nmax} :

$$B_{Nmax} = \frac{1}{2} \left(S_M - \frac{1}{S_M} \right) \quad [\text{Eq 8}]$$

The required transformer impedance ratio is:

$$N_z = \frac{R_o}{2Z_T} \left(S_M + \frac{1}{S_M} \right) \quad [\text{Eq 9}]$$

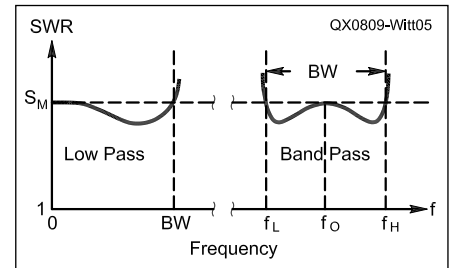


Figure 5 — SWR versus frequency for optimum transformer/resonator matching.

The improvement in match bandwidth with transformer matching is modest. If $S_M = 2:1$, for example, by deliberately mismatching at resonance so that $S_L = S_{Lopt} = 1.25:1$, the 2:1 SWR bandwidth is improved by only about 6%.

Transformer/Resonator Matching

In dramatic contrast to transformer matching, a matching network using a transformer in combination with a resonant circuit yields a significant improvement in match bandwidth. It is important, however, to properly account for losses in the matching network since these losses will influence the values of the design parameters in most practical applications. Fortunately, though somewhat tedious to derive, the results may be expressed as explicit formulas.

The antenna system for this case is shown in Figure 4A. In the matching network, the transformer is used to deliberately raise the generator impedance seen by the antenna at midband to a high but acceptable value. The resonant circuit, which has the same resonant frequency as the antenna, is used to partially compensate for the reactance of the antenna for frequencies away from resonance. All of the losses in the matching network are rep-

represented by the Q of the matching network resonator, Q_N . In addition to the transmission line and antenna parameters, Q_N is assumed to be known.

The same analysis approach used in the transformer matching case is used here. Refer to Figure 5. The parameters of the matching network are chosen so that the SWR at mid-band and at the band edges equals S_M . The optimization process involves determining the transformer impedance ratio, N_Z , and the matching resonator impedance level, Z_N , so that maximum bandwidth is achieved. Z_N is the impedance of the resonator inductor or capacitor at the antenna resonant frequency. [In subsequent writing, including Chapter 9 of *The ARRL Antenna Book*, the author changed the notation for the matching network impedance level (the reactance of the matching inductor or matching capacitor at antenna resonance) from Z_N to X_{NO} . We did not make that change in this article.—Ed.]

Referring to the low-pass equivalent circuit of Figure 4B, at dc:

$$N_Z = \frac{S_M Q_N Z_N R_O}{Z_T (Q_N Z_N + R_O)} \quad [\text{Eq 10}]$$

Implicit in this equation is the assumption that the optimum condition occurs when the SWR is equal to S_M at the center of the band as well as at the band edges. The author has been able to prove this for the lossless case and has been unable to disprove it for the lossy case.

The matching network loss, L_{MN} , is defined as the ratio, expressed in decibels, of the total power delivered by the transmission line to the power delivered to the antenna load. It is given by:

$$L_{MN} = 10 \log \frac{G_A + \left(\frac{1}{Q_N Z_N} \right)}{G_A} \quad [\text{Eq 11}]$$

where G_A is the antenna conductance, which is given by:

$$G_A = \frac{1}{R_O \left\{ 1 + \left[\left(\frac{f}{F_O} \right) Q_O \right]^2 \right\}} \quad [\text{Eq 12}]$$

Thus:

$$L_{MN} = 10 \log \left\{ 1 + \frac{R_O}{Q_N Z_N} \left\{ 1 + \left[\left(\frac{f}{F_O} \right) Q_O \right]^2 \right\} \right\} \quad [\text{Eq 13}]$$

In the band-pass domain, at midband:

$$L_{MNO} = 10 \log \left(1 + \frac{R_O}{Q_N Z_N} \right) \quad [\text{Eq 14}]$$

and at the band edges:

$$L_{MNE} = 10 \log \left[1 + \frac{R_O}{Q_N Z_N} (1 + B_N^2) \right] \quad [\text{Eq 15}]$$

For any application, the matching network loss is highest at the edges of the band, so L_{MNE} will usually be the most important loss parameter.

The expressions for transformer impedance ratio and matching network loss pertain to the topology of Figure 4A and are very general. They apply for any matching network impedance level and normalized bandwidth. Some expressions for impedance level, normalized bandwidth and band edge loss for cases of particular interest are presented next.

Maximum Bandwidth

It is possible to write an explicit expression that relates Z_N and B_N . This is done by first determining the generator conductance, G_G , necessary to achieve SWR = S_M at resonance.

$$G_G = \frac{R_O + Q_N Z_N}{S_M R_O Q_N Z_N} \quad [\text{Eq 16}]$$

The admittance, $Y(f)$, facing the generator is given by:

$$Y(f) = \frac{1}{Q_N Z_N} + j \frac{f}{F_O Z_N} + \frac{1}{R_O \left[1 + j \left(\frac{f}{F_O} \right) Q_O \right]} \quad [\text{Eq 17}]$$

The magnitude of the reflection coefficient is then:

$$|\rho(f)| = \frac{|Y(f) - G_G|}{|Y(f) + G_G|} = \frac{SWR - 1}{SWR + 1} \quad [\text{Eq 18}]$$

At the band edges, $f = BW$ and SWR = S_M . With these substitutions, the general expressions for B_N and Z_N may be derived:

$$B_N = \left[2 \left(S_M + \Delta \right) \frac{Z_N Q_O}{R_O S_M} - \left(\frac{Z_N Q_O}{R_O S_M} \right)^2 - 1 \right]^{\frac{1}{2}} \quad [\text{Eq 19}]$$

and

$$Z_N = \frac{R_O S_M}{Q_O} \left\{ S_M + \Delta \pm \left[(S_M + \Delta)^2 - 1 - B_N^2 \right]^{\frac{1}{2}} \right\} \quad [\text{Eq 20}]$$

where:

$$\Delta = \frac{Q_O}{2 Q_N} \left(S_M - \frac{1}{S_M} \right)$$

Note that for the lossless matching network case, $\Delta = 0$. The optimum impedance level, Z_{Nopt} , which yields the maximum bandwidth, is determined by setting

$$\frac{dB_N(Z_N)}{dZ_N} = 0 \quad [\text{Eq 21}]$$

and solving for Z_N .

The maximum normalized bandwidth, B_{Nmax} is:

$$B_{Nmax} = \left[(S_M + \Delta)^2 - 1 \right]^{\frac{1}{2}} \quad [\text{Eq 22}]$$

The large bandwidth enhancement obtained by using the transformer/resonator matching network is seen from the following example: For the lossless case and $S_M = 2:1$,

$$B_{Nref} = \frac{1}{\sqrt{2}} \quad \text{and} \quad B_{Nmax} = \sqrt{3}.$$

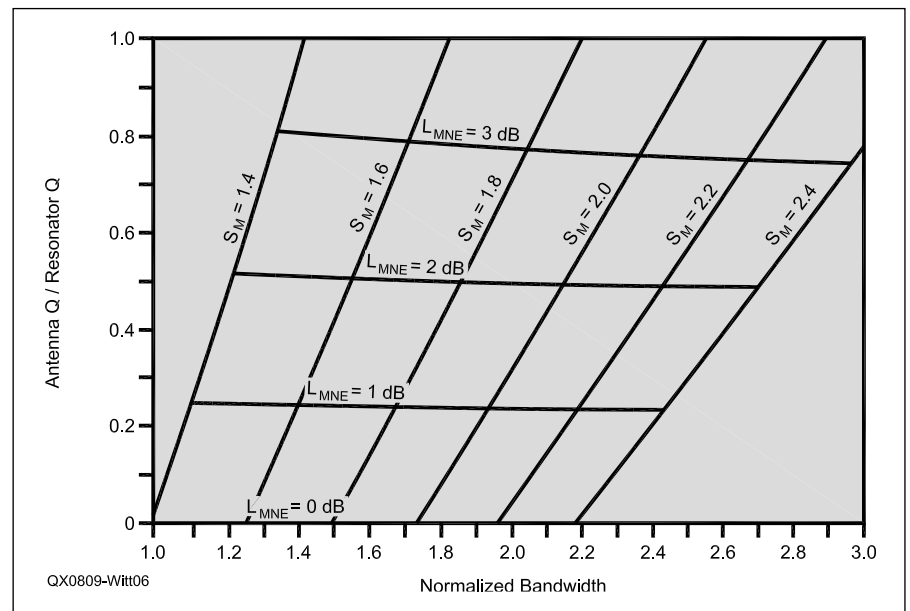


Figure 6 — Tradeoff between bandwidth, match quality and matching network loss.

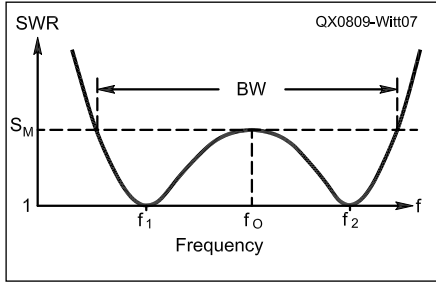


Figure 7 — Perfect match at two frequencies.

Hence, the bandwidth is increased by a factor of 2.45 over the case of a dipole matched at resonance. It is clear from Equation 22 that the bandwidth is increased even further when a lossy matching network is used.

The matching network loss at the band edges, L_{MNE} , is given by:

$$L_{MNE} = 10 \log \left\{ 1 + \frac{Q_o}{Q_N} \left[\frac{Q_o}{2Q_N} \left(1 - \frac{1}{S_M^2} \right) + 1 \right] \right\} \quad [\text{Eq 23}]$$

Notice the weak dependence on S_M . For cases when the matching network resonator Q is at least an order of magnitude greater than the antenna Q , the band edge loss simplifies to:

$$L_{MNE} = 10 \log \left(1 + \frac{Q_o}{Q_N} \right) \quad [\text{Eq 24}]$$

The above analysis provides the basis for a graphical representation of the relationship between normalized bandwidth, matching network loss,

$$\frac{Q_o}{Q_N}$$

and S_M . See Figure 6. For a particular application, where antenna Q and matching network resonator Q are given, this figure is very useful for quickly determining the tradeoff among match quality, bandwidth and matching network loss.

In most practical situations, the operating band over which matching is desired is given. In those cases, one wishes to know the best match achievable, S_{Mmin} , for a given normalized bandwidth, B_N . Solving Equation 22 for S_M yields:

$$S_{Mmin} = \frac{(B_N^2 + 1)^{\frac{1}{2}} + \left\{ B_N^2 + 1 + \left(\frac{2Q_o}{Q_N} \right) \left[1 + \left(\frac{Q_o}{2Q_N} \right) \right] \right\}^{\frac{1}{2}}}{2 \left[1 + \left(\frac{Q_o}{2Q_N} \right) \right]} \quad [\text{Eq 25}]$$

Minimizing Matching Network Loss

For situations where either the maximum possible bandwidth or minimum possible SWR is not required, Equation 20 may be used to determine the necessary value of Z_N . Notice that for values of normalized bandwidth less than B_{Nmax} there are two values of

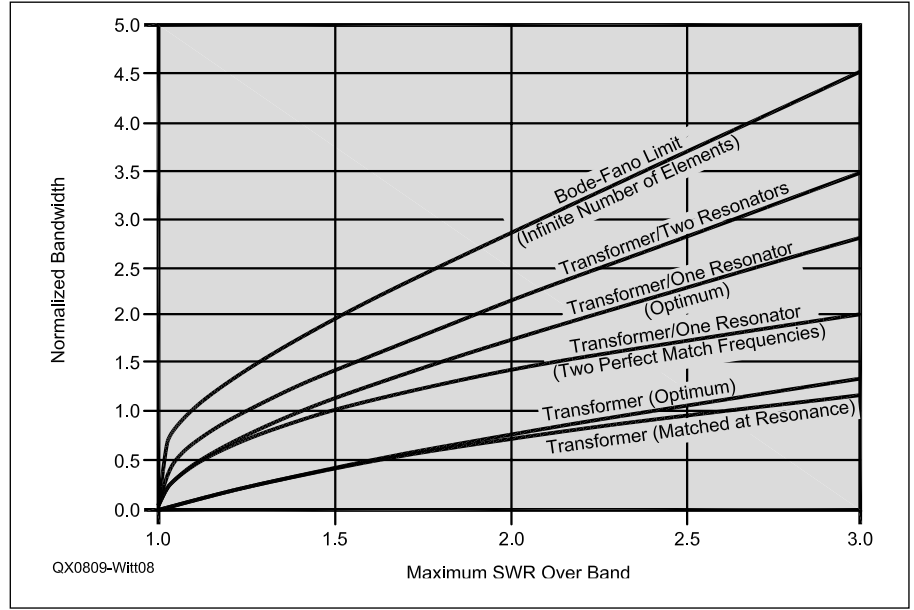


Figure 8 — Normalized bandwidth versus maximum SWR over the band for the lossless matching network case.

Z_N . The larger one is usually selected in order to minimize the matching network loss. An example later will show the potentially large impact of making the proper selection.

Perfect Matching at Two Frequencies

It is possible to find a value of Z_N that provides a perfect match at two frequencies, as seen in Figure 7.² For this case,

$$Z_N = \frac{R_o}{Q_o} \left[S_M + \frac{Q_o}{Q_N} (S_M - 1) \right] \quad [\text{Eq 26}]$$

and

$$B_N = (S_M - 1)^{\frac{1}{2}} \left\{ 2 + \frac{Q_o}{Q_N} \left[2 + \left(1 + \frac{Q_o}{Q_N} \right) \left(1 - \frac{1}{S_M} \right) \right] \right\}^{\frac{1}{2}} \quad [\text{Eq 27}]$$

This case may satisfy a special need, but it yields smaller bandwidth and more loss than the case presented in the previous section. For the case when $S_M = 2:1$, the achievable bandwidth is about 18% smaller than the maximum attainable with the same topology. This result is analogous to the transformer matching case, where obtaining perfect match at a frequency within the band does not yield maximum bandwidth.

The perfect match frequencies are given by:

$$F_1 = (F_o^2 + F_M^2)^{\frac{1}{2}} - F_M \quad [\text{Eq 28}]$$

and

$$F_2 = \frac{F_o^2}{F_1} \quad [\text{Eq 29}]$$

where:

$$F_M = \frac{F_o}{2Q_o} \left[\left(1 + \frac{Q_o}{Q_N} \right) (S_M - 1) \right]^{\frac{1}{2}}$$

Comparison with Earlier Results

Much has been reported regarding the design of optimum matching networks when the load is complex. In these analyses, the assumption has usually been made that the matching network is made up of lossless elements. In order to compare the results of this investigation with the earlier results, it is necessary to set $\Delta = 0$. The comparison may be made by showing the relationship between the normalized bandwidth and S_M , the maximum SWR over the operating band; see Figure 8.

Equation 6 and Equation 8 provide the required formulas for the dipole matched at resonance and optimum transformer matching, respectively. For the case of transformer/resonator optimum bandwidth matching, from Equation 22,

$$B_{Nmax} \Big|_{\Delta=0} = (S_M^2 - 1)^{\frac{1}{2}} \quad [\text{Eq 30}]$$

For the case of transformer/resonator matching with two perfect match frequencies, from Equation 27,

$$B_N \Big|_{\Delta=0} = [2(S_M - 1)]^{\frac{1}{2}} \quad [\text{Eq 31}]$$

In addition to the relationships derived above, Figure 8 gives the Bode-Fano limiting case, which shows the maximum bandwidth theoretically attainable with an infinite number of elements in the matching network.¹⁰ For this case,

$$B_{Nmax} = \frac{\pi}{\ln \left(\frac{S_M + 1}{S_M - 1} \right)} \quad [\text{Eq 32}]$$

The cases of transformer and transformer/resonator matching for maximum bandwidth exactly coincide with Fano's results for the equivalent situations; his results were achieved using a more general technique, which involved a graphical solution for the final result. (See Note 10.) Incidentally, the terminology of Fano is different than that used in this paper, but the necessary translations were made to prepare Figure 8.

For comparison, the case that shows how much additional bandwidth could be obtained if one more resonator were added to the matching network is also given in Figure 8. This result is derived from Fano and Levy; the two-resonator topology is shown in Figure 9. (See Notes 10 and 11.) It has been shown that the analytically derived matching network optimization is not always optimum.^{15, 16} Thus, for the two-resonator case, the curve shown may not be optimum, however, for the lossless matching network cases presented in this paper, it may be shown that the true optimum has indeed been found.

Practical Matching Networks

Two types of matching networks are presented: an LC network and a transmission line resonator. Each is based on the transformer/single resonator topology of Figure 4A. The lumped LC resonator/transformer exhibits low matching network loss and has the potential for providing the balun function, allowing an unbalanced feed line to drive a balanced antenna without radiation from the feed line. The transmission line resonator may lead to more loss, but has the advantage that it may be integrated with the radiator.

In order to illustrate some of the important practical points associated with the design of a matching network, a specific example will be considered. The antenna to be matched is a half-wave dipole in free space resonant at 4 MHz. The desired operating bandwidth is 500 kHz. The method of moments using the program, *MININEC*, was used to compute the driving point impedance of an uncompensated version of the antenna to be matched.¹⁷ The effect of the simplifying assumptions made through the use of the antenna model of Figure 1 may thus be seen. In practice, one may estimate R_o and Q_o , or better still, build the uncompensated version of the antenna and measure its feed point impedance prior to a final design of the matching network.

In the examples that follow, unless otherwise noted, the designs achieve the minimum SWR over the operating band. Other assumptions are:

$$F_L = 3.758 \text{ MHz}$$

$$F_H = 4.258 \text{ MHz}$$

$$Z_T = 50 \Omega$$

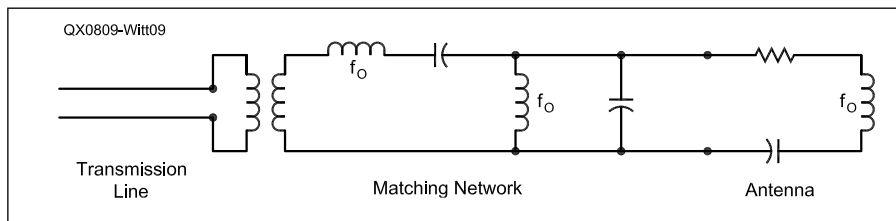


Figure 9 — Transformer/two-resonator matching.

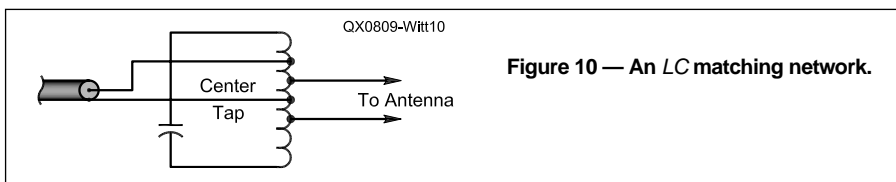


Figure 10 — An LC matching network.

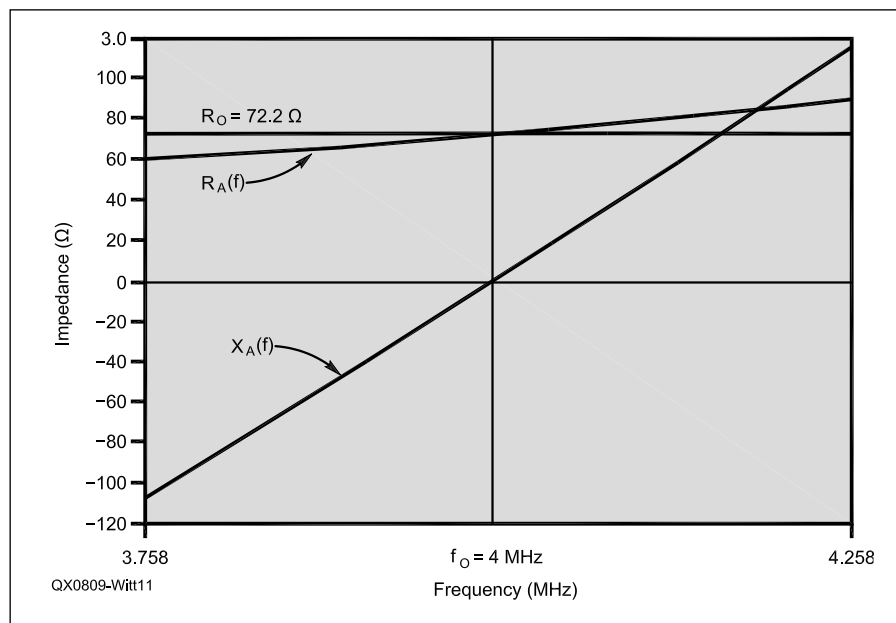


Figure 11 — Impedance versus frequency for a 4 MHz half-wave dipole in free space.

LC Matching Network

A practical LC matching network is shown in Figure 10. (See Note 2.) The function of a transformer is realized by providing primary and secondary taps on the coil. For the case when a coaxial transmission line is used and the resonant antenna load is balanced, such as a symmetrically-situated center-fed half-wave dipole, the network also serves as a balun. This is accomplished by connecting the shield of the coaxial cable to the center tap of the coil. By connecting the capacitor as shown in the figure, an optimum selection of matching network components may be made. In effect, the inductor is an autotransformer with three functional windings: a primary, a secondary and a capacitor winding.

Figure 11 shows the computed impedance of the 4 MHz half-wave dipole for the case when it is made of no. 14 AWG wire (diameter = 0.064 inch). Forty segments were used in the computer analysis. From these data, the antenna Q and radiation resistance at resonance are determined:

$$Q_o = 12.2$$

$$R_o = 72.2 \Omega$$

$$\text{Dipole length} = 120.1 \text{ feet}$$

By assuming $Q_N = 300$, which is a readily attainable value in most practical situations, the following results are obtained:

$$F_o = 4 \text{ MHz}$$

$$S_{Mmin} = 1.798:1$$

$$Z_{Nopt} = 19.41 \Omega$$

$$N_Z = 2.58:1$$

$$L_{MNE} = 0.176 \text{ dB}$$

After selecting the capacitor, the tapped inductor of Figure 10 may be designed. This procedure will not be covered here. It is important to realize that the components chosen must be capable of withstanding the large electrical stresses encountered when high transmitted power is involved. In the author's experience, high radio frequency currents that flow in the capacitor in this kind of service place particularly high demands on that component.

Figure 12A shows the SWR and matching network loss versus frequency characteristic for this example when the idealized *RLC* dipole model is assumed. Also shown for comparison is the SWR of a dipole when optimum transformer matching is employed. It is noteworthy from Figure 12B that when the actual dipole impedance frequency dependence is accounted for, the differences in SWR and loss are small. Note also from Figure 12D that the SWR characteristic may be made symmetrical by a slight perturbation of the dipole resonant frequency (-0.15%), and an increase of the resonator natural frequency ($+0.6\%$).

Transmission Line Resonator Matching Network

Another way to realize a transformer/resonator is to use a resonant length of transmission line. (See Notes 3 and 4.) The simplest form is a transmission line one-quarter wavelength long terminated with a short circuit at one end and an open circuit at the other end. In what follows, this form of resonator will be used, although there are applications where longer transmission line resonators could be used. In these latter cases, the power handling capacity of the matching network would be larger, but the resonator *Q* would be unchanged from the quarter-wave case.

Figure 13 shows a quarter-wave resonator/transformer.^{7,8} By driving and loading the resonator at different points, the function of a transformer is realized. The resonator has a *Q* that is related to the loss of the transmission line at the resonant frequency:

$$Q_N = \frac{2.774F_o}{AV} \quad [\text{Eq 33}]$$

where:

A = transmission line attenuation at $f=F_o$ (dB/100 feet)

V = velocity factor.

It is worth noting that since $A \propto \sqrt{f}$ for many transmission lines, $Q_N \propto \sqrt{F_o}$ (approximately). Hence, using the same cable type, higher *Q* values are obtained at higher frequencies. First order approximations to the equivalent circuit parameters are:

$$Z_N = \frac{4Z_R}{\pi} \sin^2 \theta_s \quad [\text{Eq 34}]$$

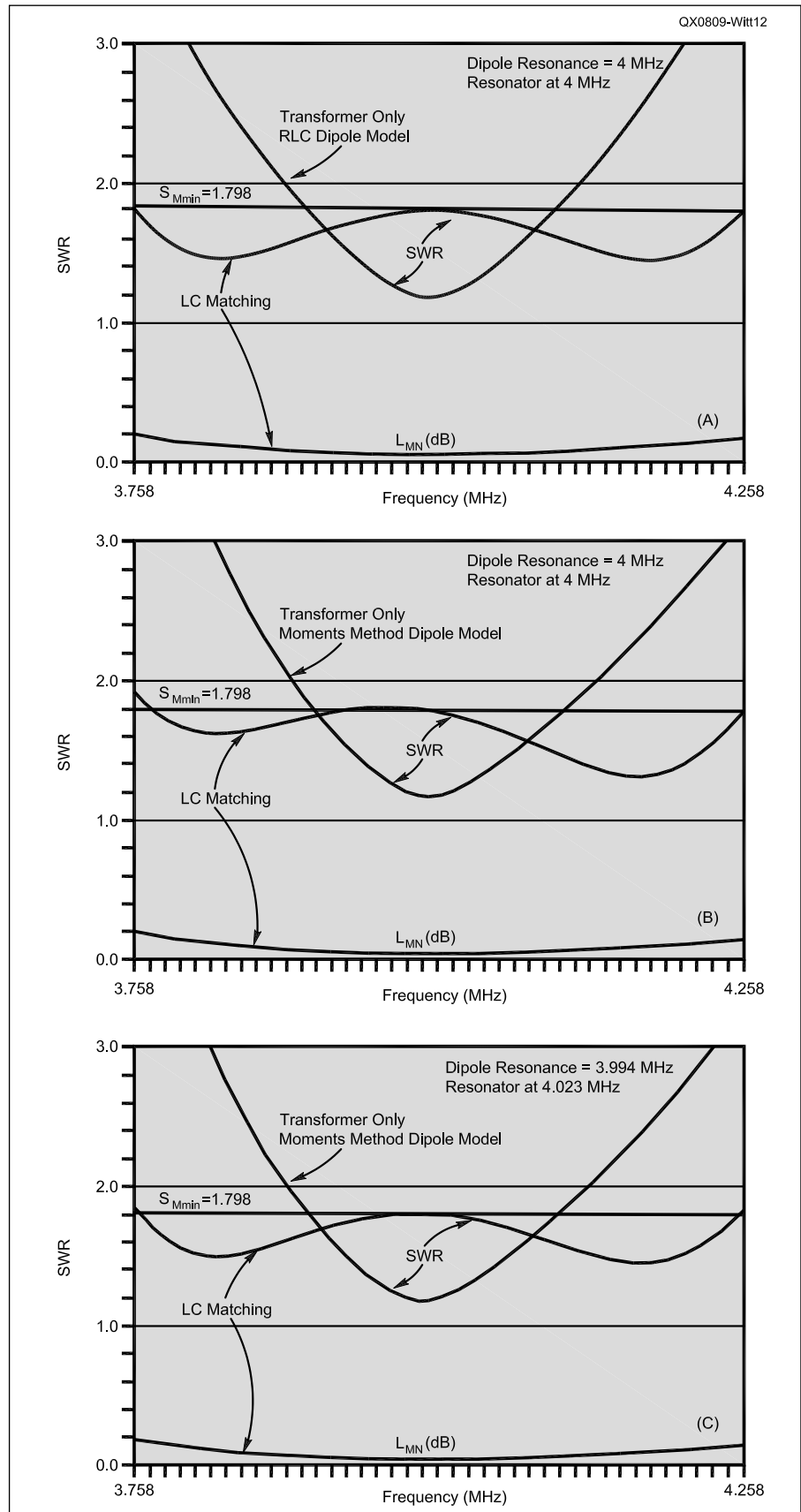


Figure 12 — SWR and matching network loss for LC matching network example. Part A shows the calculated matching network parameters, *RLC* dipole model. Part B shows the calculated matching network parameters, moments method dipole model. Part C shows the perturbed dipole and matching network resonances, moments method dipole model.

and:

$$N_Z = \frac{\sin^2 \theta_S}{\sin^2 \theta_P} \quad [\text{Eq 35}]$$

where:

Z_R = characteristic impedance of the resonator transmission line (ohms), and θ_S and θ_P are the electrical angles of the secondary and primary taps, respectively, measured from the shorted end of the resonator.

These approximations are useful only if other significant resonances are well separated from the band of interest. For example, the anti-resonance of the open stub occurs above the operating band and as the secondary tap approaches the short, that frequency approaches the operating band of the antenna system. In most practical cases, however, the equivalent circuit shown provides a sufficiently accurate initial set of matching network parameter values.

The application of the quarter-wave resonator/transformer as a matching network is shown in Figure 14. First the electrical angles (in radians), θ_S and θ_P , are determined:

$$\theta_S = \sin^{-1} \left(\frac{\pi Z_N}{4Z_R} \right)^{\frac{1}{2}} \quad [\text{Eq 36}]$$

and

$$\theta_P = \sin^{-1} \left(\frac{\pi Z_N}{4Z_R N_Z} \right)^{\frac{1}{2}} \quad [\text{Eq 37}]$$

These results are used to determine the lengths (in feet) of the transmission line segments as defined in Figure 14:

Shorted stub:

$$L_S = \frac{492V\theta_P}{\pi F_O} \quad [\text{Eq 38}]$$

Link:

$$L_L = \frac{492V\theta_S}{\pi F_O} - L_S \quad [\text{Eq 39}]$$

Open stub:

$$L_O = \frac{246V}{F_O} - L_S - L_L \quad [\text{Eq 40}]$$

Incidentally, it may be shown that L_S is independent of R_O , a fact that may be used to advantage in a situation when R_O is not known accurately.

The Coaxial Resonator Match

By recognizing that the fields and currents in a resonator made from coaxial cable are mostly confined to be within the cable, one can, in effect, integrate the resonator within the antenna radiator. This has been called the *coaxial resonator match* and is shown in Figure 15 for the case of a half-wave dipole.³

⁴ Note that the elements of the matching network in Figure 14 are contained within the structure. Currents flowing on the inside of the resonator shield are associated with the

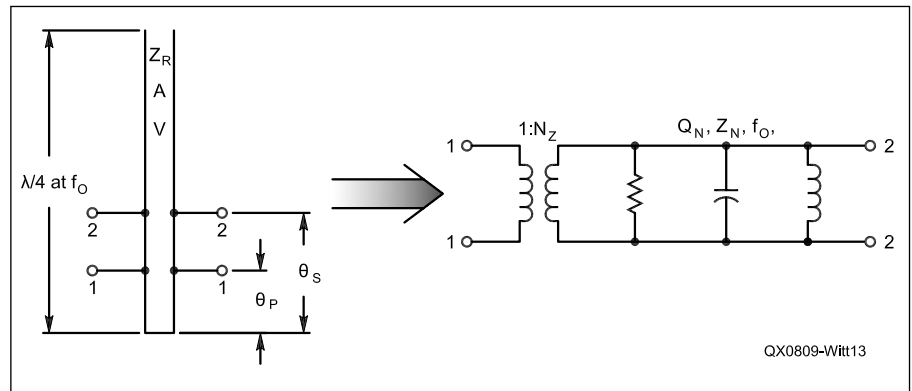


Figure 13 — The quarter-wave resonator/transformer.

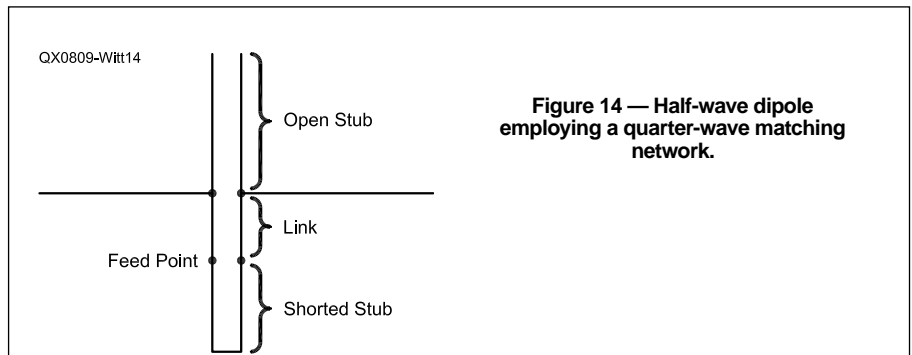


Figure 14 — Half-wave dipole employing a quarter-wave matching network.

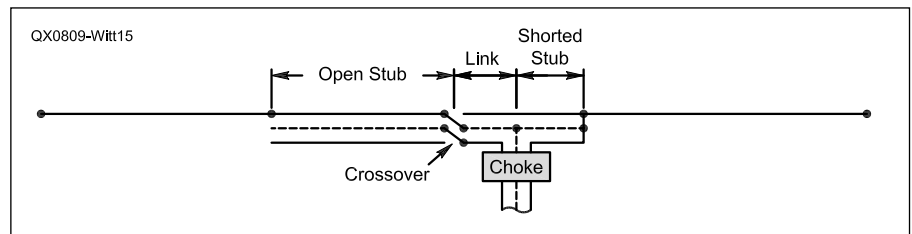


Figure 15 — The coaxial resonator match.

resonator; currents flowing on the outside of the shield are the usual dipole radiator currents. Radiation from the feed line, which is connected off-center for the above design equations to apply, is avoided by the use of a longitudinal choke as seen in the figure. A minor modification of the design procedure would permit the feed line to be connected to the physical center of the antenna but this would not eliminate the desirability of a longitudinal choke when an arbitrary length of feed line is used.

In Figure 15 the extensions necessary to build out the antenna length to one-half wavelength are made from wire. These lengths could be made from the same coaxial cable material as the resonator; the results are similar. Assuming that the entire dipole is made from RG213U coaxial cable (shield diameter = 0.3 inch), the following design input parameters were derived using MININEC:

$$Q_O = 10.2$$

$$R_O = 72.1 \Omega$$

$$\text{Dipole length} = 119.5 \text{ feet}$$

$$\text{For RG213U cable,}$$

$$Z_R = 50 \Omega$$

$$A = 0.4 \text{ dB}/100 \text{ feet at } 4 \text{ MHz}$$

$$V = 0.66$$

Hence, $Q_N = 42.0$, leading to the following results:

$$F_O = 4 \text{ MHz}$$

$$S_{\text{Mmin}} = 1.516:1$$

$$Z_{\text{Nopt}} = 17.36 \Omega$$

$$N_Z = 1.99:1$$

$$L_{\text{MNE}} = 1.00 \text{ dB}$$

$$L_S = 9.8 \text{ feet}$$

$$L_L = 4.4 \text{ feet}$$

$$L_O = 26.4 \text{ feet}$$

Figure 16A shows the SWR and matching network loss for the case when the RLC dipole model and lumped matching network approximation are used. In Figure 16B, a simulation program that uses the MININEC-derived dipole model and an accurate representation of the transmission line segments

was used to determine the SWR and matching network loss. One observes that the simulation yields results that closely match those predicted from the approximate analysis. An interesting observation is that a degree of serendipitous self-compensation for the imperfections of the lumped element dipole and matching network models takes place when a moments method dipole model and transmission line matching network are used. This is made clear when Figure 12B (where self-compensation is not present) and Figure 16B are compared.

A matter of practical interest is the electrical stress on the coaxial cable in this application. At 4 MHz, the loss in the cable is primarily resistive. To accurately calculate the current and voltage distribution within the resonator, it is necessary to use the complex value of characteristic impedance, Z_R . The segment lengths associated with Figure 16B were used. When the total power into the antenna plus matching network is one kilowatt, the maximum equivalent power stress (occurring at the low end of the operating band) is 12.5 kW. It is the current in the center conductor that places the highest stress on the cable. The peak voltage at the open circuit occurs at the high end of the operating band. When the total power into the antenna plus matching network is one kilowatt, this voltage is 826 V.

Minimizing Matching Network Loss

In many applications, the allowable SWR over the operating band is larger than the minimum achievable SWR, S_{Mmin} . By designing for this larger SWR, lower matching network loss may be obtained. The matching network loss may be improved by using Equation 20 to find Z_N . An example will illustrate this point.

In the previous example, the SWR over the 500 kHz operating band was 1.516:1. It will be assumed that the application allows, instead, $SWR < 2.1$. Using Equations 10, 15 and 20, the following results are obtained:

$$Z_N = 51.5 \Omega$$

$$N_Z = 2.79:1$$

$L_{MNE} = 0.36$ dB (compared to 1.00 dB for the "optimum" case)

Note that in the use of Equation 20, the "+" root was chosen in order to minimize the loss. This case is shown in Figure 17A when the approximate dipole and lumped element coaxial resonator match models are used. The more accurate dipole and matching network models were used to obtain the results of Figure 17B. By perturbing the dipole resonant frequency and segment lengths, an SWR shape similar to that of Figure 17A is obtained, as shown in Figure 17C.

The electrical stress on the resonator coaxial cable is reduced when match quality is traded for improved matching network

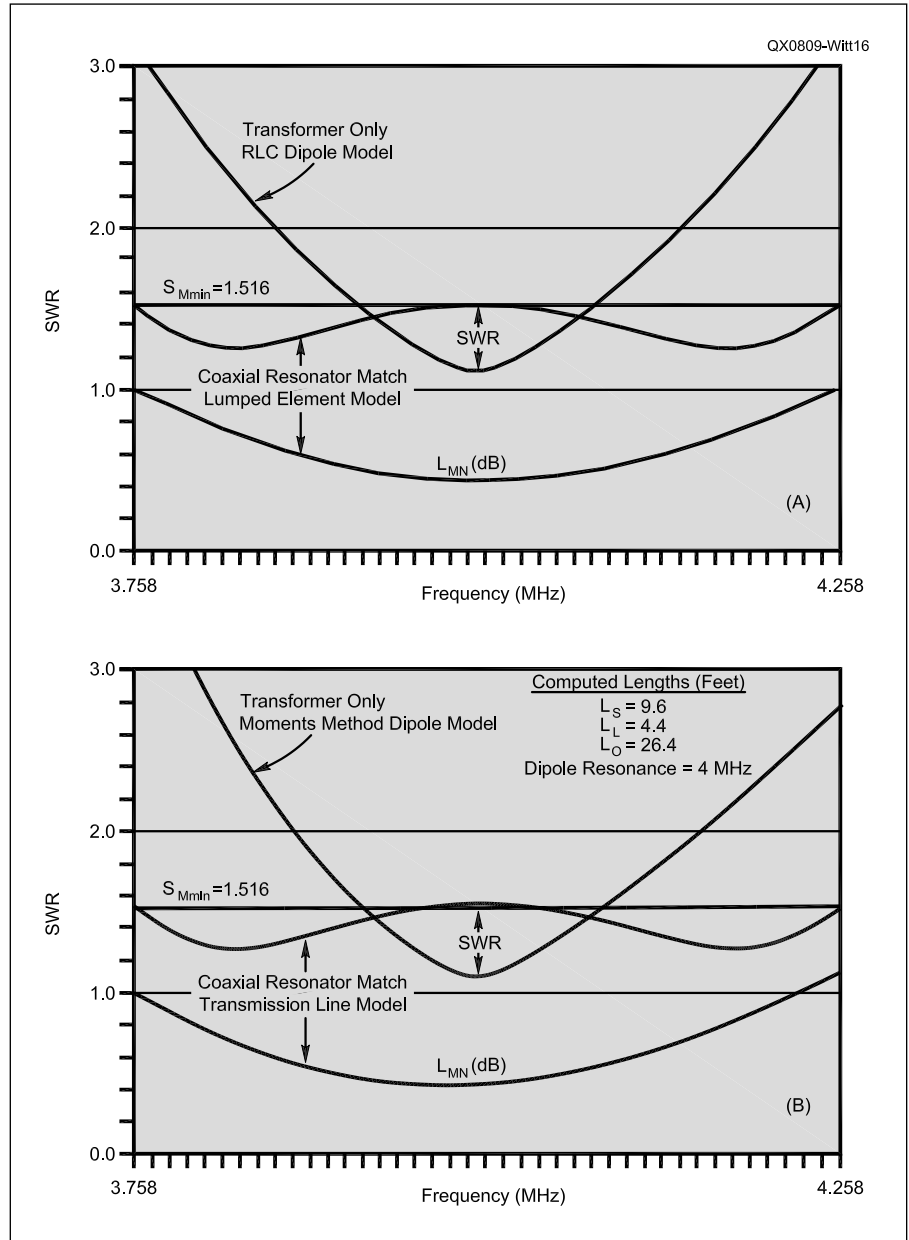


Figure 16 — SWR and matching network loss for coaxial resonator match example. Part A shows the RLC dipole model and lumped element matching network. Part B shows the moments method dipole model and transmission line matching network.

loss. For the case of Figure 17C, when the total power into the antenna plus matching network is one kilowatt, the maximum equivalent power stress is 6.2 kW and the peak voltage at the open is 507 V (compared to 12.5 kW and 826 V, respectively, for the "optimum" case of Figure 16B).

If the "-" root had been chosen, the following parameters would have been obtained:

$$Z_N = 10.2 \Omega$$

$$N_Z = 2.47:1$$

$$L_{MNE} = 1.59 \text{ dB}$$

Compare this result, shown in Figure 18, with Figure 17A; the matching network loss is higher by a factor of 4.4. In general, the

solution that yields the highest value of Z_N will have the lowest loss.

Conclusion

An important matching network for resonant antennas has been analyzed in detail. The importance stems from the large match improvement that a simple transformer/resonator matching network provides. The degree of improvement relative to simple transformer matching on one end and higher order matching on the other has been provided. Design equations, which account for the losses in the matching network, have been derived and applied to specific examples.

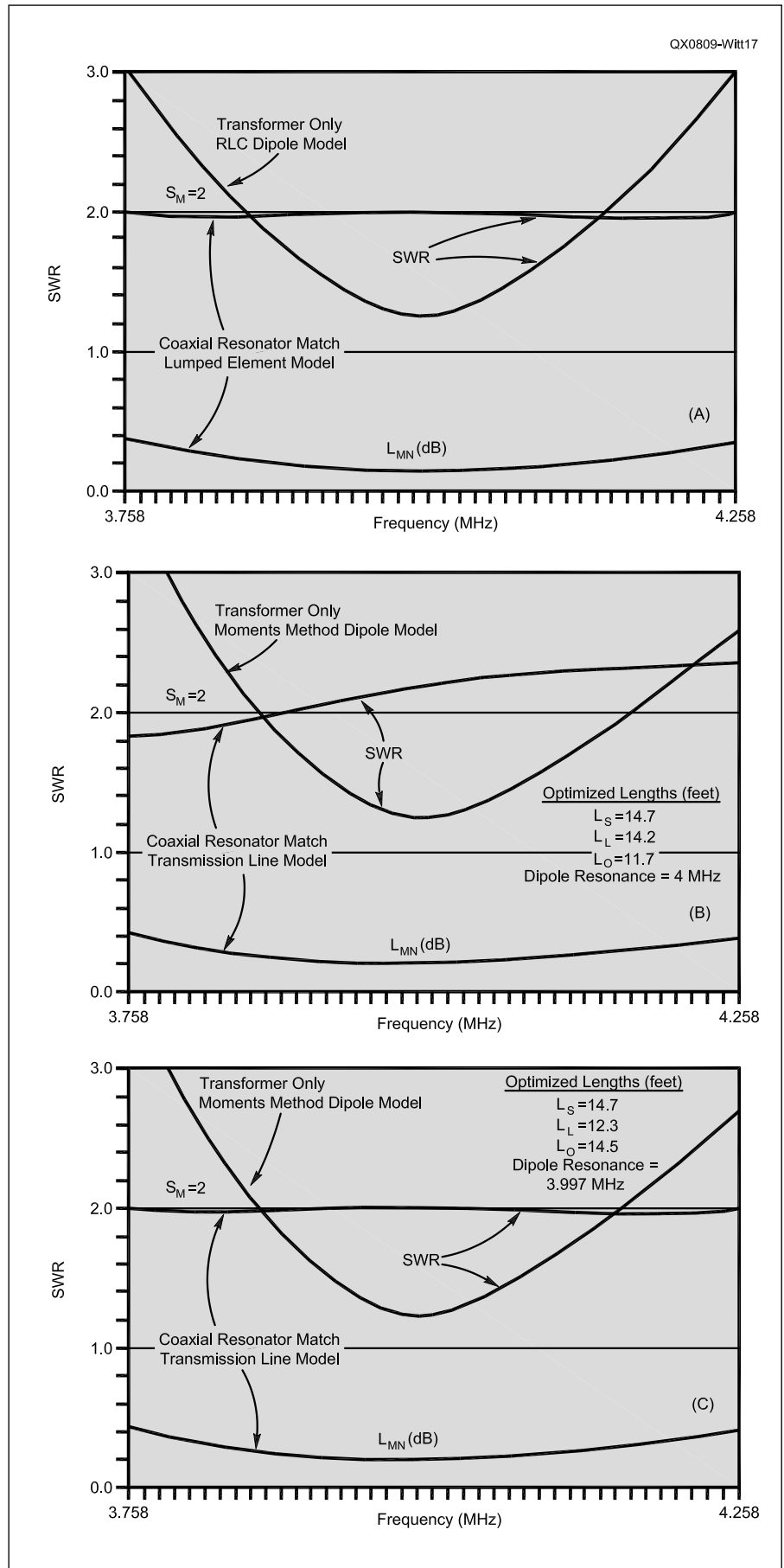
Acknowledgement

The author gratefully acknowledges the value of the stimulating discussions with J. J. Kenny and R. E. Fisher, which influenced the work reported in this paper.

Notes

- ¹Frank Witt, "Optimum Lossy Broadband Matching Networks for Resonant Antennas," *RF Design*, Apr 1990, pp 44-51 and July 1990, p 10.
- ²Frank Witt, "Broadband Dipoles - Some New Insights," *QST*, Oct 1986, pp 27-37.
- ³Frank Witt, "The Coaxial Resonator Match and the Broadband Dipole," *QST*, Apr 1989, pp 22-27.
- ⁴Frank Witt, "The Coaxial Resonator Match," *The ARRL Antenna Compendium*, Volume 2, (Newington: ARRL 1989), pp 110-118.
- ⁵Frank Witt, "Match Bandwidth of Resonant Antenna Systems," *QST*, Oct 1991, pp 21-25 and with A. Griffith, "Match Bandwidth Revisited," *QST*, June 1992, Technical Correspondence, pp 71-72.
- ⁶Frank Witt, "A Simple Broadband Dipole for 80 Meters," *QST*, Sept 1993, pp 27-30, 76.
- ⁷Frank Witt, "Broadband Matching with the Transmission Line Resonator," *The ARRL Antenna Compendium*, Volume 4, (Newington: ARRL 1995), pp 30-37.
- ⁸Frank Witt, "Optimizing the 80-Meter Dipole," *The ARRL Antenna Compendium*, Volume 4, (Newington: ARRL 1995), pp 38-48.
- ⁹R. Dean Straw, N6BV, Ed, *The ARRL Antenna Book*, 19th, 20th and 21st Editions, Chapter 9 (Frank Witt, AI1H), "Broadband Antenna Matching," (Newington: ARRL 2000, 2003 and 2007, respectively), pp 9-1 to 9-18.
- ¹⁰R. M. Fano, "Theoretical limitations on the broadband matching of arbitrary impedances," *J. Franklin Inst.*, vol. 249, pp. 57-83, Jan. 1950; pp. 139-154, Feb. 1950.
- ¹¹R. Levy, "Explicit formulas for Chebyshev impedance matching networks, filters and interstages," *Proc. Inst. Elec. Eng.*, vol. 111, pp. 1099-1106, June 1964.
- ¹²R. C. Hansen, "Evaluation of the Snyder Dipole," *IEEE Trans. Antennas Propagat.*, vol. AP-35, pp. 207-210, Feb. 1987.
- ¹³R. D. Snyder, "Broadband antennae employing coaxial transmission line sections," United States Patent No. 4 479 130, issued Oct. 23, 1984.
- ¹⁴J. D. Kraus, *Antennas*. New York: McGraw-Hill; 2nd ed., 1988, pp. 736-741.
- ¹⁵H. J. Carlin and P. Amstutz, "On optimum broadband matching," *IEEE Trans. Circuits*

Figure 17 — SWR and matching network loss characteristic when match quality is traded for reduced loss. Part A shows the RLC dipole model and lumped element matching network. Part B shows the moments method dipole model and calculated segment lengths. Part C is the same as B, except dipole resonance and segment lengths have been perturbed to restore the SWR characteristic of Part A.



Syst., vol. CAS-28, pp. 401-405, May 1981.

¹⁶J. Pandel and A. Fettweis, "Numerical solution to broadband matching based on parametric representations," *AEU*, vol. 41, pp. 202-209, April 1987.

¹⁷J. C. Logan and J. W. Rockway, "The new MININEC (Version 3): initial concept of employment," Naval Ocean Systems Center Technical Document 938, Sept. 1986.

Frank Witt, AI1H was first licensed in 1948. He holds BS and MS degrees in Electrical Engineering from Johns Hopkins University. He is retired from Bell Telephone Laboratories, where he worked for 37 years. He is a Life Member of the IEEE.

Frank has written about 20 articles related to Amateur Radio. His novel contributions include the top-loaded delta loop, the coaxial resonator match, the transmission line resonator match and the geometric resistance box. He received the 1995 ARRL Technical Excellence Award, and serves as an ARRL Technical Advisor. His other interests include golf and tennis.

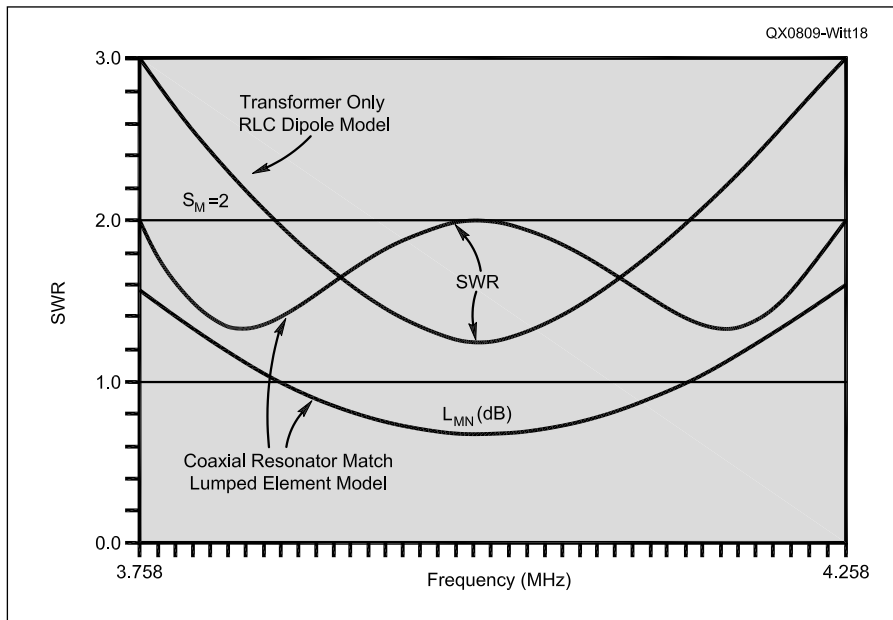


Figure 18 — SWR and matching network loss when the “-” root of Equation 20 is chosen.





Chicago — “Your Kind of Town” for the 2008 ARRL/TAPR Digital Communications Conference



September 26-28

Chicago plays host to the largest gathering of Amateur Radio digital enthusiasts in the country. Make your reservations now for three days of education and camaraderie, including a Sunday seminar on Software Defined Radio by **Phil Harman, VK6APH**.

See the Digital Communications Conference site on the Web at www.tapr.org/dcc/ or call TAPR at **972-671-8277** to make your reservations today.

Letters to the Editor

May/June Issue of QEX

Hi Larry;

I really didn't know that giving the Editor of a publication I enjoy, a good poke in the ribs from time to time could enhance my reading pleasure so much!

Regarding the 2008 May/June issue, not bad but...

I see another construction article with limited construction information slithered in under the tent. The SCR Preselector article sucked me in pretty well until I realized that there was limited construction info available except the enclosure. Harrumph, I say!

The *real* Jewell is the DDS article by James Hagerty, WA1FFL. Now, that's worth a huzzah or two. I liked it so much that I bought the semi kit. I haven't received it yet but the spectral plots have me a bit excited.

N2ADR's Digital SSB Exciter is also a winner! Now, that's more like it. This guy is sharp.

— 73, Bob McCulla, K7HBG, 5025 E Pacific Coast Hwy, Suite P340, Long Beach, CA 90804; k7hbg@arrl.net

Hi Bob,

It's always good to hear from you. I appreciate hearing what you liked and what you didn't like in the May/June issue of QEX. Poke me in the ribs anytime you like!

I was pleased to have N2ADR write about his digital SSB exciter. He had that project on display at the ARRL/TAPR Digital Communications Conference last September. I talked to him about the project and asked him to consider writing about it. The VFO article by WA1FFL was also a very interesting article, I agree. Let me know how that kit works out for you.

I remain enthusiastic about the SCR Preselector. There may not be a lot of construction information, but the microprocessor code for the project, as well as the computer control program are available for free download, either from the author's Web site or from the QEX Web site, so I think it is buildable.

— 73, Larry Wolfgang, WR1B, QEX Editor; lwolfgang@arrl.org

Some Thoughts on Crystal Parameter Measurement (Jul/Aug 2008)

Dear Editor, QEX Magazine,

Measuring quartz crystal parameters is one of those tasks that turns out to be much more complicated than it appears at first sight. The excellent article by VE5FP discusses some of the reasons for that, such as nonlinear effects (changes in crystal parameters with drive level) and issues associated with the measurement technique.¹

There is, however, a more basic theoretical complication associated with the equations of the equivalent circuit model of a quartz crystal. People often speak of "series-resonant" frequency without specifying precisely what is meant by that term. There are at least three possible definitions. One is simply the series-resonant frequency of the motional inductance and capacitance, $f_{sm} = 1 / (2\pi \sqrt{L_m C_m})$, where L_m and C_m are the motional parameters. The other definitions are the frequency of minimum impedance, f_{sz} , and the frequency at which the impedance has zero phase (is purely resistive), $f_{s\phi}$.

It turns out that all three definitions of "series-resonant frequency" give different answers. It is not difficult (although tedious) to show that the standard crystal model (Figure 1) consisting of the series combination of L_m , C_m and R_m , all in parallel with the holder capacitance, C_0 , gives:

$$f_{sz} = f_{sm} - \Delta$$

$$f_{s\phi} = f_{sm} + \Delta$$

where:

$$\Delta = f_{sm} (1 / 2Q^2) (C_0 / C_m)$$

$$Q = 2\pi f_{sm} L_m / R_m$$

There are similar equations for parallel resonance:

$$f_{pm} = f_{sm} \sqrt{1 + C_m / C_0} \cong f_{sm} (1 + 0.5 C_m / C_0)$$

$$f_{pz} = f_{sm} + \Delta$$

$$f_{p\phi} = f_{sm} - \Delta$$

For many crystals, Δ is small enough that

¹Notes appear on page 00.

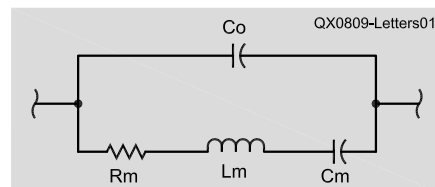


Figure 1 — Equivalent circuit for a quartz crystal.

it can be ignored. In other crystals (especially overtone types), however, it can result in an error of several hundred Hz. For example, using estimated values for the crystal tested in the article ($f_{sm} = 55.25$ MHz, $Q = 35500$, $C_0 = 4.5$ pF, $C_m = 0.00156$ pF) gives $\Delta = 63$ Hz.

The traditional crystal-impedance (C/I) meter is an oscillator with the crystal under test in the feedback path. (See Figure 2.) There is also a tuned circuit that is tuned to achieve zero phase across the crystal. The measurement uses the substitution method — a variable resistor may be switched in place of the crystal. When the tuned circuit and resistor are adjusted so that there is no change in amplitude or frequency when the resistor is substituted, then the resistor equals the equivalent series resistance, R_m , and the frequency of oscillation is the series-resonant frequency of zero phase, $f_{s\phi}$.

Most C/I meters also have provision for switching a capacitor in series with the crystal. The difference in frequency with and without the capacitor can be used to calculate L_m and C_m , given that C_0 and R_m are known. It is interesting to note that the series capacitor can also be used to measure the parallel-resonant frequency directly. It is easy to show that (ignoring the effect of R_m) the parallel-resonant frequency of a crystal with a capacitor in parallel is the same as the series-resonant frequency with the same capacitor in series.

The pi-network measurement circuit used in Jim Koehler's first measurement method is similar to the one outlined in an IEEE publication.² The main difference is his use of a low source and load impedance

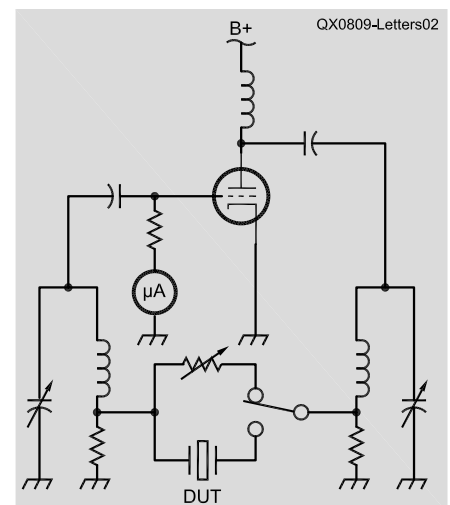


Figure 2 — Traditional crystal-impedance (C/I) meter.

instead of the 50 Ω usually used in the IEEE method. Compared to a C/I meter, this method has the advantage of a well-defined and adjustable drive level. It also allows measurements far from the resonant frequency to search for spurious resonances and to measure C_0 , and is well-suited to automated testing. Several other key references on the subject of crystal testing are listed in Notes 3, 4, 5 and 6.

The frequency of maximum transmission of the pi-network circuit is not equal to any of the three previous definitions of series-resonant frequency! Based on an equation given in the IEEE publication listed in Note 2, the following correction factor may be derived:

$$f_{\pi} = f_{sm} - \Delta (1 + 4 R_T / R_m)$$

where R_T is the source and load resistance (assumed equal) in the fixture. If R_T is much less than R_m , then f_{π} approaches f_{sz} , the frequency of minimum impedance, as expected.

The pi circuit in the article has $R_T = 25 \Omega$. Again using the example crystal from the article ($f_{sm} = 55.25$ MHz, $\Delta = 63$ Hz, $R_m = 52 \Omega$) we get $f_{\pi} - f_{sm} = -185$ Hz. That is $185 + 63 = 248$ Hz different from f_{p0} , as would be measured by a C/I meter.

In addition to the other sources of error mentioned in the article, the pi-network method has several issues associated with the fixture. Stray series inductance can be significant when low source and load impedances are used. I have measured values in the 100 to 150 nH range in a well-constructed fixture. Also, the source and load resistance can change as a function of frequency. For example, with a nominal 8.5 Ω dc resistance, I measured 9.5 Ω at 40 MHz. Finally, the stray holder capacitance of the fixture must be subtracted from the measured C_0 value.

Of course, all of this complexity can be avoided if the designer has access to a network analyzer or spectrum analyzer with tracking generator. Simply build a ladder filter with variable capacitors in shunt and in series with each crystal and then tune for the desired passband shape. (For tuning purposes, it is not necessary to observe the stopband.) I have had good luck building 4-pole filters using such a heuristic method. The trick is first to tune a pair of 2-pole filters separately, then connect them together and do final "tweaks" to get the desired response. When satisfied with the result, replace the variable capacitors with equivalent fixed values. Such a "design" technique is probably not suitable for commercial production, but is a reasonable solution for a one-of-a-kind home construction project.

— 73, Alan Bloom, N1AL, 1578 Los Alamos Rd, Santa Rosa, CA 95409; n1al@arrl.net

Dear Alan,

I appreciate your thoughtful comments and for pointing out several oversimplifications in my article. I intended the article to deal more with an algorithm for automatically making the *usual* measurements rather than a detailed discussion of the circuit itself. Your commentary is excellent, and should be read carefully by any student of the subject of crystal parameters.

— Regards, Jim Koehler, VE5FP, 2258 June Rd, Courtenay, BC V9J-1X9, CANADA; jark@shaw.ca

Notes

- ¹Jim Koehler, VE5FP, "Some Thoughts on Crystal Parameter Measurement," QEX, Jul/Aug, 2008, pp 36-41.
- ²Standard Definitions and Methods of Measurement for Piezoelectric Vibrators, Publication # 177, Institute of Electrical and Electronics Engineers, N. Y. 1966. The equation cited is equation 10b in Table 5, with $b = 1$ (no shunt inductor). Applying McLaurin's series, eliminating small terms, and substituting for reactance results in the equation for f_{π} .
- ³Basic Method for the Measurement of Reso-

nance Frequencies and Equivalent Series Resistance of Quartz Crystal Units by Zero Phase Technique in a Pi-Network, Publication # 444, International Electrotechnical Commission, Geneva, 1973.

⁴Virgil E. Bottom, *The Theory and Design of Quartz Crystal Units*, McMurray Press, Abilene, TX, 1968. This is the "Bible" for quartz crystal resonator design, with concise coverage of all the equations and design considerations. That book has long been out of print, but I see two copies of a similar book by the same author currently listed as being available on amazon.com: *Introduction to Quartz Crystal Unit Design*, Van Nostrand Reinhold, NY, 1982.

⁵W. G. Cady, *Piezoelectricity; An Introduction to the Theory and Applications of Electro-mechanical Phenomena in Crystals*, (New revised edition in two volumes), Dover Publications, NY, 1964. This is the seminal work on piezoelectric crystals, based on the original research of Dr. Cady at Wesleyan University (Middletown, CT).

⁶*Fundamentals of Quartz Oscillators*, AN 200-2, Hewlett Packard Co. This application note includes a good introduction to quartz crystals and their use in oscillators. It is still available for download from the Agilent Web site: www.agilent.com.

1010 Jorie Blvd. #332
Oak Brook, IL 60523
1-800-985-8463
www.atomictime.com

ATOMIC TIME



14" LaCrosse Black Wall
WT-3143A \$21.45

This wall clock is great for an office, school, or home. It has a professional look, along with professional reliability. Features easy time zone buttons, just set the zone and go! Runs on 1 AA battery and has a safe plastic lens.



Digital Chronograph Watch
ADWA101 \$49.95

Our feature packed Chrono-Alarm watch is now available for under \$50! It has date and time alarms, stopwatch backlight, UTC time, and much more!



LaCrosse Digital Alarm
WS-8248U-A \$49.95

This deluxe wall/desk clock features 4" tall easy to read digits. It also shows temperature, humidity, moon phase, month, day, and date. Also included is a remote thermometer for reading the outside temperature on the main unit. approx. 12" x 12" x 1.5"



LaCrosse WT-3143A - \$21.45



LaCrosse Digital Alarm
WS-8248 - \$49.95



LaCrosse WT-5720U - \$24.95

LaCrosse WT-5720UU Clock \$24.95

This digital projection clock is great for travel and fits in a small space. Shows 12 or 24 hour time, time zone, and alarm time. Size 5.25"x 1.25"x 4"

Tell time by the U.S. Atomic Clock -The official U.S. time that governs ship movements, radio stations, space flights, and warplanes. With small radio receivers hidden inside our timepieces, they automatically synchronize to the U.S. Atomic Clock (which measures each second of time as 9,192,631,770 vibrations of a cesium 133 atom in a vacuum) and give time which is accurate to approx. 1 second every million years. Our timepieces even account automatically for daylight saving time, leap years, and leap seconds. \$7.95 Shipping & Handling via UPS. (Rush available at additional cost) Call M-F 9-5 CST for our free catalog.

Upcoming Conferences

ARRL/TAPR Digital Communications Conference

September 26-28, 2008
Chicago, IL

The conference location is the Holiday Inn Hotel, Elk Grove Village, IL.

The ARRL and TAPR Digital Communications Conference is an international forum for radio amateurs to meet, publish their work, and present new ideas and techniques. Presenters and attendees will have the opportunity to exchange ideas and learn about recent hardware and software advances, theories, experimental results, and practical applications. Topics include, but are not limited to:

- Software defined radio (SDR)
- Digital voice (D-Star, P25, WinDRM, FDMDV, DRMDV, G4GUO)
- Digital satellite communications
- Global position system
- Precise Timing
- Automatic Position Reporting System (APRS)
- Short messaging (a mode of APRS)
- Digital Signal Processing (DSP)
- HF digital modes
- Internet interoperability with Amateur Radio networks
- Spread spectrum
- IEEE 802.11 and other Part 15 license-exempt systems adaptable to Amateur Radio
- Using TCP/IP networking over Amateur Radio
- Mesh and peer to peer wireless networking
- Emergency and Homeland Defense backup digital communications in Amateur Radio
- Updates on AX.25 and other wireless networking protocols
- Topics that advanced the amateur radio art

This is a 3 day Conference, with technical and introductory sessions presented all day Friday and Saturday. Join others at the conference for a Friday evening social get together. The Saturday Evening Banquet will feature an invited speaker, and conclude with award presentations and prize drawings.

The ever-popular Sunday Seminar focuses on a topic and provides an in-depth four-

hour presentation by an expert in the field. This year Phil Harman, VK6APH, presents "Software Radio Through the Looking-Glass." The presentation will be highly interactive, so be sure to bring along that SDR question that has been puzzling you for so long!

One-day only registration, Friday or Saturday is \$45. Registration for both days is \$80. The Sunday seminar is \$25. Lunch both days and the Saturday Banquet are available at an additional cost.

For further details about the Conference, and for Conference registration information, see the TAPR Web page at www.TAPR.org/dcc.htm.

Microwave Update 2008

October 17-18, 2008
Bloomington, MN

Microwave Update 2008 will be held on Friday, October 17 through Saturday, October 18 in Bloomington, Minnesota.

This is a microwave conference, and presentations will be on topics for frequencies above 900 MHz. Examples of such topics include microwave theory, construction, communication, deployment, propagation, antennas, activity, transmitters, receivers, components, amplifiers, communication modes, LASER, software design tools, and practical experiences. Please contact Jon Platt, W0ZQ, at w0zq@aol.com or Barry Malowanchuk, VE4MA, at ve4ma@shaw.ca for additional information.

2008 AMSAT North America Space Symposium

24-26 October 2008
Atlanta, Georgia

The Atlanta Radio Club announces that the 2008 AMSAT Space Symposium will be held at the Atlanta Buckhead Doubletree Hotel on Friday, October 24 through Sunday, October 26, 2008.

Call for Papers

Papers are solicited for the 2008 AMSAT Space Symposium and Annual Meeting.

Proposals for papers, symposium presentations, and poster presentations are invited on any topic of interest to the amateur satellite program. An emphasis for this year is an educational outreach to middle and high school students. Another topic of interest is using amateur satellite tracking systems to

monitor deep space network objects.

In particular, papers on the following topics are solicited:

- Students and Education
- ARISS
- AO-51
- P3E
- Eagle
- Deep Space Network monitoring
- Any additional satellite-related topics.

We request a one-page abstract as soon as possible. Camera ready copy on paper or in electronic form will be due by September 1, 2008 for inclusion in the printed symposium proceedings. Papers received after this date may not be included in the printed proceedings.

Abstracts and papers should be sent to n8fgv@amsat.org.

Registration

Symposium registration is \$40 prior to Sep 8, \$45 after Sep 8 and \$50 at the door. The Saturday evening banquet is \$45.



In the Next Issue of QEX

George Murphy, VE3ERP, and Robert DeHoney describe a Dual Output Power Supply. DeHoney's innovative double bridge rectifier design provides nearly equal positive and negative dc output voltages with a common ground from a single ac power transformer. A conventional circuit using plus and minus half wave rectifiers presents some danger of saturating the transformer core, unless the positive and negative loads are carefully balanced. The double bridge rectifier eliminates that possibility.

George and Robert take us through the design calculations, and even offer a software solution to the math problem! If you work with dual supply op-amps or have other needs for equal positive and negative power supply output voltages, you will want to experiment with this circuit. Don't miss it!

Out of the Box

CADSTAR Express Version 10.0 Available

Free Schematic/PCB Design Software

Zuken has released version 10.0 of *CADSTAR Express*. This replaces Version 9.0 and has some significant improvements. This free version has all the schematic entry, PCB layout, and library generation necessary to do a board with up to 300 pins and 50 components. There are facilities in the layout editor to constrain the characteristic impedance of traces so that microstrip designs can be achieved. There are actually three different PCB layout tools included in the package: the standard router/autorouter, the P.R. Editor XR, and the P.R. EditorXR HS/SI.

New in Version 10.0

The top of the list in new features is support for Windows *Vista*.

The library tools now allow libraries to have versions, and you can create a new library from a PCB or schematic. In version 9.0, changes to a parts library required a manual step to index the library for searching. The new version detects when a new index needs to be created and prompts the user to see if they want it updated. The new version includes a sample of the on-line library. The full library that you get with a paid version of *CADSTAR 10.0* has over 200,000 parts. The *Express* copy of the on-line library has about 20,000 parts.

There are upgrades to the user interface for both schematic capture and board layout.

Features

CADSTAR Express is a very useful tool for making small printed circuit boards. I use it in my "day job" to make small prototypes rather than get the CAD people in our California plant to do a full blown design in *PADS PCB*. My experience has been with version 9.0, but it is relevant to the new version. The biggest task in any board is to create a PCB component (some packages call it a footprint) if one does not exist. There are wizards in the library editor to create basically any type of surface mount or through hole part, so the job is very easy once you have done it a couple of times.

The best part of this package is that it is fully integrated from library generation to schematic capture and on to PCB manufacturing. There are wizards at each step of the process to help you through normal tasks. There is also a very well written tutorial that comes with the package. You can follow the examples in the tutorial in

an afternoon or two and learn all of the basics of the process.

I have been doing electronics for over 40 years and the new standards for schematic symbols still seem foreign to me. The example libraries from Zuken are heavy on ISO and European style symbols. Traditional symbols are also available, but you have to search for them. Schematic entry is straightforward and similar enough to other CAD packages that you will learn it quickly.

Once you have a schematic, it is a simple task to export it (from the File menu) into the PCB layout editor. You can do either manual component placement or automatic placement, or a combination of both. Likewise, you can do manual routing or autorouting, or both. I usually make 2 sided boards that are big enough that the autorouter can complete the job without my intervention.

The last step of the process is to start a batch job from the File menu to create all of the manufacturing files necessary to send to a circuit board house. The *Express* version contains a command file that handles 2 layer boards and another for 6 layer boards. You can create your own boards for other configurations using the supplied files as examples.

Each transformation step checks the input data for errors and allows you to go back and clean up the design before proceeding.

Full Featured CADSTAR

CADSTAR has varying levels of cost for varying levels of additional capability. You can purchase a more capable version of *CADSTAR* for about \$2000. Even at this price level there are some restrictions on the number of components and the number of pins, but the level is sufficient for moderately complex designs.

Zuken USA, Inc.
www.zuken.com
 USA Distributor:
 Doug Boone
 PCE Texas, Suite 100
 15441 Knoll Trail Dr
 Dallas, TX 75248
 800-755-6628

New L Band FETs

HVVi Semiconductor has created a new line of UHF power FETs. Current power FETs for L band use are LDMOS FETs that have lateral flow of current through the transistor. HVVi has created vertical FETs with a structure similar to an upside down TMOS FET as used in power supplies. The difference is that the source and gate are positioned on the heat sink with the drain above. The vertical structure pro-

vides a much higher voltage rating than a lateral transistor. The new construction results in higher power capability (due to the higher voltage) in a smaller package. The combination of inverted packaging and smaller size reduces parasitic capacitance and decreases thermal resistance.

The current devices are designed with pulsed avionics and radar applications in mind, but these devices can also be used in linear applications with appropriate allowances for differences. The devices range from 30 W output to 300 W output and cover the 1030-1090 MHz and 1200-1400 MHz bands. The V_{dd} is rated at 48 V and drain efficiency is nearly 50% in pulsed applications. They are not rated for linear or class C operation yet. The 1030 MHz devices can be persuaded to work as low as the 900 MHz amateur band.

These devices are available from Richardson Electronics.

HVVi Semiconductors, Inc.
 Phoenix, AZ
 480-776-3800
www.hvvi.com

New RF Power Detector IC

Linear Technology has added a new part to their line of RF power detectors that produce true RMS readings. The LT5570 joins the LT5004, LT5534, LT5537, and LT5538. Each of these parts convert an input signal to an RMS dc equivalent voltage.

The LT5570 has more than 50 dB linear range over the frequency range of 40 MHz to 2700 MHz. The linearity error at a given frequency is significantly less than 1 dB from -35 dBm to +15 dBm. The output voltage versus input voltage decreases with increasing frequency, so operation at known frequencies can be calibrated. Operation over wide bands (such as a wideband power meter) will require frequency compensation.

At the low end of the frequency range, the part is linear from -53 dBm to +13 dBm. The output voltage is also very accurate for measuring modulated systems with high crest factors such as SSB and CDMA.

The part is currently available from DigiKey for \$11.80 each.

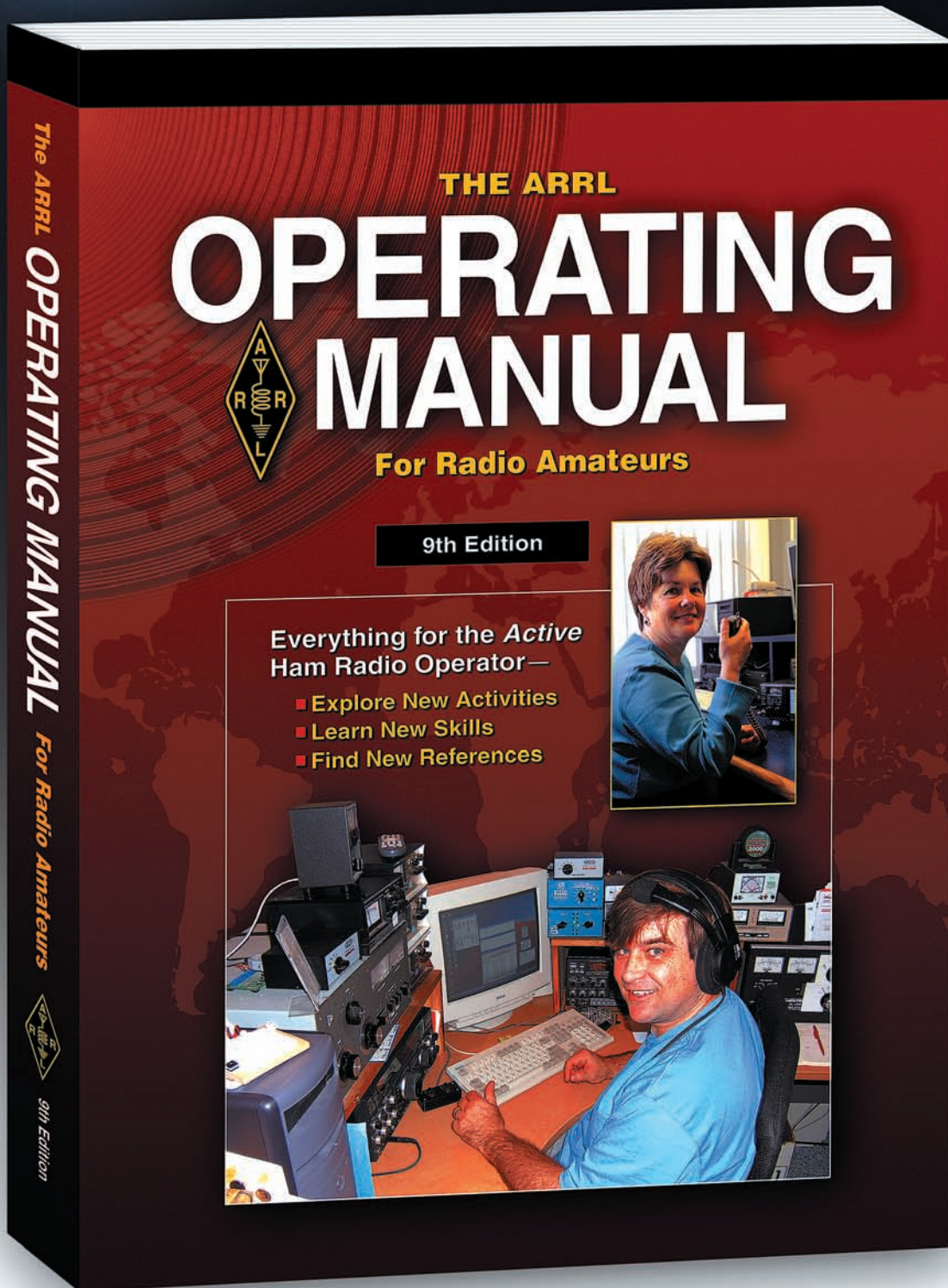
There is no evaluation kit for the LT5570, but Linear Technology has kits available for \$100 each for the LT5534 and LT5537.

Linear Technology
 1630 McCarthy Blvd.
 Milpitas, CA 95035-7417
 Phone: 408-432-1900
 Fax: 408-434-0507
www.linear.com



NEW! Available Now!

ARRL Order No. 1093 **Only \$29.95***



ARRL The national association for
AMATEUR RADIO

SHOP DIRECT or call for a dealer near you.
ONLINE WWW.ARRL.ORG/SHOP
ORDER TOLL-FREE 888/277-5289 (US)

*shipping \$8 US(ground)/\$13.00 International

QEX 9/2008

KENWOOD

Listen to the Future

Kenwood & AvMap The Ultimate APRS[®] Combination

TM-D710A



AvMap G5



Two Great Companies...Providing One Outstanding Solution!

KENWOOD U.S.A. CORPORATION
Communications Sector Headquarters
3970 Johns Creek Court, Suite 100, Suwanee, GA 30024
Customer Support/Distribution
P.O. Box 22745, 2201 East Dominguez St., Long Beach, CA 90801-5745
Customer Support: (310) 639-4200 Fax: (310) 537-8235



www.kenwoodusa.com
ADS#01308



JQA-1205 ISO9001 Registered
Communications Equipment Division
Kenwood Corporation
ISO9001 certification



AvMAP
SATELLITE NAVIGATION



www.avmap.us • e-mail: info@avmap.us
1.800.363.2627